

JUSTUS-LIEBIG-UNIVERSITÄT GIESSEN
INSTITUT FÜR ANORGANISCHE UND ANALYTISCHE CHEMIE



**Syntheses, structures and properties of metal complexes
of bis(2-pyridylmethyl) derivatives of o-, m-, and p-
phenylenediamine and aniline**

Inaugural-Dissertation

zur Erlangung des Doktorgrades der Naturwissenschaften im Fachbereich Biologie
und Chemie der Justus-Liebig-Universität Gießen

vorgelegt von

Sabrina Turba

aus

Gießen

Erstgutachter:	Prof. Dr. Siegfried Schindler
Zweitgutachter:	Prof. Dr. Richard Göttlich
Abgabe der Dissertation im Prüfungsamt:	22.01.2008
Tag der mündlichen Prüfung:	29.02.2008

For my parents

Acknowledgements

The work described in this doctoral thesis has been carried out between December 2004 and February 2008 at the Institute of Inorganic and Analytical Chemistry at the Justus-Liebig-University of Gießen under the supervision of Prof Dr. Siegfried Schindler.

I would like to express my sincere gratitude to my supervisor Prof. Dr. Siegfried Schindler for his excellent guidance and for his great support, patience and enthusiasm during these years.

Furthermore I wish to thank my colleagues and labmates Anja Henss, Sandra Kisslinger, Alexander Beitat, Jörg Müller (every work group deserves a person like him), Thomas Nebe, Christian Würtele, Tobias Hoppe, Dr. Jing-Yuan Xu, Dr. Ildikó Kerezsi, Dr. Jörg Astner, Janine Will, Sabrina Schäfer and Tatjana Neuwert for their friendship and encouragement. We shared rooms, discussions and litres of sparkling wine. Thank you for a great time!

I would like to express my gratitude to Christian Würtele and Dr. Olaf Walter for their friendly support in handling out the X-Ray Crystallography.

Furthermore I would like to thank the people of the Institute of Inorganic and Analytical Chemistry and of the Institute of Organic Chemistry at the Justus-Liebig-University in Gießen for their support of my work

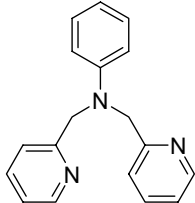
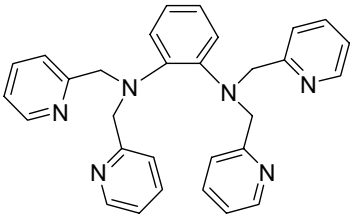
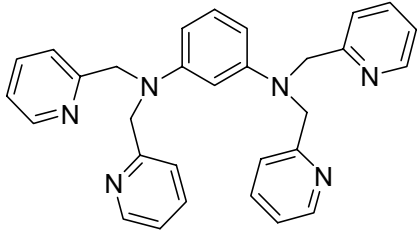
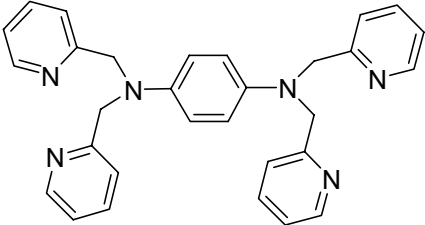
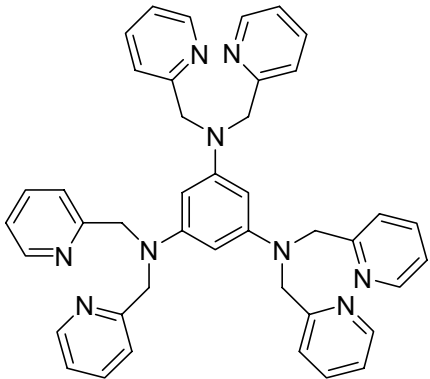
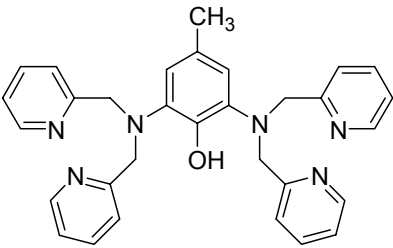
Surely my words will not encompass the love and gratitude that I have for my friends and family who have influenced my life and have formed me to the person I am now. I will not list them here purely out of confidence that they know who they are.

Unfortunately, most of the endeavors that one would like to undertake are loaded with financial barriers. For the reduction of these barriers I owe my parents a big IOU.

Ligand precursors used

<p>1,3-Phenyldiamine</p> <chem>Nc1cccc(N)c1</chem>	<p>Aniline</p> <chem>Nc1ccccc1</chem>
<p>1,3,5-Triaminobenzene trihydrochloride</p> <chem>Nc1cc(N)cc(N)c1</chem> * 3 HCl	<p>2,6-Diamino-<i>p</i>-cresole dihydrochloride</p> <chem>Cc1cc(N)cc(O)c1N</chem> * 2 HCl
<p>2-(Chloromethyl)pyridine hydrochloride</p> <chem>ClCC1=CC=CC=N1</chem> * HCl	<p>1,2-Phenyldiamine</p> <chem>Nc1ccccc1N</chem>

Ligands used

<p><i>N,N</i>-Bis(2-pyridylmethyl)aniline (phbpa)</p> 	<p>1,2-Bis[bis(2-pyridylmethyl)amino]benzene (1,2-tbpd)</p> 
<p>1,3-Bis[bis(2-pyridylmethyl)amino]benzene (1,3-tbpd)</p> 	<p>1,4-Bis[bis(2-pyridylmethyl)amino]benzene (1,4-tbpd)</p> 
<p>1,3,5-Tris[bis(2-pyridylmethyl)amino]benzene (1,3,5-hpbt)</p> 	<p>2,6-Bis[bis(2-pyridylmethyl)amino]-<i>p</i>-cresole (2,6-tpcd)</p> 

Abbreviations

d	Doublet (NMR)
dd	Doublet of Doublet (NMR)
δ	chemical shift in ppm (NMR)
DMSO	Dimethylsulfoxide
e. g.	for example (Latin: <i>exempli gratia</i>)
$\{^1\text{H}\}$	Proton-decoupled (NMR)
Hc	Hemocyanin
IR	Infrared
m	Multiplet
MeOH	Methanol
NMR	Nuclear Magnetic Resonance
Ph	Phenyl
RT	Room temperature
s	Singlet (NMR)
t	Triplet (NMR)
TLC	Thin Layer Chromatography
UV/Vis	Ultraviolet-visible

Table of contents

Acknowledgements	I
Ligand precursors used	II
Ligands used	III
Abbreviations	IV
Table of contents	V
Table of Figures and Schemes	VIII
Chapter 1 - Introduction	1
1.1 Motivation	1
1.2 Copper proteins.	1
1.3 Model complexes for copper proteins	2
1.4 m-phenylenediamine based ligands.....	3
1.5 Magnetic properties of copper(II) complexes with the ligand 1,3-tpbd.	5
1.6 Projects.....	6
1.6.1 Metal complexes with the ligand 1,3-tpbd.....	6
1.6.2 Copper(II) complexes with derivatives of the ligand 1,3-tpbd.	7
Chapter 2 - Syntheses and Characterisation of Copper(II) Complexes with the Ligand 1,3-Bis[bis(2-pyridylmethyl)amino]benzene (1,3-tpbd).	9
2.1 Introduction	9
2.2 Results and Discussion.....	10
2.2.1 Syntheses.....	10
2.2.2 $[\text{Cu}_4(1,3\text{-tpbd})_2(\text{H}_2\text{O})_4(\text{NO}_3)_4](\text{NO}_3)_4 \times 13 \text{ H}_2\text{O}$ (1).....	11
2.2.3 $[\text{Cu}_4(1,3\text{-tpbd})_2(\text{AsO}_4)(\text{ClO}_4)_3(\text{H}_2\text{O})](\text{ClO}_4)_2 \times 2 \text{ H}_2\text{O} \times 0.5 \text{ CH}_3\text{OH}$ (2).....	12
2.2.4 $[\text{Cu}_4(1,3\text{-tpbd})_2(\text{PO}_4)(\text{ClO}_4)_3(\text{H}_2\text{O})](\text{ClO}_4)_2 \times 2 \text{ H}_2\text{O} \times 0.5 \text{ CH}_3\text{OH}$ (3).....	13
2.2.5 $[\text{Cu}_2(1,3\text{-tpbd})((\text{PhO})_2\text{P}(\text{O})_2)_2](\text{ClO}_4)_4$ (4).....	15
2.2.6 $[\text{Cu}_2(1,3\text{-tpbd})((\text{PhO})\text{PO}_3)_2(\text{H}_2\text{O})_{0.69}(\text{CH}_3\text{CN})_{0.31}]_2(\text{BPh}_4)_4 \times \text{Et}_2\text{O} \times \text{CH}_3\text{CN}$ (5).....	16
2.3 Magnetic Measurements.....	17
2.4 Conclusion	19
2.5 Experimental Section	19
2.5.1 General Remarks.....	19
2.5.2 Ligand synthesis.....	20
2.5.3 Complex Syntheses.....	20
2.5.4 Magnetic Measurements.	21
2.5.5 X-ray Crystallographic Studies.....	21
Chapter 3 - Syntheses, structures and properties of copper(II) complexes of bis(2-pyridylmethyl) derivatives of o-, m-, and p-phenylenediamine and aniline.....	26
3.1 Introduction	26
3.2 Results and Discussion.....	28

Table of contents

3.2.1	Ligand Syntheses.	28
3.2.2	[CuCl ₂ (phbpa)] (6).	29
3.2.3	[Cu(1,2-tpbd)](PF ₆) ₂ (7).	30
3.2.4	[Cu ₂ Cl ₄ (1,3-tpbd)] x 0.84 CH ₃ OH (8).	31
3.2.5	[{Cu ₂ Cl ₂ (ClO ₄)(1,3-tpbd)}Cl{Cu ₂ Cl ₂ (OH ₂)(1,3-tpbd)}](ClO ₄) ₂ (9).	32
3.2.6	[Cu ₂ (OH ₂) ₂ (S ₂ O ₆)(1,3-tpbd)]S ₂ O ₆ x 2 H ₂ O x CH ₃ OH (10).	34
3.2.7	[Cu ₂ Cl ₄ (1,4-tpbd)] (11).	35
3.2.8	Magnetic properties.	35
3.3	Conclusion	44
3.4	Experimental Section	44
3.4.1	Materials and Methods.	44
3.4.2	Preparation of the Ligands and Complexes.	45
3.4.3	Magnetic measurements.	47
3.4.4	Computational Methodology.	47
3.4.5	X-Ray Crystallography.	47
Chapter 4 - Syntheses, Characterization and Reactivity of Iron(II), Nickel(II), Copper(II) and Zinc(II) Complexes of the Ligand 1,3-Bis[bis(2-pyridylmethyl)amino]benzene (1,3-tpbd) and its phenol derivative 2,6-Bis[bis(2-pyridylmethyl)amino]-p-cresol (2,6-tpcd).		
4.1	Introduction	52
4.2	Results and Discussion.....	53
4.2.1	Ligand Syntheses	53
	Syntheses of the complexes.....	55
4.2.2	Iron complexes.	55
4.2.3	Nickel complex.....	58
4.2.4	Zinc complexes.....	59
4.2.5	Heterodinuclear zinc(II) and copper(II) complexes.	62
4.2.6	"Zinc ion assisted" formation of a dinuclear copper complex.	64
4.2.7	[Cu ₂ (2,6-tpcd)(H ₂ O)(Cl)](ClO ₄) ₂ x 2 H ₂ O (19).	69
4.2.8	Conclusion	70
4.3	Experimental Section	71
4.3.1	General Remarks.....	71
4.3.2	Physical Measurements.....	71
4.3.3	Ligand Syntheses.	71
4.3.4	Syntheses of Complexes.	72
4.3.5	Computational Methods.....	74
4.3.6	X-ray Crystallographic Studies.....	74

Table of contents

Chapter 5 - Synthesis of 1,3,5-Triaminobenzene Trihydrochloride in a soft way reveals interesting NMR-Spectra.....	84
5.1 Introduction.....	84
5.2 Results and Discussion.....	85
5.2.1 Synthesis of 1,3,5-triaminobenzene trihydrochloride.	85
5.2.2 Synthesis of the ligand 1,3,5-hpbt.....	87
5.3 Experimental Section	88
5.3.1 General Remarks.....	88
5.3.2 Physical Measurements.....	88
5.3.3 Synthesis of 1,3,5-triaminobenzene trihydrochloride. ^[139]	88
5.3.4 Synthesis of the ligand 1,3,5-hpbt. ^[26]	89
5.3.5 X-ray Crystallographic Studies.....	89
Summary	92
Zusammenfassung	96
Publications	100
Curriculum Vitae	101
Bibliography.....	103

Table of Figures and Schemes

Figure 1-1. Schematic representation of the copper-peroxo complex [Cu ₂ (tmpa) ₂ (O ₂)] ²⁺ .	2
Scheme 1-1. Selected Cu/O ₂ species.	3
Figure 1-2. Oxidation reaction of the complex [Cu ₂ (PD)] ²⁺ .	3
Figure 1-3. Synthesis of the ligand 1,3-bis[bis(2-pyridylmethyl)amino]benzene (1,3-tpbd)	4.
Figure 1-4. Schematic representation of the cation of [Cu ₂ (1,3-tpbd)(H ₂ O) ₂ (ClO ₄) ₃][ClO ₄].	5
Figure 1-5. Schematic representation of the complex anion [Cu ₂ (η ² :η ² - <i>N,N'</i> -1,3- phenylenebis(oxamate)) ₂] ⁴⁻ .	6
Figure 1-6. Expected oxidized product of the reaction of 1,3-tpbd with dioxygen (R = H) / The ligand 2,6-Bis[bis(2-pyridylmethyl)amino]- <i>p</i> -cresole (2,6-tpcd, R = CH ₃).	7
Figure 1-7. The ligand <i>N,N',N''</i> -1,3,5-benzenetris(oxamate).	7
Figure 1-8. The ligand precursor 1,3,5-triaminobenzene trihydrochloride (a) and the ligand 1,3,5-Tris[bis(2-pyridylmethyl)amino]benzene (1,3,5-hpbt) (b)	8
Figure 2-1. Molecular structure of the cation of [Cu ₄ (1,3-tpbd) ₂ (H ₂ O) ₄ (NO ₃) ₄] (NO ₃) ₄ × 13 H ₂ O (1).	11
Figure 2-2. Molecular structure of the cation of [Cu ₄ (1,3-tpbd) ₂ (AsO ₄)(ClO ₄) ₃ (H ₂ O)](ClO ₄) ₂ × 2 H ₂ O × 0.5 CH ₃ OH (2).	12
Figure 2-3. Molecular structure of the cation of [Cu ₄ (1,3-tpbd) ₂ (PO ₄)(ClO ₄) ₃ (H ₂ O)](ClO ₄) ₂ × 2 H ₂ O × 0.5 CH ₃ OH (3).	14
Figure 2-4. Connecting unit of the cation of the polymeric chain of [Cu ₂ (1,3- tpbd)((PhO) ₂ P(O) ₂) ₂] ₂ (ClO ₄) ₄ (4).	15
Figure 2-5. Molecular structure of the cation of [Cu ₂ (1,3-tpbd)((PhO)PO ₃) ₂	

Table of Figures and Schemes

$(\text{H}_2\text{O})_{0.69}(\text{CH}_3\text{CN})_{0.31}]_2(\text{BPh}_4)_4 \times \text{Et}_2\text{O} \times \text{CH}_3\text{CN}$ (5).	17
Figure 2-6. μ_{eff} versus H plot for 3 .	18
Figure 2-7. Thermal variation of $\chi \cdot T$ for 3 .	18
Figure 2-8. Thermal variation of $1/\chi$ for 3 .	19
Scheme 3-1. The ligands: phbpa and 1, n -tpbd ($n = 2-4$).	27
Scheme 3-2. The dicopper(II) units in a and b .	27
Figure 3-1. Molecular structure of $[\text{CuCl}_2(\text{phbpa})]$ (6).	29
Figure 3-2. A view of the chain formation in 6 through π - π type interactions along the a axis.	30
Figure 3-3. Molecular structure of the cation of $[\text{Cu}(1,2\text{-tpbd})](\text{PF}_6)_2$ (7).	30
Figure 3-4. Molecular structure of $[\text{Cu}_2\text{Cl}_4(1,3\text{-tpbd})] \times 0.84 \text{ CH}_3\text{OH}$ (8).	31
Figure 3-5. Molecular structure of the cation of $[\{\text{Cu}_2\text{Cl}_2(\text{ClO}_4)(1,3\text{-tpbd})\}\text{Cl}\{\text{Cu}_2\text{Cl}_2(\text{OH}_2)(1,3\text{-tpbd})\}](\text{ClO}_4)_2$ (9).	33
Figure 3-6. Molecular structure of $[\text{Cu}_2(\text{OH}_2)_2(\text{S}_2\text{O}_6)(1,3\text{-tpbd})]\text{S}_2\text{O}_6$ (10).	35
Figure 3-7. Thermal variation of $\chi_M T$ for 6 under an applied magnetic field of 1000 G.	36
Figure 3-8. Magnetization <i>versus</i> H plot for 6 at $T = 1.85, 2.0, 2.5, 3.0$ and 3.5 K.	37
Figure 3-9. Thermal variation of $\chi_M T$ for 8 under an applied magnetic field of 0.1 T.	38
Figure 3-10. Thermal variation of $\chi_M T$ for 10 under applied magnetic fields of 0.1 T.	40
Figure 3-11. Thermal dependence of $\chi_M T$ for 9 .	40
Figure 3-12. Model systems (I-III) of the dinuclear copper(II) fragments of 9 which were used to perform the DFT type calculations.	41

Table of Figures and Schemes

Scheme 4-1. The ligands 1,3-Bis[bis(2-pyridylmethyl)amino]benzene (1,3-tpbd) and 2,6-Bis[bis(2-pyridylmethyl)amino]-p-cresol (2,6-tpcd; R = CH ₃).	52
Figure 4-1. Molecular structure of 1,3-tpbd.	54
Figure 4-2. Molecular structure of the cation of [1,3-tpbdH ₂](ClO ₄) ₂ .	54
Figure 4-3. Molecular structure of the cation of [Fe ₂ (1,3-tpbd)(CH ₃ CN) ₆](ClO ₄) ₄ x 2 CH ₃ CN x 0.5 H ₂ O (12).	56
Figure 4-4. Molecular structure of the cation of [Fe ₂ (1,3-tpbd)(DMF) ₆](ClO ₄) ₄ (13).	58
Figure 4-5. Molecular structure of the cation of [Ni ₂ (1,3-tpbd)(DMF) ₆](ClO ₄) ₄ (14).	59
Figure 4-6. Molecular structure of the cation of [Zn ₂ (1,3tpbd)(CH ₃ CN) ₂ (SO ₃ CF ₃) ₂ (H ₂ O)](SO ₃ CF ₃) ₂ (15).	60
Scheme 4-2. NMR-assignment in complexes 12 , 13 and 15 .	61
Figure 4-7. Molecular structure of [Zn ₂ (1,3-tpbd)Cl ₄] (16).	62
Figure 4-8. Molecular Structure of [CuZn(1,3-tpbd)Cl ₄] (17).	63
Figure 4-9. Molecular structure of the cation of [Cu ₂ (1,3-tpbd) ₂ (H ₂ O) ₂](ClO ₄) ₄ (18).	65
Scheme 4-3. Schematic representation of the complex with the "impurity" L' as ligand (left) in comparison to 18 (right).	66
Scheme 4-4. Scheme of reactions observed during the "zinc assisted" formation of 18 .	67
Scheme 4-5. Possible reaction scheme for the formation of an oxidation product of 1,3-tpbd.	68
Figure 4-10. Calculated structures of the copper dioxygen adduct complex of 1,3-tpbd.	69

Table of Figures and Schemes

Figure 4-11. Molecular structure of the cation of $[\text{Cu}_2(2,6\text{-tpcd})(\text{H}_2\text{O})(\text{Cl})](\text{ClO}_4)_2$ (19).	70
Figure 5-1. The ligand 1,3,5-hpbt.	84
Figure 5-2. The ligand $N,N'N''$ -1,3,5-benzenetris(oxamate).	85
Scheme 5-1. Synthesis of 1,3,5-triaminobenzene trihydrochloride.	85
Figure 5-3. Molecular structure of 1,3,5-triaminobenzene trihydrochloride.	86
Figure 5-4. NMR-Spectra of 1,3,5-triaminobenzene trihydrochloride.	86
Scheme 5-2. Synthesis of the ligand 1,3,5-hpbt.	87

Chapter 1 - Introduction

1.1 Motivation

Metalloproteins are a class of natural compounds that are involved in important chemical reactions in biological systems.^[1, 2] During breathing of animals, uptake and transport of dioxygen is performed by either iron or copper proteins. Furthermore, mainly iron or copper enzymes are involved in the selective oxidation of organic substrates, e. g. by transferring one (monooxygenases) or two (dioxygenases) oxygen atoms to the substrate molecule.^[3-5] Such reactions have inspired bioinorganic chemists because selective oxidations of hydrocarbons using air under ambient conditions are an important challenge in the laboratory and in industry. Therefore, strong efforts have been made during the last thirty years, to model the active sites of these enzymes and their catalytic oxidations reactions using low molecular weight complexes.^[6] Currently one of the biggest challenges is assigned to the catalytic selective oxidation of methane to methanol using air, an oxidation that is easily performed by methane monooxygenase that can have either iron or copper ions in its active site.

1.2 Copper proteins.

As described above, a large number of oxidation reactions in nature involves transport and activation of dioxygen by metalloproteins. Many active sites of these compounds contain copper ions.^[4, 5, 7-10] The protein hemocyanin (Hc) for example is responsible for dioxygen transport in molluscs such as snails and arthropods such as spiders, crabs or lobster.^[11] Its active site, a dinuclear copper complex, has the ability to bind and release dioxygen reversibly. Another important copper enzyme is tyrosinase, which functions as a monooxygenase and has a rather similar structure to Hc.^[9] It is found in mammals, crops, insects and fungi and catalyses the *ortho*-hydroxylation of the amino acid tyrosine (and its subsequent oxidation to the related quinone).^[1, 12, 13] After the polymerisation is completed, the pigment melanine is formed, that is responsible for the colour of our skin and furthermore for the browning reaction of vegetables and fruit.^[14, 15] The enzyme tyrosinase is also involved in the composition of insect's exoskeleton (cuticula).

1.3 Model complexes for copper proteins

A large number of model compounds for copper proteins have been studied in the past and several excellent review articles describe these investigations in great detail.^[4, 5, 16] Research groups have been interested in the development of biomimetic copper complexes, which react with dioxygen in the same way as their natural analogues.^[4, 5, 10, 17, 18] These model compounds usually are low molecular weight complexes with similar spectral, magnetic or chemical properties as the copper proteins mentioned above.^[4, 5, 10]

The most important aspect in this kind of chemistry is the detection and analysis of the active species, the transient "oxygen" copper complex that is responsible for the selective oxidation reactions. Pyridine based ligands proved to be quite useful in that regard^[4, 5, 10] and Karlin and coworkers were able to model the reversible dioxygen binding of a copper(I) complex at low temperatures using tris(2-pyridylmethyl)amine (tmpa) as a ligand.^[19] Furthermore, they also succeeded for the first time to crystallize and to structurally characterize a dinuclear copper peroxo complex $[\text{Cu}_2(\text{tmpa})_2(\text{O}_2)]^{2+}$ at low temperatures.^[20] The schematic structure of this purple complex is shown in Figure 1-1.

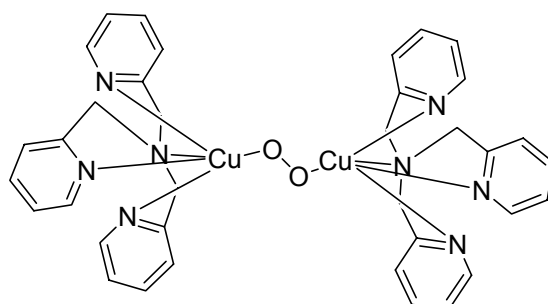
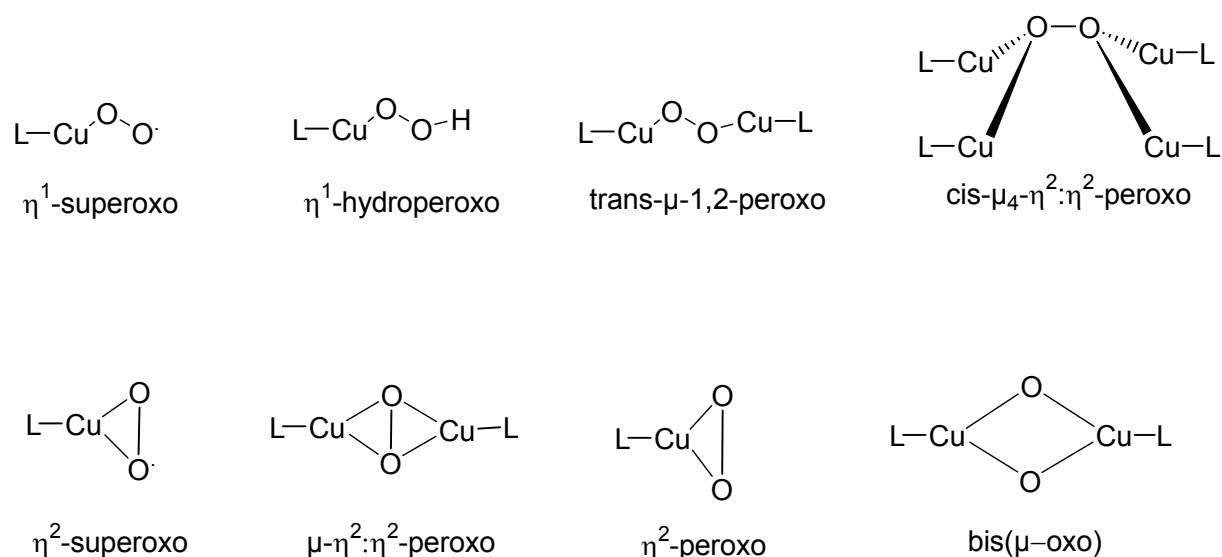


Figure 1-1. Schematic representation of the copper-peroxo complex $[\text{Cu}_2(\text{tmpa})_2(\text{O}_2)]^{2+}$.

Subsequent work showed that dioxygen can react with copper(I) complexes to a large number of "oxygen" complexes and several of these species could be fully characterized in recent work.^[4, 5, 16, 21] Some selected examples for the different binding mode of dioxygen (as superoxo, peroxo or oxo groups) to copper are presented in Scheme 1-1.^[4, 5, 10, 22] In contrast to the trans- μ -1,2-peroxo coordination in $[\text{Cu}_2(\text{tmpa})_2(\text{O}_2)]^{2+}$ it was found that in hemocyanin or tyrosinase dioxygen is coordinated as a μ - η^2 : η^2 peroxide, the so called side-on coordination mode.^[23, 24] In

methane monooxygenase it is most likely that a bis- μ -oxo unit represents the active species.



Scheme 1-1. Selected Cu/O₂ species.

1.4 *m*-phenyldiamine based ligands.

Due to the fact that many of the copper enzymes contain dinuclear active sites, model studies as well concentrated on preorganized ligands and research groups started to connect a large number of coordinating units through a variety of different bridges.^[4, 5, 16] In this aspect tetra-*N*-functionalized 1,3-benzenediamines have been previously used as ligands for the preparation of dinuclear copper complexes.^[12, 25, 26] In some cases these complexes proved to be good structural models of the active sites of copper proteins such as hemocyanin and tyrosinase.^[12, 25-27]

For example Karlin and coworkers could model tyrosinase reactivity with the dinuclear copper complex $[\text{Cu}_2(\text{PD})]^{2+}$ (PD = 1,3-bis[bis(2-pyridylethyl)amino]benzene) according to Figure 1-2.

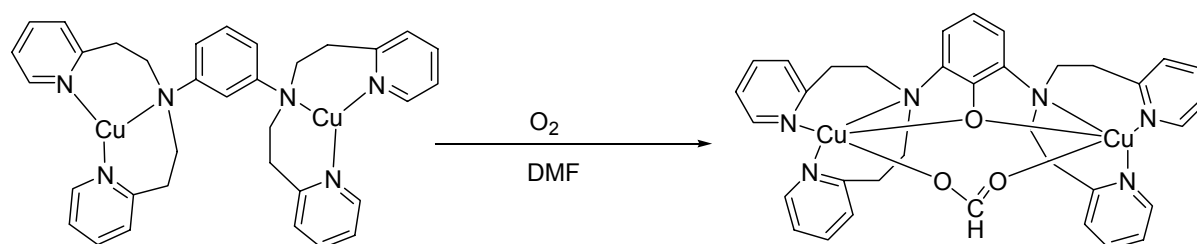


Figure 1-2. Oxidation reaction of the complex $[\text{Cu}_2(\text{PD})]^{2+}$.

During the reaction of the dicopper(I) complex with dioxygen in DMF selective hydroxylation of the benzene ring was observed, similar to the *o*-hydroxylation reactions of tyrosinase.^[27]

To gain further insight into the reaction behaviour of such dinuclear copper systems, the ligand 1,3-bis[bis(2-pyridylmethyl)amino]benzene (1,3-tpbd) was synthesized according to Figure 1-3 by Schindler et al.^[26] The ligand 1,3-tpbd is related to PD, however it differs by forming 5-membered chelate rings in contrast to the 6-membered chelate rings in PD complexes. Compared with 5-membered rings, 6-membered rings tend to stabilize copper(I) ions much more towards oxidation.

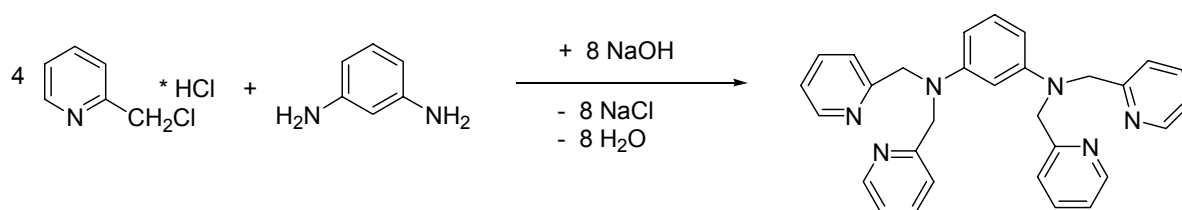


Figure 1-3. Synthesis of the ligand 1,3-bis[bis(2-pyridylmethyl)amino]benzene (1,3-tpbd).

However, in contrast to $[\text{Cu}_2(\text{PD})]^{2+}$ the air oxidation of the copper(I) complex of the ligand 1,3-tpbd did not show an intramolecular ligand hydroxylation reaction. While it was quickly oxidised, treatment of the formed copper(II) complex with an excess of aqueous ammonia (to remove the copper), 1,3-tpbd could be isolated by extraction, unchanged from the oxidation.^[26]

During these investigations however, a copper(II) complex of 1,3-tpbd, $[\text{Cu}_2(1,3\text{-tpbd})(\text{H}_2\text{O})_2(\text{ClO}_4)_3]\text{ClO}_4$, was isolated and could be structurally characterized.^[26] It contains two copper(II) cores which are overall coordinated by one 1,3-tpbd molecule, two water molecules and three perchlorate ions. The coordination sphere of the two copper(II) ions in the equatorial plane is consisting of two pyridine rings which are in a *trans* position to each other, the tertiary amine atom of the ligand and the oxygen atom from the water molecule. The basal plane contains the perchlorate ions and surprisingly one of them acts as a bridging group between the two copper ions.^[26] The schematic representation of the complex cations crystal structure is presented in Figure 1-4.

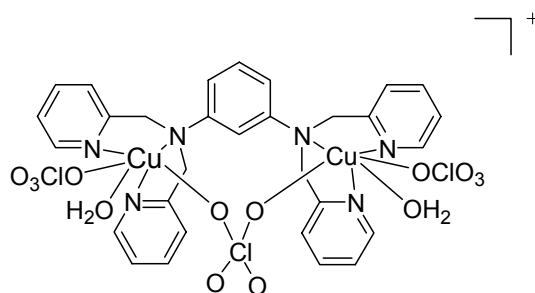


Figure 1-4. Schematic representation of the cation of $[\text{Cu}_2(1,3\text{-tpbd})(\text{H}_2\text{O})_2(\text{ClO}_4)_3]\text{ClO}_4$.

1.5 Magnetic properties of copper(II) complexes with the ligand 1,3-tpbd.

Interest in syntheses and characterisation of polynuclear copper(II) complexes furthermore derives from the efforts to understand the factors that are responsible for the magnetic exchange interactions between coupled metal centres (magnetostructural correlations and the exchange mechanism involving different bridging groups).^[28-31]

In that regard it was interesting to observe in a magnetic study on the $[\text{Cu}_2(1,3\text{-tpbd})(\text{H}_2\text{O})_2(\text{ClO}_4)_3]\text{ClO}_4$ that in this complex a significant ferromagnetic exchange coupling with $J = +9,3 \text{ cm}^{-1}$ could be measured.^[26] This result was surprising in so far that the two copper ions are separated by a quite far distance of $5,87 \text{ \AA}$ and furthermore, that related dinuclear complexes usually show antiferromagnetic exchange coupling.^[30, 32] There is only one other example of a similar complex, which is based on the ligand *N,N'*-1,3-phenylenebis(oxamate), where the two copper(II) ions are separated by a similar distance ($6,822 \text{ \AA}$) and a ferromagnetic exchange coupling ($J = +16,8 \text{ cm}^{-1}$) is observed as well.^[33] The schematic representation of the anion of this complex is shown in Figure 1-5.

The ferromagnetic coupling observed for these compounds can be assigned to a magnetic exchange pathway *via* the *m*-phenylenediamine units, the so called σ -framework.^[34] If there is an even number of bridging atoms between the two copper(II) cores, antiferromagnetic coupling is observed. When an odd number of bridging atoms is employed, ferromagnetic coupling takes place.^[34-36] The magnetic behaviour of these compounds is best explained by the so called spin polarisation mechanism.^[30, 37, 38] It describes, in which way an unpaired electron on one atom can polarize the electron cloud on the adjacent atom.

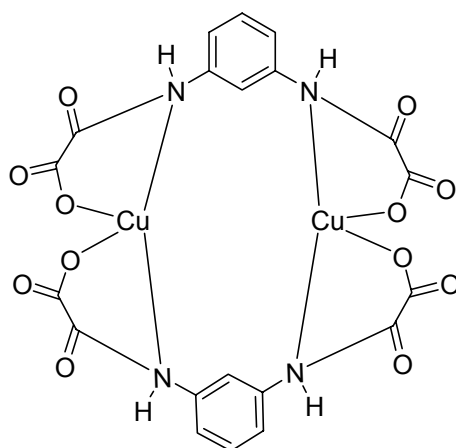


Figure 1-5. Schematic representation of the complex anion $[\text{Cu}_2(\eta^2:\eta^2\text{-}N,N'\text{-}1,3\text{-phenylenebis(oxamate)})_2]^{4-}$.

Furthermore, it was observed by Schindler and coworkers, that the magnetic behaviour of the copper(II) complexes with the ligand 1,3-tpbd could be modified through variation of the used anions or the employment of additional ligands. In contrast to $[\text{Cu}_2(1,3\text{-tpbd})(\text{H}_2\text{O})_2(\text{ClO}_4)_3]\text{ClO}_4$ the complex $[\text{Cu}_2(1,3\text{-tpbd})(\text{N}_3)_4]$ in which four azide anions are coordinated as monodentate ligands to the copper ions, shows only weak antiferromagnetic exchange coupling ($J = -2,1 \text{ cm}^{-1}$), because one of the phenyldiamine nitrogen atoms is now in the basal plane of the copper(II) ions.^[39]

On the other side, if oxalate was used as an anion it acted as a bridging ligand and strong antiferromagnetic coupling between the two copper(II) ions was observed ($J = -366 \text{ cm}^{-1}$).^[39] The copper(II) ions in this complex are now not longer coordinated to the phenyldiamine nitrogen atoms and therefore the ferromagnetic coupling pathway through the σ -framework is now impossible.^[39]

1.6 Projects.

1.6.1 Metal complexes with the ligand 1,3-tpbd.

As described above in paragraph 1.4, copper(II) complexes with the ligand 1,3-tpbd showed interesting magnetic properties that could be modified through variation of the used anions or additional ligands. To gain better insight into the magnetism of these compounds a series of 1,3-tpbd copper complexes using different anions and

additional possible ligands should be synthesized, cristallographically characterized and investigated using magnetic measurements.

1.6.2 Copper(II) complexes with derivatives of the ligand 1,3-tpbd.

As described in paragraph 1.3, no hydroxylation reaction of the ligand 1,3-tpbd was observed, when its according copper(I) complex was reacted with dioxygen. However, the expected oxidized product shown in Figure 1-6 (R = H) that did not form during oxidation could be an interesting ligand in copper chemistry. Therefore the ligand 2,6-Bis[bis(2-pyridylmethyl)amino]-*p*-cresole (2,6-tpcd, Figure 1-6, R = CH₃) and the according copper complexes should be synthesized and characterized.

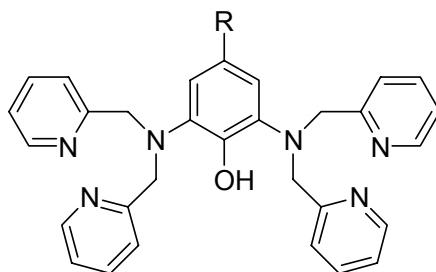


Figure 1-6. Expected oxidized product of the reaction of 1,3-tpbd with dioxygen (R = H) / The ligand 2,6-Bis[bis(2-pyridylmethyl)amino]-*p*-cresole (2,6-tpcd, R = CH₃).

Due to the fact that copper(II) complexes with the ligand 1,3-tpbd showed interesting magnetic properties, it was obvious to try to increase the complexity of this system by introducing an additional “arm” that should coordinate to a third copper ion.

A similar system which is based on the ligand *N,N',N''*-1,3,5-benzenetris(oxamate) (Figure 1-7) was developed and studied by Ottenwaelder et al.

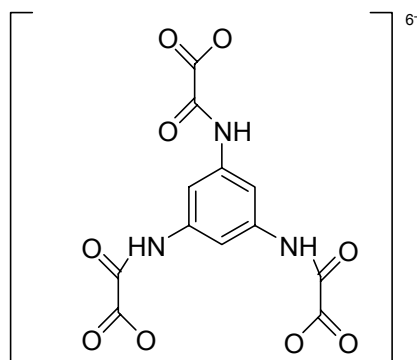


Figure 1-7. The ligand *N,N',N''*-1,3,5-benzenetris(oxamate).

The interesting magnetic properties of its copper(II) complex were reported previously.^[40]

Therefore the ligand precursor 1,3,5-triaminobenzene (Figure 1.8 a) described previously in the literature should be synthesized to obtain the new ligand 1,3,5-Tris[bis(2-pyridylmethyl)amino]benzene (1,3,5-hpbt, Figure 1-8 b) and the according copper complexes.

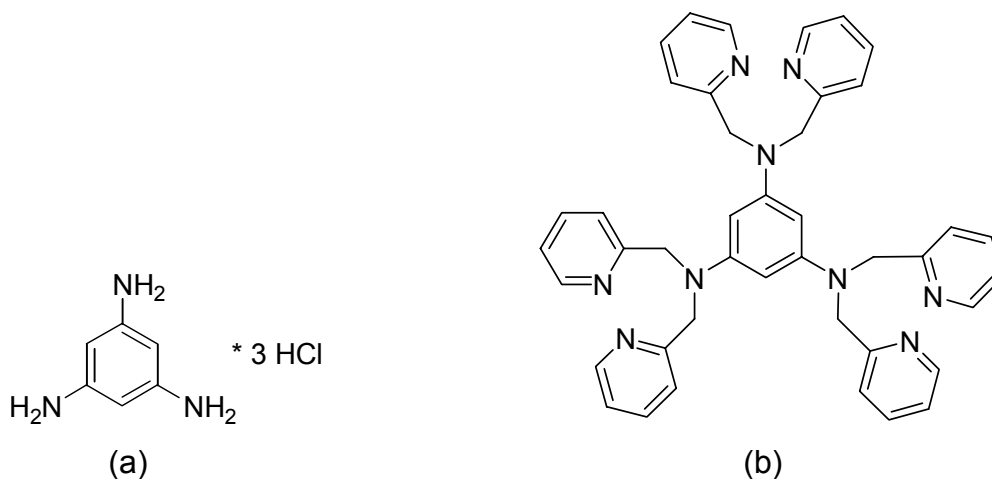


Figure 1-8. The ligand precursor 1,3,5-triaminobenzene trihydrochloride (a) and the ligand 1,3,5-Tris[bis(2-pyridylmethyl)amino]benzene (1,3,5-hpbt) (b).

Chapter 2 - Syntheses and Characterisation of Copper(II) Complexes with the Ligand 1,3-Bis[bis(2-pyridylmethyl)amino]benzene (1,3-tpbd).

This work has been submitted for publication to *European Journal of Inorganic Chemistry*.

Sabrina Turba, Simon Foxon, Frank W. Heinemann, Konstantin Petukhov, Paul Müller, Olaf Walter and Siegfried Schindler.

2.1 Introduction

Tetra-*N*-functionalized 1,3-benzenediamines have been previously used as ligands in the preparation of dicopper complexes.^[12, 25, 26] In some cases these complexes are good structural models of the active sites of the copper proteins hemocyanin and tyrosinase.^[12, 25-27] The ligand 1,3-Bis[bis(2-pyridylmethyl)amino]benzene (1,3-tpbd) and a series of its dinuclear copper complexes have been prepared for such purpose in the past by Schindler and co-workers.^[26] Moreover, the ligand 1,3-tpbd is a versatile ligand that binds various metal ions in a quite rigid framework.^[41]

Furthermore, interest in syntheses and characterisation of polynuclear copper(II) complexes derives from the efforts to understand the factors that are responsible for the magnetic exchange interactions between coupled metal centres (magnetostructural correlations and the exchange mechanism involving different bridging groups).^[28-31] Therefore further copper(II) complexes of the ligand 1,3-tpbd that showed promising magnetic properties were investigated. A magnetic study of the structurally characterized perchlorate bridged dinuclear copper complex $[\text{Cu}_2(1,3\text{-tpbd})(\text{H}_2\text{O})_2(\text{ClO}_4)_3](\text{ClO}_4)$ (with a large intramolecular Cu...Cu separation of 5.873(1) Å) had shown in the past that a significant ferromagnetic coupling ($J = 9.3 \text{ cm}^{-1}$, the Hamiltonian being defined as $H = -JS_1 \times S_2$) mediated by the benzenediamine unit was observed.^[34] The ferromagnetic coupling, following the spin polarisation mechanism, was successfully interpreted using density functional theory (DFT) calculations.^[34] This finding is in good agreement with a related benzenediamine based dinuclear complex that also showed ferromagnetic coupling between two copper(II) ions over a large distance ($J = 16.8 \text{ cm}^{-1}$).^[33]

In contrast, no magnetic exchange coupling was observed when the perchlorate group in $[\text{Cu}_2(1,3\text{-tpbd})(\text{H}_2\text{O})_2(\text{ClO}_4)_3](\text{ClO}_4)$ was substituted by acetate (which did not bridge the two copper(II) ions) or sulfate (the sulfate ion acting as both a terminal and a one-atom bridging ligand in the tetranuclear complex $[\text{Cu}_4(1,3\text{-tpbd})_2(\text{H}_2\text{O})_2(\text{SO}_4)_2](\text{SO}_4)_2$).^[34] Substitution of the perchlorate anions in $[\text{Cu}_2(1,3\text{-tpbd})(\text{H}_2\text{O})_2(\text{ClO}_4)_3](\text{ClO}_4)$ by azide anions led to the preparation of $[\text{Cu}_2(1,3\text{-tpbd})(\text{N}_3)_4]$ and structural characterisation showed that azide acts only as a non-bridging ligand.^[39] Only very weak antiferromagnetic coupling was observed ($J = -2.1 \text{ cm}^{-1}$) most likely due to an intermolecular exchange pathway. On the other hand, if oxalate was used as an anion it acted as a bridging ligand and strong antiferromagnetic coupling between the copper(II) ions was observed ($J = -366 \text{ cm}^{-1}$).^[39]

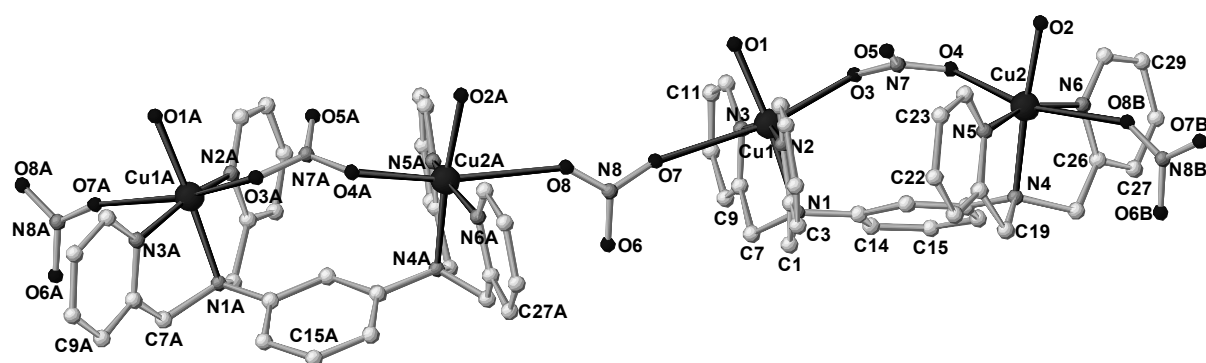
To gain more information about the behaviour of copper(II) compounds with the ligand 1,3-tpbd additional complexes were prepared and we report herein the syntheses and characterisation of $[\text{Cu}_4(1,3\text{-tpbd})_2(\text{H}_2\text{O})_4(\text{NO}_3)_4](\text{NO}_3)_4 \times 13 \text{ H}_2\text{O}$ (**1**), $[\text{Cu}_4(1,3\text{-tpbd})_2(\text{AsO}_4)(\text{ClO}_4)_3(\text{H}_2\text{O})](\text{ClO}_4)_2 \times 2 \text{ H}_2\text{O} \times 0.5 \text{ CH}_3\text{OH}$ (**2**), $[\text{Cu}_4(1,3\text{-tpbd})_2(\text{PO}_4)(\text{ClO}_4)_3(\text{H}_2\text{O})](\text{ClO}_4)_2 \times 2 \text{ H}_2\text{O} \times 0.5 \text{ CH}_3\text{OH}$ (**3**), $[\text{Cu}_2(1,3\text{-tpbd})((\text{PhO})_2\text{P}(\text{O})_2)_2](\text{ClO}_4)_4$ (**4**) and $[\text{Cu}_2(1,3\text{-tpbd})((\text{PhO})\text{PO}_3)_2(\text{H}_2\text{O})_{0.69}(\text{CH}_3\text{CN})_{0.31}]_2(\text{BPh}_4)_4 \times \text{Et}_2\text{O} \times \text{CH}_3\text{CN}$ (**5**).

2.2 Results and Discussion

2.2.1 Syntheses

1,3-Bis[bis(2-pyridylmethyl)amino]benzene (1,3-tpbd) was prepared in good yield according to a literature procedure and recrystallised from acetone.^[26] The copper(II) complexes **1-5** were obtained by mixing stoichiometric amounts of the respective copper(II) salts, 1,3-tpbd and NaH_2AsO_4 , NaH_2PO_4 , diphenylphosphate or monophenylphosphate in aqueous methanol solutions. Single crystals suitable for X-ray crystallography were obtained from slow evaporation of the solutions.

Previous efforts to obtain single crystals of a nitrate derivative of $[\text{Cu}_2(1,3\text{-tpbd})(\text{H}_2\text{O})_2(\text{ClO}_4)_3](\text{ClO}_4)$ were unsuccessful. While perchlorate anions could be readily substituted, partially or completely by nitrate ions, the crystal structure obtained could not be refined satisfactorily. Finally we recognized that the isolated crystals were quickly deteriorating due to loss of solvent molecules from the crystal lattice. Keeping the crystals in their mother liquor allowed **1** to be structurally characterized by single crystal X-ray diffraction. The cation of **1** is depicted in Figure 2-1. The crystallographic data are shown in Table 2-1, bond lengths and angles in Table 2-2.



Complex **1** crystallizes in form of a polynuclear chain that consists of dinuclear Cu-1,3-tpbd units. Two of these units are connected by one nitrate anion. **1** however, is clearly best described as a polynuclear complex in which each of the copper(II) ions are ligated by three nitrogen donor atoms, two nitrate ions and one oxygen atom of a water molecule. The nitrate ions act as bridging units, intramolecular and intermolecular, between the copper(II) ions. The distance between the two copper(II) ions in one dinuclear complex unit is 5.7976 Å, quite close to 5.873(1) Å reported earlier for [Cu₂(1,3-tpbd)(H₂O)₂(ClO₄)₃]ClO₄.^[26] Each copper(II) ion is “4+2” coordinated in a distorted octahedral environment. again quite similar to [Cu₂(1,3-tpbd)(H₂O)₂(ClO₄)₃]ClO₄. The terminal nitrate ions are coordinated weakly to the copper(II) ions as one terminal nitrate ion has been replaced by a water molecule, an

effect observed previously in a similar way for the crystallographically characterized copper(II) acetate complexes of 1,3-tpbd.^[34]

There are some more complexes where two copper ions are bridged by a nitrate anion.^[42-44]

2.2.3 $[\text{Cu}_4(1,3\text{-tpbd})_2(\text{AsO}_4)(\text{ClO}_4)_3(\text{H}_2\text{O})](\text{ClO}_4)_2 \times 2 \text{H}_2\text{O} \times 0.5 \text{CH}_3\text{OH}$ (**2**).

Initial synthesis of **2** was achieved by mixing 1,3-tpbd, $\text{Cu}(\text{ClO}_4)_2$ and Na_2HAsO_4 in a stoichiometric ratio of 1:2:1. However, as the tetranuclear copper(II) complex was always isolated as the product, the reaction conditions were modified accordingly. The blue crystals obtained were analysed by X-ray diffraction studies and the cation of **2** is shown in Figure 2-2. The crystallographic parameters are depicted in Table 2-1, bond lengths and angles in Table 2-2.

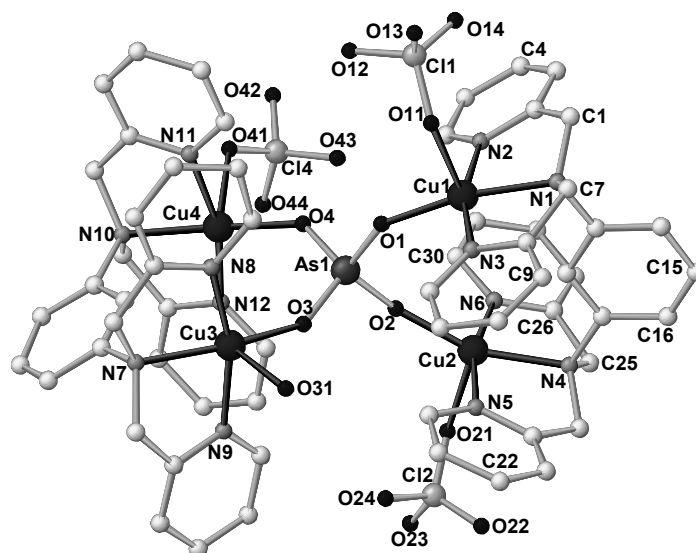


Figure 2-2. Molecular structure of the cation of $[\text{Cu}_4(1,3\text{-tpbd})_2(\text{AsO}_4)(\text{ClO}_4)_3(\text{H}_2\text{O})](\text{ClO}_4)_2 \times 2 \text{H}_2\text{O} \times 0.5 \text{CH}_3\text{OH}$ (**2**). Hydrogen atoms and solvent molecules are omitted for clarity.

Complex **2** is a tetranuclear copper(II) complex and the arsenate ion coordinates to each copper(II) ion via a different oxygen atom. Three copper(II) ions (Cu(1), Cu(2) and Cu(4)) are ligated by three nitrogen atoms of the 1,3-tpbd ligand, one arsenate oxygen atom and one perchlorate oxygen atom. The perchlorate anion of the fourth copper(II) ion (Cu(3)) has been replaced by a water molecule. The intramolecular distance between the copper(II) centres bridged by 1,3-tpbd $[\text{Cu}(1) \cdots \text{Cu}(2) = 4.358 \text{ \AA}]$

is much shorter than in **1**. The distance between the copper(II) centres (not bridged by 1,3-tpbd) [Cu(1) and Cu(4) = 6.139 Å] is considerably longer. Each of the four copper(II) ions is “4+1” coordinated in a slightly distorted square-pyramidal geometry. The trigonality index parameter^[45] τ ranges from 0.08 for Cu(1) to 0.13 for Cu(4). ($\tau = (\beta - \alpha)/60$, with α and β being the two largest coordination angles around the metal centre (for ideal square-pyramidal geometry $\tau = 0$, while for perfect trigonal-bipyramidal geometry $\tau = 1$). The basal plane of the coordination sphere around each copper(II) ion is formed by the two pyridine nitrogen atoms of 1,3-tpbd, which are *trans* to each other, the tertiary amine nitrogen of 1,3-tpbd and the coordinated arsenate oxygen atom. The apical position is occupied by a perchlorate oxygen atom, and on Cu3 by the oxygen atom of a coordinated water molecule, respectively.

The bond lengths between the three nitrogen atoms N(1), N(2) and N(3) and the copper(II) ion Cu(1) are similar [Cu(1)–N(1) = 2.039(6) Å, Cu(1)–N(2) = 1.990(7) Å and Cu(1)–N(3) = 1.986(7) Å]. Bonds between the copper(II) ions and the arsenate oxygen atom are shorter 1.865(6) Å. The longest bond is found for Cu(1)–O(11) 2.40(2) Å, respectively. Complex **2** represents, to the best of our knowledge, the first example of a μ_4 -AsO₄³⁻ coordination mode in a copper complex.

Only a small number of complexes containing a Cu–O–As bond have been structurally characterized. For example, Doyle et al. described a complex with the ligand bipyridine, in which two copper(II) ions are bridged by two H₂AsO₄⁻ molecules.^[46] Furthermore some polyoxometallates are known that contain this binding mode.^[47–49]

2.2.4 [Cu₄(1,3-tpbd)₂(PO₄)(ClO₄)₃(H₂O)](ClO₄)₂ x 2 H₂O x 0.5 CH₃OH (**3**).

The synthesis of complex **3** was analogous to the synthesis of **2**, with the difference that NaH₂AsO₄ was replaced by NaH₂PO₄. The blue needles obtained were analysed by single crystal X-ray diffraction. The molecular structure of the cation of **3** is isostructural to **2** and is shown in Figure 2-3. Crystallographic parameters are depicted in Table 2-1, selected bond lengths and angles in Table 2-2.

The separation of the copper(II) ions bridged by 1,3-tpbd [Cu(1)···Cu(2) = 4.226 Å] is similar to that found in **2**. However, the separation between the copper(II) ions not bridged by 1,3-tpbd [Cu(1)···Cu(4) = 5.869 Å] is shorter than the distance found in **2**.

The Cu–N_{py}, Cu–N_{amine} and Cu–O bond distances in **3** are all similar in length to the corresponding values found in **2**. Again the coordination sphere of the four copper(II) ions is best described as slightly distorted square pyramidal geometry. The trigonality index parameter $\tau^{[45]}$ ranges from 0.02 on Cu(1) to 0.14 on Cu(3) and Cu(4). The basal plane of the coordination sphere around each copper(II) ion in **3** is formed by the two pyridine nitrogen atoms of 1,3-tpbd, the tertiary amine nitrogen and the phosphate oxygen atom. The apical position is occupied by a perchlorate oxygen atom, and on Cu(3) by the oxygen atom O(31) of a coordinated water molecule respectively.

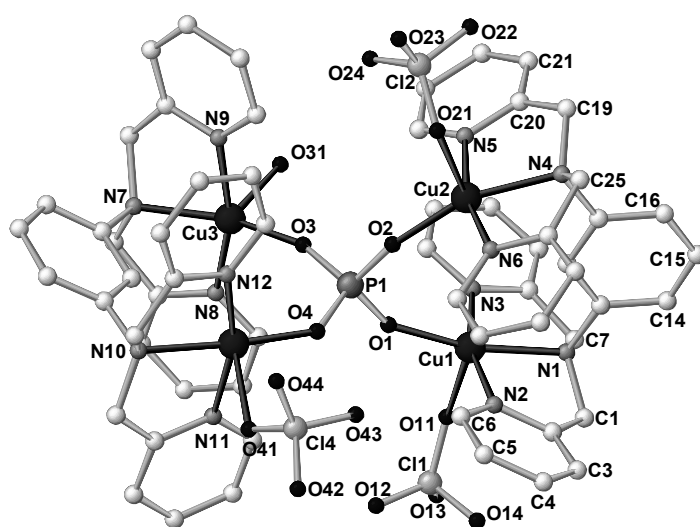


Figure 2-3. Molecular structure of the cation of $[\text{Cu}_4(1,3\text{-tpbd})_2(\text{PO}_4)(\text{ClO}_4)_3(\text{H}_2\text{O})](\text{ClO}_4)_2 \times 2 \text{H}_2\text{O} \times 0.5 \text{CH}_3\text{OH}$ (**3**). Hydrogen atoms and solvent molecules are omitted for clarity.

Dinuclear copper complexes with bridging phosphate ions are well known and have been used in the past to model the active site of purple acid phosphatases.^[50-53] In contrast the μ^4 -binding mode is less known and is usually limited to phosphate groups embedded in polyoxometallates^[54-57] and layered infinite sheets.^[58-60]

Only two other structurally characterized complexes with a discrete $\mu^4\text{-Cu-O}_{\text{Phosphate}}$ coordination mode (as observed for **3**) are reported in the literature.^[61, 62]

Anslyn et. al. developed tripodal ligands with a copper(II) core, which act as a receptor with an extraordinary capacity for binding phosphate and arsenate ions as well as various phosphate esters in neutral aqueous solutions.^[63-66]

2.2.5 $[\text{Cu}_2(1,3\text{-tpbd})((\text{PhO})_2\text{P}(\text{O})_2)_2]_2(\text{ClO}_4)_4$ (**4**).

In regard to the coordination behaviour of the phosphate and arsenate ion in complexes **2** and **3** we thought it could be interesting to investigate the effect of introducing sterically demanding organic groups on the phosphate anion and therefore used diphenylphosphate as a bridging group. By mixing this salt, 1,3-tpbd and $\text{Cu}(\text{ClO}_4)_2 \times 6 \text{H}_2\text{O}$ in a stoichiometric ratio we obtained the complex $[\text{Cu}_2(1,3\text{-tpbd})((\text{PhO})_2\text{P}(\text{O})_2)_2]_2(\text{ClO}_4)_4$ (**4**). The turquoise crystals obtained were analysed by X-ray diffraction studies and demonstrated that a polymer was obtained. The repeating unit together with the copper(II) ions connecting the individual units of **4** is shown in Figure 2-4. The crystallographic parameters are depicted in Table 2-1, selected bond lengths and angles in Table 2-2.

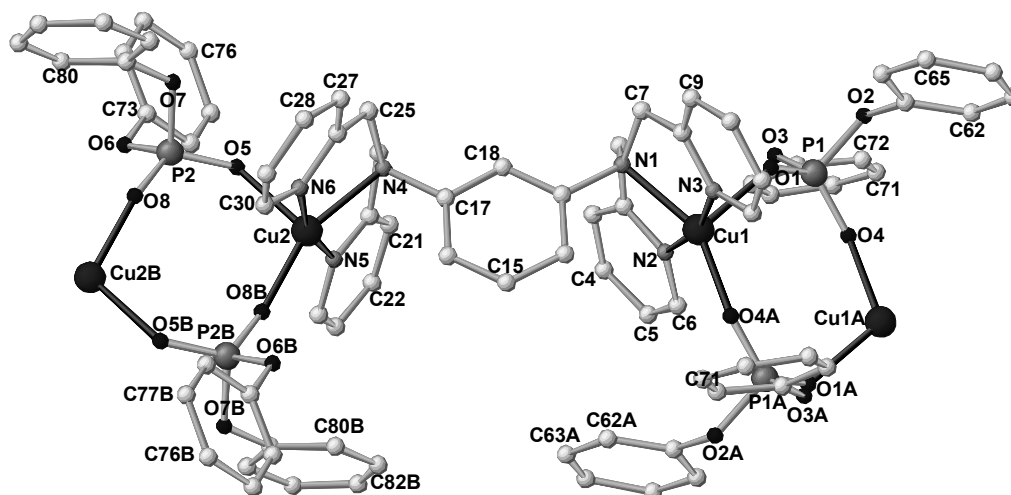


Figure 2-4. Connecting unit of the cation of the polymeric chain of $[\text{Cu}_2(1,3\text{-tpbd})((\text{PhO})_2\text{P}(\text{O})_2)_2]_2(\text{ClO}_4)_4$ (**4**). Hydrogen atoms are omitted for clarity.

In **4**, the coordination environment around both copper(II) ions is best described as “4+1” distorted square pyramidal with a τ value^[45] of 0.285 for Cu(1) and 0.123 for Cu(2). The basal plane around both copper(II) ions consists of the two pyridine nitrogen atoms of 1,3-tpbd the tertiary amine nitrogen atom and one diphenylphosphate oxygen atom. The apical position is occupied by another oxygen atom, which derives from a second diphenyl phosphate molecule. Interestingly, the diphenylphosphate molecules do not act as a bridge between the two adjacent copper(II) ions or form a tetranuclear unit such as **2** or **3**. Instead, they connect to another dinuclear complex unit, resulting in a polymeric complex chain, most likely

due to the consequence of the steric crowding of the phenyl groups. Between the two dinuclear units, an 8-membered ring is formed, which consists of two copper(II) ions, two phosphorous atoms and four oxygen atoms.

Chin et. al. discovered the interesting role that a dinuclear copper(II) complex quite similar to our earlier published $[\text{Cu}_2(2,6\text{-tpcd})(\text{H}_2\text{O})(\text{Cl})](\text{ClO}_4)_2 \times 2 \text{H}_2\text{O}$ ^[41] in the cleavage of phosphate diesters.^[67]

2.2.6 $[\text{Cu}_2(1,3\text{-tpbd})((\text{PhO})\text{PO}_3)_2(\text{H}_2\text{O})_{0.69}(\text{CH}_3\text{CN})_{0.31}]_2(\text{BPh}_4)_4 \times \text{Et}_2\text{O} \times \text{CH}_3\text{CN}$ (**5**).

To release some of the steric strain shown in **4** we used monophenyl phosphate and crystals of $[\text{Cu}_2(1,3\text{-tpbd})((\text{PhO})\text{PO}_3)_2(\text{H}_2\text{O})_{0.69}(\text{CH}_3\text{CN})_{0.31}]_2(\text{BPh}_4)_4 \times \text{Et}_2\text{O} \times \text{CH}_3\text{CN}$ (**5**) thus could be obtained. The molecular structure of the cation of **5** is shown in Figure 2-5. The crystallographic parameters are shown in Table 2-1, selected bond lengths and angles in Table 2-2.

The complex unit of **5** comprises two 1,3-tpbd molecules, each of them coordinating two copper(II) ions, and two monophenyl phosphate molecules. As in **4**, an 8-membered ring with two copper(II) ions, two phosphorous atoms and four oxygen atoms is formed. Moreno et. al. and Phuengphai et. al. both reported a similar structural motif with the ligand 1,10-Phenanthroline where mono-/diphenylphosphate was replaced by dihydrogenphosphate.^[68, 69] The Cu–O distances reported therein are in good accordance to those of **4** and **5**. Complex **5** crystallizes with an inversion centre located in the middle of the Cu–P–O 8-membered ring. The four copper(II) ions are connected via the monophenyl phosphate molecules resulting in a tetranuclear complex which is build by two dinuclear symmetry-related units. Coordination environments around the copper(II) ions in one of the two units in **5** are again “4+1” distorted square-pyramidal. The distortion differs remarkably for Cu(1) and Cu(2). The trigonality index parameter τ ^[45] has a value of 0.263 for Cu(1) and 0.023 for Cu(2). The same parameters apply to the symmetry related Cu(1A) and Cu(2A). The basal plane on Cu(1) is made up by the pyridine nitrogen atoms N(10) and N(20), the tertiary amine nitrogen atom N(1) and the monophenyl phosphate oxygen atom O(11). The apical position is occupied by the monophenyl phosphate oxygen atom O(13), which derives from a second monophenyl phosphate molecule. The coordination mode on Cu(2) is slightly different, the basal plane also comprises two pyridine nitrogen atoms [N(40) and N(50)], the tertiary amine nitrogen atom N(2)

and the monophenylphosphate oxygen atom O(12), whereas the apical position is occupied by a donor atom coming from a solvent molecule being either water (O(2); 69(2)% occupancy) or acetonitrile (N(520); 31(2)% occupancy).

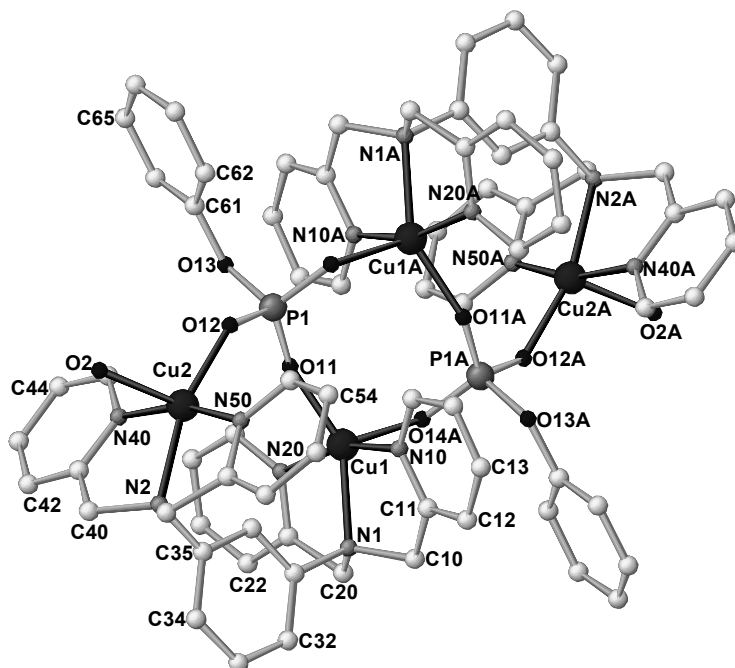


Figure 2-5. Molecular structure of the cation of $[\text{Cu}_2(1,3\text{-tpbd})((\text{PhO})\text{PO}_3)_2(\text{H}_2\text{O})_{0.69}(\text{CH}_3\text{CN})_{0.31}]_2(\text{BPh}_4)_4 \times \text{Et}_2\text{O} \times \text{CH}_3\text{CN}$ (**5**). Hydrogen atoms and solvent molecules are omitted for clarity.

2.3 Magnetic Measurements

Magnetic investigations of the copper complexes turned out to be difficult. As a consequence of the large number of solvent molecules in the new compounds loss of solvent molecules seemed to cause clear changes of the compounds and thus preventing a detailed magnetic analysis (similar problems have been observed previously for the acetate system).^[34] For the nitrate complex **1** we have indication that substitution of perchlorate through nitrate in $[\text{Cu}_2(1,3\text{-tpbd})(\text{H}_2\text{O})_2(\text{ClO}_4)_3](\text{ClO}_4)$ still retains its ferromagnetic coupling, however no solid magnetic data can be reported.

Of all the complexes **1-5** magnetic investigations could only be performed on **3**. The measurements were performed using a Quantum Design MPMS magnetometer. A plot of μ_{eff} versus H , presented in Figure 2-6, shows that at rather high temperatures (10–250 K) the compound behaves paramagnetically. At the lowest temperature of

1.8 K saturation of magnetization is observed with a value close to 4.9 Bohr magnetons at high-field limit.

This corresponds to a total spin of $S = 2$ using a g value of approximately 2. This value of total spin is consistent with 4 copper ions each having $s = \frac{1}{2}$.

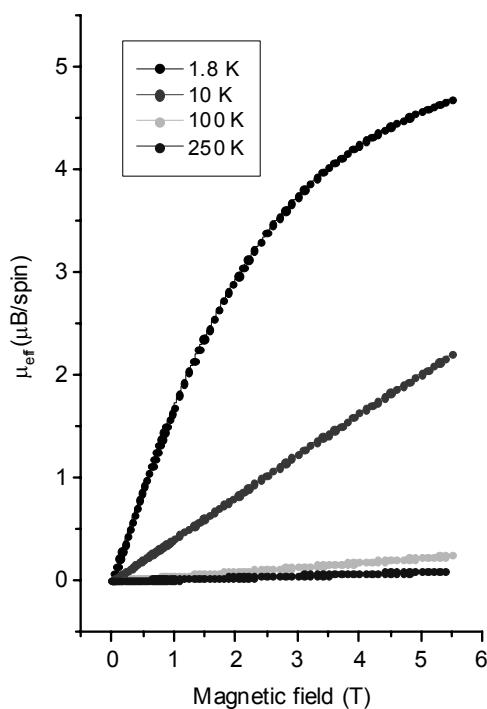


Figure 2-6. μ_{eff} versus H plot for **3**.

Plot $\chi \cdot T$ versus temperature (Figure 2-7), which is basically the plot μ^*T/B , does not show any strong magnetism.

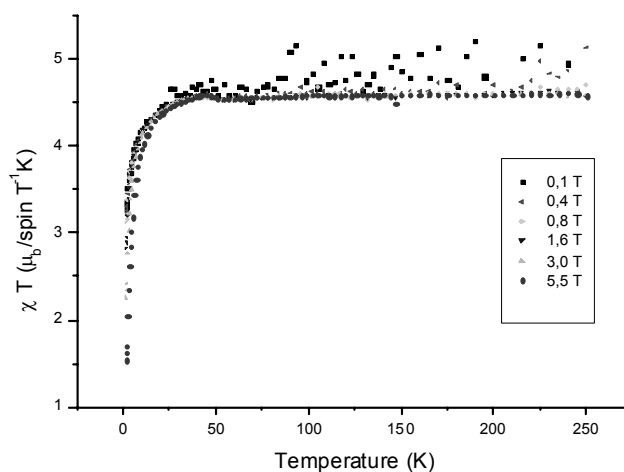


Figure 2-7. Thermal variation of $\chi \cdot T$ for **3**.

The plot $1/\chi$ versus temperature (Figure 2-8) is presented to confirm the paramagnetic behaviour of the compound. Indeed, it shows clearly Curie-like paramagnetism.

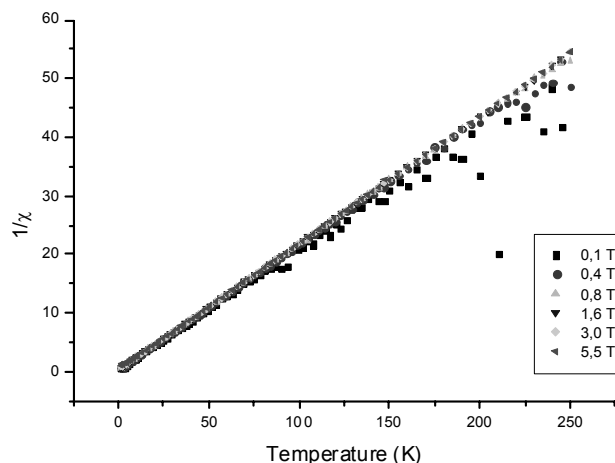


Figure 2-8. Thermal variation of $1/\chi$ for **3**.

2.4 Conclusion

The new copper(II) complexes **1-5** of the ligand 1,3-tpbd contain interesting structural properties; they show rare coordination modes of copper(II) ions with the arsenate ion in **2** or with phosphate anions in **3**. Furthermore complexes **4** and **5** show the interesting formation of an 8-membered ring between two copper(II) ions and two phosphate molecules. The magnetic measurements performed for **3** showed paramagnetic behaviour, which is expected for a complex with four copper(II) ions each having $s = \frac{1}{2}$.

2.5 Experimental Section

2.5.1 General Remarks.

All chemicals were obtained from commercial sources and used without further purification.

Caution! The syntheses and procedures described below involve compounds that contain perchlorate ions, which can detonate explosively and without warning.

Although we have not encountered any problems with the compounds used in this study, they should be handled with extreme caution.

2.5.2 Ligand synthesis.

The ligand 1,3-tpbd was prepared according to a literature procedure.^[26]

2.5.3 Complex Syntheses.

[Cu₄(1,3-tpbd)₂(H₂O)₄(NO₃)₄](NO₃)₄ × 13 H₂O (1). 1,3-tpbd (328.8 mg, 0.680 mmol) dissolved in methanol (15 mL) was added to an aqueous solution (10 mL) of Cu(NO₃)₂ × H₂O (279.5 mg; 1.360 mmol). The reaction mixture was stirred for 5 min during which time the solution turned to a dark green colour. After two days single crystals of **1** were obtained. UV/Vis (MeOH) λ_{max} = 383 nm (ε = 2762.9 M⁻¹cm⁻¹), 684 nm (ε = 604.7 M⁻¹cm⁻¹).

[Cu₄(1,3-tpbd)₂(AsO₄)(ClO₄)₃(H₂O)](ClO₄)₂ × 2 H₂O × 0.5 CH₃OH (2). / **[Cu₄(1,3-tpbd)₂(PO₄)(ClO₄)₃(H₂O)](ClO₄)₂ × 2 H₂O × 0.5 CH₃OH (3).** / **[Cu₂(1,3-tpbd)((PhO)₂P(O)₂)₂]₂(ClO₄)₄ (4).** Ligand 1,3-tpbd (100 mg; 0.21 mmol) dissolved in methanol (15 mL) was added to aqueous solutions (5 mL) of Cu(ClO₄)₂ × 6 H₂O (155 mg; 0.42 mmol) and Na₂HAsO₄ (65.5 mg; 0.21 mmol) for **2**, Cu(ClO₄)₂ × 6 H₂O (155 mg; 0.42 mmol) and Na₂HPO₄ (56.3 mg; 0.21 mmol) for **3**, and Cu(ClO₄)₂ × 6 H₂O (155 mg; 0.42 mmol) and diphenyl phosphate (52.5 mg; 0.21 mmol) for **4**. The green coloured reaction solutions were each stirred for 5 min. After two days crystals suitable for X-ray diffraction formed. Intensive blue coloured crystals of **2**; UV/Vis (MeOH) λ_{max} = 380 nm (shoulder, ε = 859 M⁻¹cm⁻¹), 713 nm (ε = 471 M⁻¹cm⁻¹). **3** UV/Vis (MeOH) λ_{max} = 706 nm (ε = 550.5 M⁻¹cm⁻¹), and light blue coloured crystals of **4**.

[Cu₂(1,3-tpbd)((PhO)PO₃)₂(H₂O)_{0.69}(CH₃CN)_{0.31}]₂(BPh₄)₄ × Et₂O × CH₃CN (5). To a mixture of 1,3-tpbd (50.0 mg; 0.105 mmol) and NaBPh₄ dissolved in methanol the aqueous solutions (5 mL) of Cu(ClO₄)₂ × 6 H₂O (78.4 mg; 0.210 mmol) and the sodium salt of phenyl phosphate (27.0 mg; 0.105 mmol) were added. The turquoise precipitate was filtered and dissolved in CH₃CN. Crystals suitable for X-ray diffraction analyses were obtained by slow diffusion of diethyl ether into the solution.

2.5.4 Magnetic Measurements.

Magnetic susceptibility data for **3** was collected in the temperature range of 1.8–300 K on a Quantum Design MPMS-7 SQUID magnetometer. Two samples of each compound were investigated.

The powder sample (15.32 mg) was mixed with apiezon grease and fixed on a plastic straw. The signal of the grease could be subtracted from the experimental measurements, whereas the signal due to the straw was negligible.

2.5.5 X-ray Crystallographic Studies.

Intensity data of **1–4** were collected on a Siemens SMART CCD 1000 diffractometer by the ω -scan technique collecting a full sphere of data with irradiation times of 10 to 20 s per frame and $\Delta\omega$ ranges between 0.3° and 0.45° . The collected reflections were corrected for absorption, Lorentz and polarization effects^[70] All structures were solved by direct methods and refined by least-squares techniques using the SHELX-97 programme package^[71]. The hydrogen atoms were positioned geometrically and all non-hydrogen atoms were refined anisotropically, if not mentioned otherwise. Further data collection parameters are summarised in Table 1.

Intensity data of **5** were collected on a Bruker-Nonius Kappa CCD diffractometer. Absorption effects were corrected by semi-empirical methods based on equivalent reflexes.^[70] The structure was solved by direct methods; full-matrix least-squares refinement was carried out on F^2 using SHELXTL NT 6.12.^[72] All non-hydrogen atoms were refined anisotropically. Hydrogen atoms were geometrically positioned, their isotropic displacement parameters were tied to those of their corresponding carrier atoms by a factor of 1.2 or 1.5. Both of the BPh_4^- anions show disordered phenyl groups. SIMU and SAME restraints were applied in the refinement of these anions. The co-ligand at Cu(2) is disordered. The sixth coordination site is either occupied by an aqua ligand (O(2), 69(2)%) for which no hydrogens have been included in the structure model or by an acetonitril (N(520) – C(522), 31(2)%). A disordered Et_2O molecule (O(500) – C(504)) is partially present when the aqua ligand is coordinated to Cu(2). SIMU, SADI, SAME and ISOR restraints were applied in the treatment of this disordered part of the structure.

CCDC 661254 (**1**), CCDC 661255(**2**), CCDC 661256(**3**), CCDC 661257(**4**) and CCDC 658344 (**5**) contain the supplementary crystallographic data for this paper. These data can be obtained free of charge at www.ccdc.cam.ac.uk/conts/retrieving.html [or from the Cambridge Crystallographic Data Center, 12, Union Road, Cambridge CB2 1EZ, UK; Fax: (internat.) +44-1223-336-033; E-mail: deposit@ccdc.cam.ac.uk].

Table 2-1. Crystallographic data and experimental details for **1-5**.

Compound	1	2	3	4	5
Empirical formula	C ₃₀ H ₄₅ Cu ₂ N ₁₀ O _{19.5}	C _{60.5} H ₆₄ AsCl ₅ Cu ₄ N ₁₂ O _{27.5}	C _{60.5} H ₆₄ Cl ₅ Cu ₄ N ₁₂ O _{27.5} P	C ₁₀₈ H ₁₀₄ Cl ₄ Cu ₄ N ₁₂ O ₃₂ P ₄	C _{177.25} H _{166.63} B ₄ Cu ₄ N _{14.63} O _{10.38} P
<i>M_r</i>	984.84	1905.57	1861.62	2601.87	3026.97
Temperature [K]	200(2)	200(2)	200(2)	200(2)	100(2)
Radiation (λ [Å])	Mo-K _α , 0.71073	Mo-K _α , 0.71073	Mo-K _α , 0.71073	Mo-K _α , 0.71073	Mo-K _α , 0.71073
Crystal shape	green block	blue prism	blue block	green prism	green rhomboid
Crystal size [mm]	0.4 × 0.4 × 0.4	0.3 × 0.2 × 0.045	0.4 × 0.3 × 0.3	0.33 × 0.25 × 0.04	0.24 × 0.18 × 0.08
Crystal system	Monoclinic	monoclinic	monoclinic	Triclinic	monoclinic
Space group	<i>C2/c</i> (No. 15)	<i>P2₁/c</i> (No. 14)	<i>P2₁/c</i> (No. 14)	<i>P</i> -1 (No. 2)	<i>P2₁/n</i> (No. 14)
<i>a</i> [Å]	36.691(2)	18.662(2)	18.566(2)	16.312(2)	15.664(2)
<i>b</i> [Å]	8.9054(6)	19.355(2)	19.326(2)	18.040(2)	27.742(3)
<i>c</i> [Å]	24.997(2)	22.504(2)	22.596(2)	22.835(3)	17.767(1)
α [°]	90.0	90.0	90.0	105.968(2)	90.0
β [°]	96.667(1)	109.639(1)	109.328(1)	103.670(2)	94.20(1)
γ [°]	90.0	90.0	90.0	105.645(2)	90.0
<i>V</i> [Å ³]	8112.7(9)	7655.9(8)	7650(1)	5080(1)	7700(2)
<i>Z</i>	8	4	4	2	2
ρ _{calcd.} [g·cm ⁻³]	1.613	1.653	1.616	1.474	1.306
μ [mm ⁻¹]	1.140	1.787	1.379	0.944	0.632
<i>F</i> (000)	4072	3860	3788	2672	3163
Scan range θ [°]	1.64 to 28.29	1.42 to 28.32	1.42 to 28.32	1.29 to 28.34	3.35 to 25.68
Index ranges	-48 ≤ <i>h</i> ≤ 48	-24 ≤ <i>h</i> ≤ 24	-24 ≤ <i>h</i> ≤ 24	-21 ≤ <i>h</i> ≤ 21	-19 ≤ <i>h</i> ≤ 19
	-11 ≤ <i>k</i> ≤ 11	-25 ≤ <i>k</i> ≤ 25	-25 ≤ <i>k</i> ≤ 25	-24 ≤ <i>k</i> ≤ 23	-33 ≤ <i>k</i> ≤ 33
	-33 ≤ <i>l</i> ≤ 32	-29 ≤ <i>l</i> ≤ 29	-30 ≤ <i>l</i> ≤ 29	-30 ≤ <i>l</i> ≤ 30	-21 ≤ <i>l</i> ≤ 21
Reflections collected	46831	92298	90912	59537	69542
Unique reflections	9915	18858	18761	27966	14426
<i>R</i> _{int}	0.0437	0.1445	0.1039	0.2432	0.1062
Data/restraints/parameters	9915/36/572	18858/43/1056	18761/56/1047	27966/28/1492	14426/1950/1331
Goodness-of-fit on <i>F</i> ²	1.059	1.019	1.018	0.928	1.006
Final <i>R</i> indices [<i>I</i> > 2σ(<i>I</i>)]	<i>R</i> 1 = 0.0665	<i>R</i> 1 = 0.0776	<i>R</i> 1 = 0.0761	<i>R</i> 1 = 0.1021	<i>R</i> 1 = 0.0648
	<i>wR</i> 2 = 0.1927	<i>wR</i> 2 = 0.2133	<i>wR</i> 2 = 0.2150	<i>wR</i> 2 = 0.1957	<i>wR</i> 2 = 0.1225
<i>R</i> indices (all data)	<i>R</i> 1 = 0.0924	<i>R</i> 1 = 0.1967	<i>R</i> 1 = 0.1667	<i>R</i> 1 = 0.3480	<i>R</i> 1 = 0.1495
	<i>wR</i> 2 = 0.2100	<i>wR</i> 2 = 0.2585	<i>wR</i> 2 = 0.2586	<i>wR</i> 2 = 0.2940	<i>wR</i> 2 = 0.1478
Largest diff. peak/hole [e·Å ⁻³]	2.087/-0.950	1.496/-1.320	1.556/-2.091	1.639/-0.830	0.653/-0.405

Table 2-2. Selected bond lengths [Å] and angles [°] for **1-5**.

Atoms	1	Atoms	2	3	Atoms	4	Atoms	5
Cu(1)–O(1)	1.972(3)	Cu(1)–O(1)	1.865(6)	1.874(4)	Cu(1)–O(4)	1.964(7)	Cu(1)–O(11)	1.941 (3)
Cu(1)–N(2)	1.972(3)	Cu(1)–N(3)	1.986(7)	1.988(6)	Cu(1)–N(3)	1.970(9)	Cu(1)–N(10)	2.026 (3)
Cu(1)–N(3)	1.986(3)	Cu(1)–N(2)	1.990(7)	1.989(5)	Cu(1)–N(2)	1.971(9)	Cu(1)–N(20)	2.002 (3)
Cu(1)–N(1)	2.091(3)	Cu(1)–N(1)	2.039(6)	2.061(5)	Cu(1)–N(1)	2.072(9)	Cu(1)–N(1)	2.086 (3)
Cu(1)–O(3)	2.313(3)	Cu(1)–O(11)	2.40(2)	2.36(2)	Cu(1)–O(1)	2.168(7)	Cu(1)–O(14A)	2.115 (3)
Cu(1)–O(7)	2.729(3)	Cu(2)–O(2)	1.877(6)	1.884(5)	Cu(2)–O(8)	1.958(7)	Cu(2)–O(12)	1.935 (3)
Cu(2)–N(5)	1.966(4)	Cu(2)–N(5)	1.978(8)	1.990(8)	Cu(2)–N(6)	1.967(9)	Cu(2)–N(50)	1.991 (4)
Cu(2)–N(6)	1.974(4)	Cu(2)–N(6)	2.003(8)	1.988(7)	Cu(2)–N(5)	1.980(9)	Cu(2)–N(40)	1.992 (3)
Cu(2)–O(2)	1.979(4)	Cu(2)–N(4)	2.055(7)	2.066(6)	Cu(2)–N(4)	2.057(8)	Cu(2)–N(2)	2.081 (3)
Cu(2)–N(4)	2.097(3)	Cu(2)–O(21)	2.383(8)	2.410(8)	Cu(2)–O(5)	2.152(7)	Cu(2)–O(2)	2.221 (7)
Cu(2)–O(4)	2.313(3)	Cu(3)–O(3)	1.906(6)	1.885(5)				
Cu(2)–O(8B)	2.792(4)	Cu(3)–N(8)	1.999(7)	1.994(6)				
		Cu(3)–N(9)	2.016(8)	2.011(6)				
		Cu(3)–N(7)	2.050(7)	2.057(5)				
		Cu(3)–O(31)	2.268(6)	2.269(5)				
		Cu(4)–O(4)	1.888(6)	1.871(5)				
		Cu(4)–N(12)	1.994(8)	1.999(6)				
		Cu(4)–N(11)	2.012(8)	2.014(6)				
		Cu(4)–N(10)	2.069(7)	2.051(6)				
		Cu(4)–O(41)	2.396(6)	2.424(5)				
N(2)–Cu(1)–O(1)	94.97(2)	O(1)–Cu(1)–N(3)	94.6(3)	95.7 (2)	O(4)–Cu(1)–N(3)	95.4(3)	O(11)–Cu(1)–N(20)	91.0 (2)
N(2)–Cu(1)–N(3)	161.13(2)	O(1)–Cu(1)–N(2)	100.7(3)	99.1 (2)	O(4)–Cu(1)–N(2)	97.2(3)	O(11)–Cu(1)–N(10)	100.9 (2)
O(1)–Cu(1)–N(3)	96.41(2)	N(3)–Cu(1)–N(2)	163.7(3)	164.0 (2)	N(3)–Cu(1)–N(2)	165.3(4)	N(20)–Cu(1)–N(10)	161.2 (2)
N(2)–Cu(1)–N(1)	83.58(2)	O(1)–Cu(1)–N(1)	168.7(3)	165.7 (2)	O(4)–Cu(1)–N(1)	148.2(3)	O(11)–Cu(1)–N(1)	145.6 (2)
O(1)–Cu(1)–N(1)	174.09(2)	N(3)–Cu(1)–N(1)	82.0(3)	82.6 (2)	N(3)–Cu(1)–N(1)	82.7(4)	N(20)–Cu(1)–N(1)	80.9 (2)
N(3)–Cu(1)–N(1)	83.57(2)	N(2)–Cu(1)–N(1)	81.9(3)	81.6 (2)	N(2)–Cu(1)–N(1)	82.6(4)	N(10)–Cu(1)–N(1)	81.1 (2)
N(2)–Cu(1)–O(3)	106.59(2)	O(1)–Cu(1)–O(11X)	103.6(6)	106.2 (4)	O(4)–Cu(1)–O(1)	113.8(3)	O(11)–Cu(1)–O(14A)	108.8 (2)
O(1)–Cu(1)–O(3)	87.33(2)	N(3)–Cu(1)–O(11X)	94.3(7)	99.5 (4)	N(3)–Cu(1)–O(1)	91.9(3)	N(20)–Cu(1)–O(14A)	94.6 (2)
N(3)–Cu(1)–O(3)	88.95(2)	N(2)–Cu(1)–O(11X)	87.9(6)	82.2 (4)	N(2)–Cu(1)–O(1)	90.0(3)	N(10)–Cu(1)–O(14A)	95.2 (2)
N(1)–Cu(1)–O(3)	98.57(2)	N(1)–Cu(1)–O(11X)	87.5(6)	88.2 (4)	N(1)–Cu(1)–O(1)	98.0(3)	N(1)–Cu(1)–O(14A)	105.2 (2)
N(5)–Cu(2)–N(6)	160.58(2)	O(1)–Cu(1)–O(11)	96.0(6)	101.4 (4)	O(8)–Cu(2)–N(6)	99.7(3)	P(1)–O(11)–Cu(1)	150.4 (2)
N(5)–Cu(2)–O(2)	94.91(2)	N(3)–Cu(1)–O(11)	78.9(6)	78.3 (3)	O(8)–Cu(2)–N(5)	93.6(3)	P(1)–O(14)–Cu(1A)	125.1 (2)
N(6)–Cu(2)–O(2)	96.24(2)	N(2)–Cu(1)–O(11)	105.1(4)	104.4 (4)	N(6)–Cu(2)–N(5)	165.2(4)	O(12)–Cu(2)–N(50)	93.0 (2)
N(5)–Cu(2)–N(4)	83.39(2)	N(1)–Cu(1)–O(11)	94.0(6)	92.2 (4)	O(8)–Cu(2)–N(4)	157.8(3)	O(12)–Cu(2)–N(40)	102.3 (2)
N(6)–Cu(2)–N(4)	83.94(2)	O(11X)–Cu(1)–O(11)	17.7(6)	22.2 (3)	N(6)–Cu(2)–N(4)	83.3(4)	N(50)–Cu(2)–N(40)	164.1 (2)
O(2)–Cu(2)–N(4)	174.26(2)	O(2)–Cu(2)–N(5)	102.1(3)	99.6 (3)	N(5)–Cu(2)–N(4)	82.0(4)	O(12)–Cu(2)–N(2)	162.7 (2)
N(5)–Cu(2)–O(4)	106.66(2)	O(2)–Cu(2)–N(6)	92.7(3)	95.5 (3)	O(8)–Cu(2)–O(5)	106.6(3)	N(50)–Cu(2)–N(2)	81.6 (2)
N(6)–Cu(2)–O(4)	89.46(2)	N(5)–Cu(2)–N(6)	164.9(3)	164.7 (3)	N(6)–Cu(2)–O(5)	92.4(3)	N(40)–Cu(2)–N(2)	82.5 (2)
O(2)–Cu(2)–O(4)	88.65(2)	O(2)–Cu(2)–N(4)	159.0(3)	158.6 (3)	N(5)–Cu(2)–O(5)	89.8(3)	O(12)–Cu(2)–O(2)	105.4 (2)
N(4)–Cu(2)–O(4)	97.09(2)	N(5)–Cu(2)–N(4)	82.8(3)	82.4 (3)	N(4)–Cu(2)–O(5)	95.2(3)	N(50)–Cu(2)–O(2)	89.0 (3)
		N(6)–Cu(2)–N(4)	82.3(3)	82.6 (3)			N(40)–Cu(2)–O(2)	91.3 (3)
		O(2)–Cu(2)–O(21)	102.9(3)	104.9 (3)			N(2)–Cu(2)–O(2)	91.0 (2)
		N(5)–Cu(2)–O(21)	95.8(3)	101.3 (3)			P(1)–O(12)–Cu(2)	132.9 (2)

Chapter 2

N(6)–Cu(2)–O(21)	83.4(3)	77.0 (3)
N(4)–Cu(2)–O(21)	96.9(3)	95.5 (3)
O(3)–Cu(3)–N(8)	104.4(3)	101.3 (3)
O(3)–Cu(3)–N(9)	91.8(3)	95.0 (2)
N(8)–(3)–N(9)	163.3(3)	163.2 (3)
O(3)–Cu(3)–N(7)	156.0(3)	154.8 (2)
N(8)–Cu(3)–N(7)	82.8(3)	82.6 (3)
N(9)–Cu(3)–N(7)	80.8(3)	80.9(3)
O(3)–Cu(3)–O(31)	94.4(3)	97.5(2)
N(8)–Cu(3)–O(31)	91.9(3)	91.2(2)
N(9)–Cu(3)–O(31)	90.5(3)	90.6(2)
N(7)–Cu(3)–O(31)	108.4(3)	107.3(2)
O(4)–Cu(4)–N(12)	101.7(3)	100.3(3)
O(4)–Cu(4)–N(11)	94.3(3)	96.4(3)
N(12)–Cu(4)–N(11)	163.8(3)	163.1(3)
O(4)–Cu(4)–N(10)	171.5(3)	171.6(2)
N(12)–Cu(4)–N(10)	81.6(3)	81.1(2)
N(11)–Cu(4)–N(10)	82.2(3)	82.0(3)
O(4)–Cu(4)–O(41)	96.7 (2)	101.0(2)
N(12)–Cu(4)–O(41)	96.4(3)	96.1(2)
N(11)–Cu(4)–O(41)	84.6(2)	82.8(2)
N(10)–Cu(4)–O(41)	90.7(2)	87.0(2)

Chapter 3 - Syntheses, structures and properties of copper(II) complexes of bis(2-pyridylmethyl) derivatives of o-, m-, and p-phenylenediamine and aniline.

This work has been submitted for publication to *Inorganic Chemistry*.

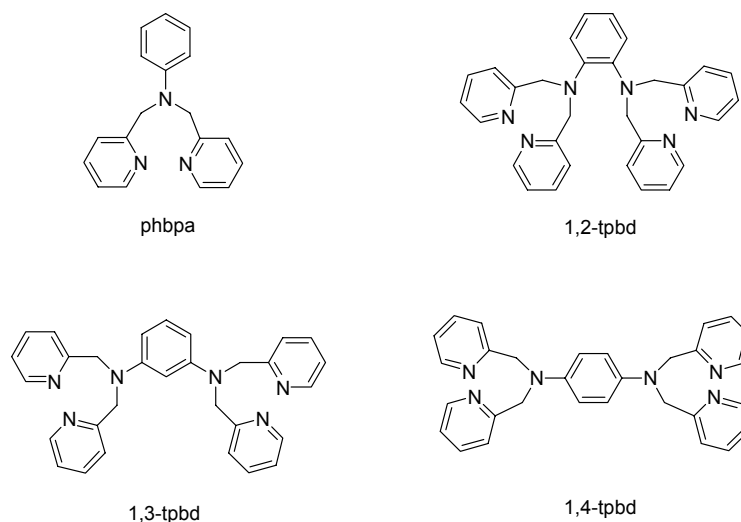
Sabrina Turba, Olaf Walter, Siegfried Schindler, Lars Preuss Nielsen, Alan Hazell, Rita Hazell, Christine Mc Kenzie, Francese Lloret, Joan Cano and Miguel Julve.

3.1 Introduction

The parallel spin alignment (ferromagnetic coupling) in magnetic systems is not an easy task and two main strategies are used to achieve it. These are based either on the orbital symmetry or on the spin polarization mechanism.^[30, 38, 73-75] The first one requires the strict or accidental orthogonality between the interacting magnetic orbitals and it has been illustrated by a good number of magneto-structural studies on heterobimetallic species^[30, 76] and meta-radical systems.^[32] However, the second one has received less attention in the context of the metal complexes^[33, 35, 77-82] when looking at the extensive work dealing with the high-spin organic polyradicals.^[83-85]

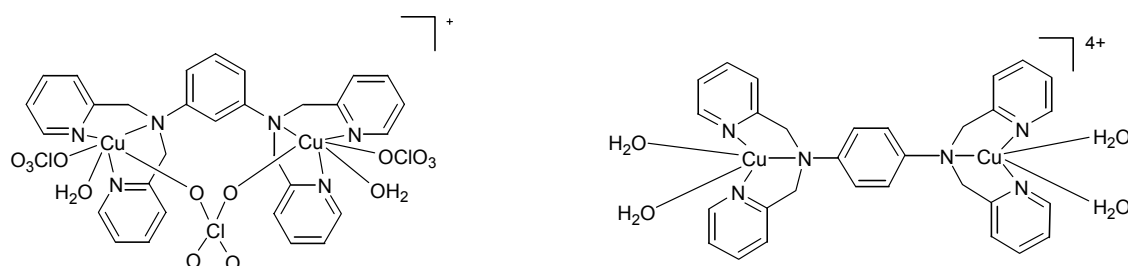
The series of ligands, 1,*n*-bis[bis(2-pyridylmethyl)amino]benzene with *n* = 2-4 [see Scheme 3-1] appear to offer an opportunity for testing the spin polarization mechanism for the magnetic exchange coupling in coordination compounds. At this respect, in previous works we have found that significant intramolecular magnetic interactions occur in the dicopper(II) complexes [Cu₂(ClO₄)₃(OH₂)₂(1,3-tpbd)]ClO₄ (**a**) (*J* = +9.3 cm⁻¹)^[34] and [Cu₂(OH₂)₄(1,4-tpbd)](S₂O₆)₂ (**b**) (*J* = -15.6 cm⁻¹)^[86] [see Scheme 3-2], the values of the intramolecular Cu...Cu distances being 5.873(1) and 8.259(4) Å, respectively.

The ferromagnetic coupling in **a**, was successfully interpreted using density functional theory (DFT) calculations^[34] and this finding is in good agreement with the properties of a related *N,N'*-1,3-phenylenebis(oxamate) dicopper(II) complex which also showed ferromagnetic coupling.^[33] As illustrated by Scheme 3-2, the coordination spheres of the copper atoms in **a** and **b** are not identical because a O,O'-perchlorate bridging group is present in **a** in addition to the phenylenediamine unit.



Scheme 3-1. The ligands: phbpa and 1,*n*-tpbd (*n* = 2-4).

However, no exchange pathway was associated to this perchlorate group in **a** in contrast to what occurs with other auxiliary bridges between the copper atoms in other dicopper(II) complexes of 1,3-tpbd where they are found to be significant in the provision and attenuation of magnetic exchange pathways.^[34, 39]



Scheme 3-2. The dicopper(II) units in **a** (left) and **b** (right).

In order to better elucidate whether or not the magnetic behaviour of the dicopper(II) complexes of the geometrical isomers of tpbd follows the spin polarisation mechanism, we prepared several dinuclear copper(II) species with the ligands 1,3- and 1,4-tpbd. In principle, these complexes would contain copper(II) ions with chemically identical coordination spheres. Furthermore we would prepare the unknown geometrically isomeric 1,2-tpbd ligand and its corresponding dicopper(II) compound. This latter species is expected to exhibit an antiferromagnetic interaction between the copper(II) centres as for the corresponding complex with the 1,4-tpbd ligand. Thus the target dinuclear systems should have the formulation [Cu₂(1,*n*-tpbd)L_x] with *n* = 2 - 4 and L being a terminal monodentate or a chelating ligand which does not furnish a secondary bridging group. We focused on the use of terminal water or chloride ligands, given that some of these systems with 1,3- and

1,4-tpbd were available to us although the series was incomplete. For example, the already known $[\text{Cu}_2(\text{OH}_2)_4(1,4\text{-tpbd})]^{4+}$ seemed an appropriate prototype. Copper(II) complexes of the monotopic ligand, *N,N*-Bis(2-pyridylmethyl)aniline, phbpa such as $[\text{CuCl}_2(\text{phbpa})]$ (**6**)^[87-90] were useful for geometric, spectroscopic and magnetic comparisons. In the present work, we report on the syntheses, structural and magnetic characterisation of mono- and dinuclear copper(II) complexes of 1,*n*-tpbd (*n* = 2-4) and phbpa.

3.2 Results and Discussion

3.2.1 Ligand Syntheses.

The ligand phbpa was synthesized without any problems according to a previously published procedure.^[87] For the reaction of 2-(chloromethyl)pyridine with *meta*- and *para*-phenylenediamine we have now optimized the syntheses in order to favour the formation and isolation of the tetrasubstituted 1,3-tpbd and 1,4-tpbd ligands.

All our attempts to prepare 1,2-tpbd by using reaction conditions similar to those used for the related 1,3-tpbd and 1,4-tpbd derivatives did not provide us with a pure sample of the tetrasubstituted *ortho* compound. It was always contaminated by the trisubstituted derivative, *N,N,N'*-tri(2-pyridylmethyl)benzene-1,3-diamine. The reactions were carried out under inert conditions with careful control of the pH in a variety of solvents. In general, the reaction mixtures became dark red more rapidly than for the corresponding 1,3-tpbd and 1,4-tpbd derivatives. This colour is probably an indication of the presence of oxidized by-products formed by radical formation in the *o*-phenylenediamine unit and consequent side reactions similar to those described above for 1,4-tpbd. Notably, although Sato *et al.* also attempted the preparation of 1,2-tpbd, they succeeded in the isolation of only its trisubstituted derivative.^[91] These authors suggested that the tetrasubstituted derivative is not formed for steric reasons. Our results at least contrast to this in that we were able to prepare a mixture containing both the tri- and the tetra-substituted products. However, we failed to separate them satisfactorily in a pure form using the usual chromatographic techniques. In one preparation, 1,2-tpbd was successfully separated from the mixture *via* the isolation of the copper(II) complex $[\text{Cu}(1,2\text{-tpbd})](\text{PF}_6)_2$ (**7**) whose molecular structure is described below.

Copper(II) complexes. Copper(II) complexes of all four ligands were isolated and characterized. Here described are $[\text{CuCl}_2(\text{phbpa})]$ (**6**), $[\text{Cu}(1,2\text{-tpbd})](\text{PF}_6)_2$ (**7**), $[\text{Cu}_2\text{Cl}_4(1,3\text{-tpbd})] \times 0.84 \text{ CH}_3\text{OH}$ (**8**), $\{[\text{Cu}_2\text{Cl}_2(\text{ClO}_4)(1,3\text{-tpbd})]\text{Cl}\}[\text{Cu}_2\text{Cl}_2(\text{OH}_2)(1,3\text{-tpbd})](\text{ClO}_4)_2$ (**9**), $[\text{Cu}_2(\text{OH}_2)_2(\text{S}_2\text{O}_6)(1,3\text{-tpbd})]\text{S}_2\text{O}_6 \times 2 \text{ H}_2\text{O} \times \text{CH}_3\text{OH}$ (**10**) and $[\text{Cu}_2\text{Cl}_4(1,4\text{-tpbd})]$ (**11**). Compounds **6**, **8** and **11** are lime green coloured while the complexes which include either water ligands, or a combination of water and anion-oxygen atoms in the copper environment are dark green.

3.2.2 $[\text{CuCl}_2(\text{phbpa})]$ (**6**).

The crystal structure of **6** has been described previously,^[90] however, due to the fact that different complexes can form when copper(II) salts are reacted with phbpa^[89, 90] we performed the reaction of phbpa with CuCl_2 under our conditions and crystallographically characterized the product. Its molecular structure is shown in Figure 3-1 and selected bond lengths and angles are listed in Table 3-2. The copper environment in **6** is intermediate between square pyramidal and trigonal bipyramidal, the value of the trigonality parameter^[45] being $\tau = 0.559$ [$\tau = (\beta - \alpha)/60$, where α and β are the two largest coordination angles around the five-coordinated copper atom; for ideal square-pyramidal geometry $\tau = 0$, while for perfect trigonal-bipyramidal geometry $\tau = 1$]. The three nitrogen atoms of the phbpa ligand and the copper atom are almost coplanar, with Cu-N_{py} bond distances are 1.988(2) and 1.997(2) Å and $\text{Cu-N}_{\text{amine}} = 2.216(2)\text{Å}$. They are all shorter than the Cu-Cl bond lengths [2.276(1) and 2.368(2) Å].

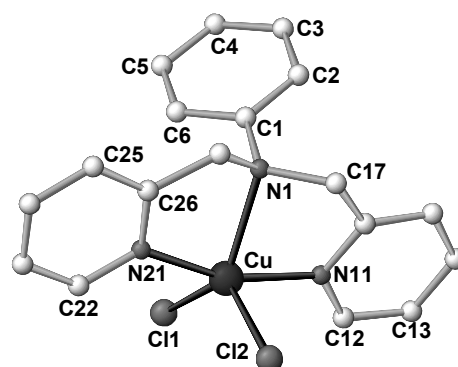


Figure 3-1. Molecular structure of $[\text{CuCl}_2(\text{phbpa})]$ (**6**). Hydrogen atoms are omitted for clarity.

A closer inspection of the intermolecular interactions in **6** shows the presence of off-set π - π type interactions between adjacent pyridyl rings along the crystallographic *a*

axis (shortest interplanar carbon-carbon distance of ca. 3.350 Å) leading to a chain of weakly interacting mononuclear copper(II) units (see Figure 3-2).

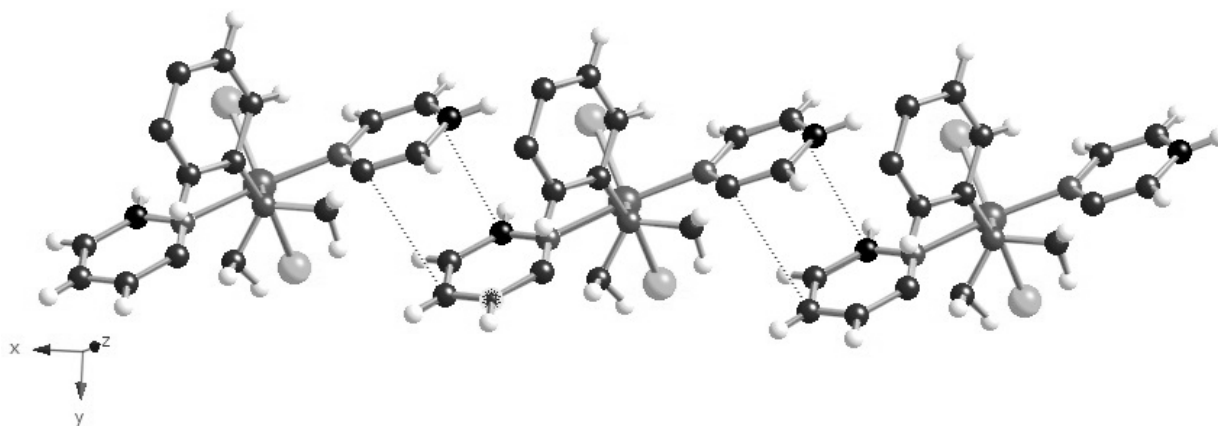


Figure 3-2. A view of the chain formation in **6** through π - π type interactions (dotted lines) along the *a* axis.

3.2.3 [Cu(1,2-tpbd)](PF₆)₂ (**7**).

Not unexpectedly a mononuclear, rather than a dinuclear, copper(II) complex was obtained with the *ortho*-substituted ligand, 1,2-tpbd. However, the addition of different copper(II) salts to mixtures of 1,2-tpbd and its trisubstituted derivative (see the Experimental Section) led to the isolation of several products. Only very few crystals were obtained in one batch and fortunately they were suitable for X-ray diffraction.

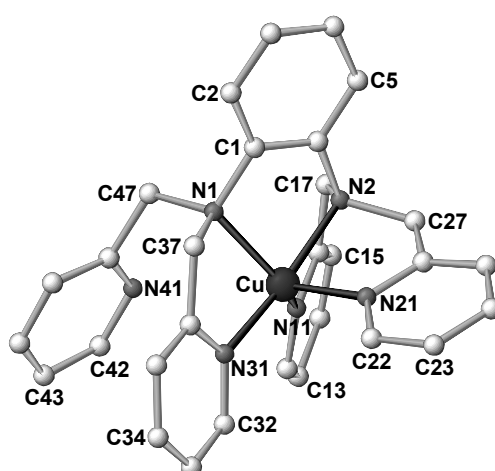


Figure 3-3. Molecular structure of the cation of [Cu(1,2-tpbd)](PF₆)₂ (**7**). Hydrogen atoms are omitted for clarity.

The molecular structure of **7** is shown in Figure 3-3. The structure contains two crystallographically independent copper atoms [Cu(1) and Cu(2)], the corresponding [Cu(1,2-tpbd)]²⁺ mononuclear cations being very similar. Their positive charge is neutralized by PF₆⁻ anions. Selected bond lengths and angles are listed in Table 3-2.

The coordination at the copper atoms is close to trigonal bipyramidal with N(2) and N(31) defining the ternary axis. The value of the trigonality parameter τ is 0.728. The copper atoms are bonded to three pyridine-nitrogen atoms and two amine nitrogen atoms leaving one pendant methylpyridine group which is uncoordinated. Cu-N_{py} distances are in the range 1.970(3) to 2.102(3) Å, Cu-N_{amine} distances vary between 2.013(2) and 2.091(2) Å.

3.2.4 [Cu₂Cl₄(1,3-tpbd)] x 0.84 CH₃OH (**8**).

The reaction of 1,3-tpbd with the stoichiometric amount of CuCl₂ x 2 H₂O in a water/methanol mixture afforded X-ray quality crystals of **8** as a methanol solvate. The structure of this compound, which is depicted in Figure 3-4, consists of discrete [Cu₂Cl₄(1,3-tpbd)] units and uncoordinated methanol molecules.

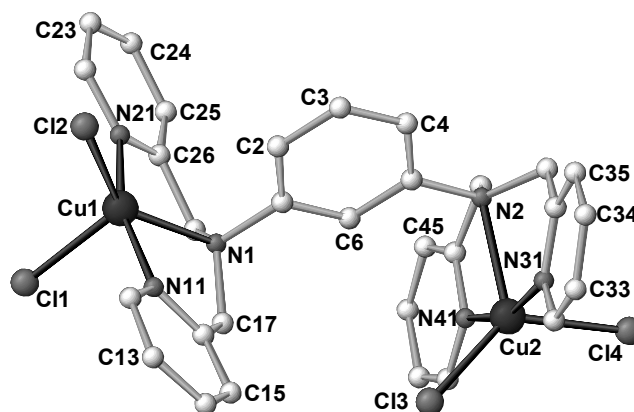


Figure 3-4. Molecular structure of [Cu₂Cl₄(1,3-tpbd)] x 0.84 CH₃OH (**8**) showing the atom numbering. Hydrogen atoms are omitted for clarity.

Selected bond lengths and angles for **8** are summarized in Table 3-2. The dinuclear unit contains two crystallographically independent copper atoms [Cu(1) and Cu(2)] which are only linked via the 1,3-phenylenediamine group causing an intramolecular Cu...Cu distance of 7.434(1) Å. The coordination geometry around Cu(1) is best described as distorted square pyramidal ($\tau = 0.335$) with N(11), N(21), N(1) and Cl(2) defining the basal plane and Cl(1) occupying the axial position. In contrast, the

coordination around Cu(2) with $\tau = 0.535$ is intermediate between square pyramidal and trigonal bipyramidal. It could be viewed as a trigonal bipyramidal with the N(31) and N(41) atoms in the ternary axis [N(31)-Cu(2)-N(41) = 161.7(1)°]. The three nitrogen atoms of the tridentate end of the 1,3-tpbd ligand and the copper atom to which they are bonded are almost coplanar, Cu-N_{py} distances are in the range 1.922(3) to 2.003(4) Å and Cu-N_{amine} distances are 2.138(3) and 2.224(3) Å. Cu-Cl distances are in the range 2.276(1) to 2.375(1) Å. The values of the C(6)-C(1)-N(1)-Cu(1) and C(6)-C(5)-N(2)-Cu(2) torsion angles are 179.9 and 53.2°, respectively. Consequently, Cu(1) is within the plane of the bridging phenylene ring whereas Cu(2) is well below this ring.

The crystal structures of **6** and **8** reveal similar coordination geometries of the two complexes. However, the coordination sphere around the copper(II) core in **6** is very close to that of Cu(2) in **8**, the values of the trigonality parameter τ being practically identical [0.559 in **6** versus 0.535 for Cu(2) in **8**]. The three nitrogen atoms and the copper(II) ion are almost coplanar at both cores.

Five coordination around the copper atoms is also observed in the previously reported complex [Cu₂(N₃)₄(1,3-tpbd)]^[39] where the azide groups act as terminal ligands. However, a less distinctive distortion of the square-pyramidal geometry on Cu(2) occurs there. The Cu-N_{azide} distances in this complex are in the range 1.955(2)-1.979(2) Å values which are remarkably shorter than the Cu-Cl distances in **8**. Interestingly, the two Cu-N_{amine} bonds in [Cu₂(1,3-tpbd)(N₃)₄] [2.474(2) and 2.138(2) Å for Cu(1)-N_{amine} and Cu(2)-N_{amine}, respectively] are significantly different, the shorter one being closer to the Cu-N_{amine} bond lengths in **8**. Finally, the Cu-N_{py} distances in [Cu₂(1,3-tpbd)(N₃)₄] vary in the range 2.029(2)-2.176(2) Å, which stands in good agreement with the Cu-N_{py} distances in **8**.

3.2.5 [{Cu₂Cl₂(ClO₄)(1,3-tpbd)}Cl{Cu₂Cl₂(OH₂)(1,3-tpbd)}](ClO₄)₂ (**9**).

A chloro-bridged tetracopper(II) compound (**9**) was isolated as a product when a mixture of perchlorate and chloride salts of copper(II) was used for the reaction with 1,3-tpbd. Its molecular structure is shown in Figure 3-5. This result lends support to an oligomeric/polymeric formulation in the case of compound **9** described below.

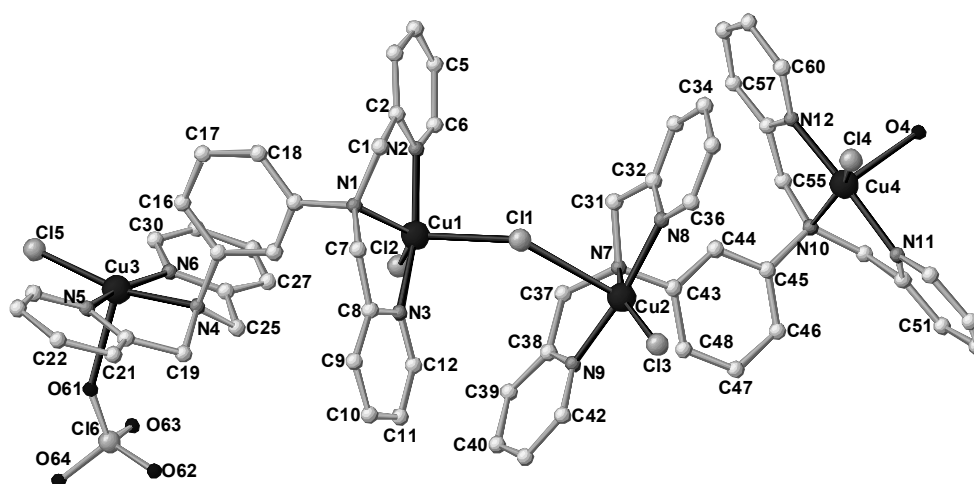


Figure 3-5. Molecular structure of the cation of $[\{\text{Cu}_2\text{Cl}_2(\text{ClO}_4)(1,3\text{-tpbd})\}\text{Cl}\{\text{Cu}_2\text{Cl}_2(\text{OH}_2)(1,3\text{-tpbd})\}](\text{ClO}_4)_2$ (**9**) with the atom numbering. Hydrogen atoms are omitted for clarity.

The structure of **9** consists of tetranuclear $[\{\text{Cu}_2\text{Cl}_2(\text{ClO}_4)(1,3\text{-tpbd})\}\text{Cl}\{\text{Cu}_2\text{Cl}_2(\text{OH}_2)(1,3\text{-tpbd})\}]^{2+}$ cations and uncoordinated ClO_4^- anions. Selected bond lengths and angles for this compound are given in Table 3-2. Four crystallographically independent copper atoms [Cu(1), Cu(2), Cu(3) and Cu(4)] occur in **9**. They are all five-coordinated. The environment at Cu(2), Cu(3) and Cu(4) is best described as distorted square-pyramidal with values of τ ranging from 0.06 [Cu(3)] to 0.22 [Cu(4)]. The apical positions at Cu(2), Cu(3) and Cu(4) are filled by the Cl(1), O(61) and O(4) atoms, respectively and the copper atoms are shifted by 0.152 [Cu(2)], 0.132 [Cu(3)] and 0.145 Å [Cu(4)] from the respective mean basal planes. Notably, Cu(1) has a significantly distorted coordination between square-pyramidal and trigonal-bipyramidal with a τ value of 0.520, which is most likely due to geometrical constraints. If described as trigonal bipyramidal, the ternary axis would roughly correspond to the N(2)-Cu(1)-N(3) vector. The Cu- N_{amine} bond lengths of all the four copper cores vary in the range 2.070(4) [at Cu(3)] to 2.143(4) Å [at Cu(1)], values which are somewhat longer than those concerning the Cu- N_{py} bond distances [1.985(4)-1.996(4) Å]. The values of the distances of copper to terminally bound chloro atoms cover the range 2.221(2)-2.310(2) Å, the longer value corresponding to the Cu(1)-Cl(2) bond [that is to the copper with the greater τ value]. These values are all shorter than those concerning the single chloro bridge [2.412(2) and 2.741(2) Å for Cu(1)-Cl(1) and Cu(2)-Cl(1), respectively], as expected because of the bridging role of Cl(1).

Chloride-bridged crystal structures like the one observed for **9** were also reported for monotopic copper(II) complexes with the ligand phbpa. Ugozzoli *et al.* described the complex $[\text{Cu}_2\text{Cl}_3(\text{phbpa})_2]\text{PF}_6 \times 0.5 \text{ CH}_3\text{OH}$.^[90] The reported Cu-Cl bond distances at the chloro bridge in this compound are 2.568(2) and 2.504(2) Å and that of the angle at the chloro bridge is 159.9(1)°, the differences observed with the respective values in **9** being most likely due to the presence of sterically demanding coordinated perchlorate groups in **9**. Nielsen *et al.* described the complex $[\text{Cu}_2\text{Cl}_2(\text{CH}_3\text{CO}_2)(\text{phbpa})_2]\text{PF}_6 \times 1.5 \text{ CH}_3\text{OH}$, where in contrast to the complex reported by Ugozzoli, one chloro ligand is replaced by an acetate group.^[89] Nevertheless, the values of the Cu-Cl bond distances and the Cu(x)-Cl-Cu(y) bond angle agree with the Ugozzoli's earlier described results.

3.2.6 $[\text{Cu}_2(\text{OH}_2)_2(\text{S}_2\text{O}_6)(1,3\text{-tpbd})]\text{S}_2\text{O}_6 \times 2 \text{ H}_2\text{O} \times \text{CH}_3\text{OH}$ (**10**).

The dithionate copper complex with the 1,3-tpbd ligand (complex **10**) was prepared in the hope that a compound structurally isomeric to the previously reported **b** (e.g. uncoordinated dithionate, this dianion acting exclusively as counter ion) would be obtained.^[86] Compound **10** shows structural similarities to **a**. The structure of **10** consists of $[\text{Cu}_2(\text{OH}_2)_2(\text{S}_2\text{O}_6)(1,3\text{-tpbd})]^{2+}$ cations (Figure 3-6) $\text{S}_2\text{O}_6^{2-}$ anions, water molecules of crystallization and a noncoordinated methanol molecule which is disordered over two sites with the oxygen position common to both molecules. Selected bond lengths and angles for **10** are listed in Table 3-2. The environment of the two crystallographically independent copper atoms [Cu(1) and Cu(2)] is close to square pyramidal with $\tau = 0.130$. The dithionate-oxygen atoms O(2) [at Cu(1)] and O(1) [at Cu(2)] fill the axial positions whereas a water molecule and three nitrogen atoms (one amine and two pyridyl ones) occupy the equatorial positions at each copper atom. The two copper atoms are linked by a bis-terdentate 1,3-tpbd ligand and a bis-monodentate dithionate group. The intramolecular copper...copper distance is 5.736(1) Å, a value which is larger than the shortest intermolecular metal-metal separation. The Cu-N_{py} bond lengths cover the range 1.970(2)-1.972(2) Å, values which are shorter than the Cu-N_{amine} distances [2.091(2) and 2.110(2) Å]. The Cu-O_{water} distances are 1.992(2) and 1.994(2) Å which are considerably shorter than those to the apical oxygen atoms provided by the bridging dithionate, Cu-O_{dithionate} = 2.275(2) and 2.342(2) Å. The Cu-O_{dithionate} distances to the non-bridging dithionate

anions are with 2.444(6) Å (for Cu(1)-O(8)) and 2.967(4) Å (for Cu(2)-O(9A)) small enough to provide at least electronic interactions.

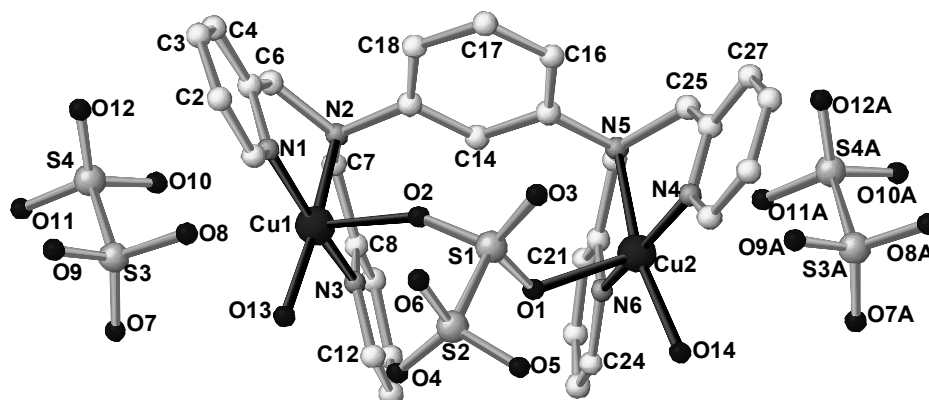


Figure 3-6. Molecular structure of $[\text{Cu}_2(\text{OH}_2)_2(\text{S}_2\text{O}_6)(1,3\text{-tpbd})]\text{S}_2\text{O}_6$ (**10**). One dithionate-anion of the next asymmetric unit is shown. Hydrogen atoms are omitted for clarity.

3.2.7 $[\text{Cu}_2\text{Cl}_4(1,4\text{-tpbd})]$ (**11**).

The reaction of copper(II) chloride with 1,4-tpbd yields compound **11** as a very finely divided microcrystalline solid and despite our numerous attempts, X-ray suitable crystals of this material could not be obtained. The formula of **11** on the basis of the elemental analysis, $[\text{Cu}_2\text{Cl}_4(1,4\text{-tpbd})]$, represents only the stoichiometry of the compound, and it is not necessarily the molecular unit, e.g., a polynuclear compound with chloro bridges between the copper atoms cannot be excluded. Indeed, the structure of **9** shows one mode of chloro bridging which could occur in **11**.

3.2.8 Magnetic properties.

Results of previous magnetic studies on copper(II) complexes of 1,3-tpbd and 1,4-tpbd were discussed in the introduction. Our efforts to prepare copper(II) complexes of all ligands with identical anions led to the isolation of **6**, **8** and **11**. Unfortunately, we could not obtain X-ray quality crystals of **11** because this compound seems to form a highly insoluble polymer. Because of the lack of structural characterisation of **11** and the small amount of crystals of **7** that we got together with its mononuclear nature, the magnetic properties of these two compounds were not investigated.

Magnetic susceptibility measurements were carried out on polycrystalline samples of the structurally characterized complexes **6** and **8-10** in the temperature range 1.9-300 K. The magnetic properties of **6** under the form of $\chi_M T$ versus T plot [χ_M is the magnetic susceptibility per one copper(II) ion] are shown in Figure 3-7. At room temperature $\chi_M T$ is equal to $0.420 \text{ cm}^3 \text{ mol}^{-1} \text{ K}$, a value which is as expected for two magnetically isolated spin doublets. Upon cooling, this value remains constant until $T = 50 \text{ K}$ and it further decreases sharply to $0.050 \text{ cm}^3 \text{ mol}^{-1} \text{ K}$ at 1.9 K . The susceptibility versus T plot (see inset of Figure 3-7) exhibits a maximum at *ca.* 3.7 K . These features are characteristic of a weak antiferromagnetic interaction between the local spin doublets. Most likely, the weak π - π overlap between adjacent monomeric units along the x axis in **6** (see Fig. 3-2) provides the exchange pathway. The position of this maximum is field dependent being shifted toward lower temperatures when the field is increased from 1000 G to 4 T (see inset of Fig. 3-8) and it disappears under an applied field of 4 T , the magnetic susceptibility exhibiting a plateau at $T < 3 \text{ K}$ for $H \geq 4 \text{ T}$. These features correspond to a metamagnetic behaviour: when the magnitude of applied magnetic field overcomes the small intrachain antiferromagnetic interaction, the maximum of the magnetic susceptibility disappears and the magnetic susceptibility tends to a constant value.

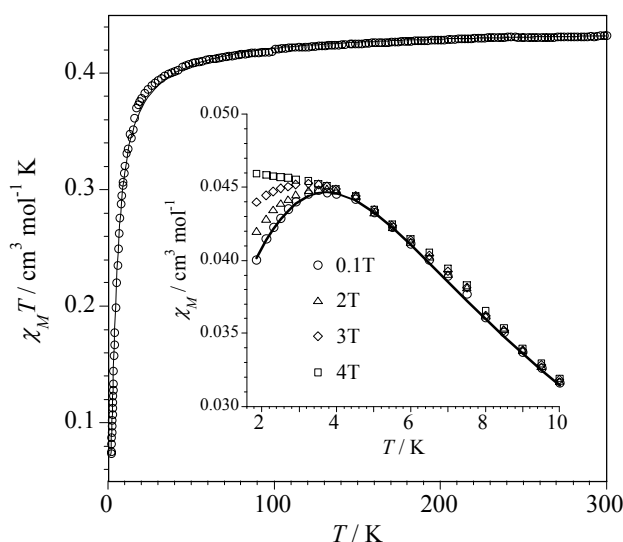


Figure 3-7. Thermal variation of $\chi_M T$ for **6** under an applied magnetic field of 1000 G : (o) experimental data; (—) best fit curve through eqn. (1) (see text). The inset shows the maximum of the magnetic susceptibility in the low temperature region.

The analysis of the magnetic behaviour of **6** have been analyzed through the theoretical expression (the Hamiltonian being $H = -J \sum_i \mathbf{S}_i \cdot \mathbf{S}_{i+1}$) proposed by Hall^[92] for a uniform chain of local spins $S = 1/2$, [eqn. (1)]

$$\chi_M = (N\beta^2 g^2 / kT) [(0.25 + 0.14995x + 0.30094x^2) / (1 + 1.9862x + 0.68854x^2 + 6.0626x^3)] (1)$$

where N , β and g have their usual meanings, $x = J/kT$ and J is the exchange coupling constant describing the magnetic interaction between the two nearest-neighbor spin doublets. Such an expression derives from the numerical results from Bonner and Fisher^[93] and it has been normally used to treat the magnetic data of uniform copper(II) chains. Least-squares fit leads to the following parameters: $J = -4.1(1) \text{ cm}^{-1}$, $g = 2.10(1)$ and $R = 6.1 \times 10^{-5}$ (R is the agreement factor defined as $\sum_i [(\chi_M)_{\text{obs}}(i) - (\chi_M)_{\text{calc}}(i)]^2 / \sum_i [(\chi_M)_{\text{obs}}(i)]^2$). The curves of the magnetization versus H plot at very low temperatures (see Figure 3-8) exhibit a crossing point 4.0 T which corresponds to the situation where the magnetic field overcomes the magnetic interaction. The magnitude of the magnetic field at the crossing point provides an evaluation of the magnetic interaction: J would be ca. 4.2 cm^{-1} with $g = 2.10$, a value which agrees with that obtained by the above fit. This example is analogous to that previously reported by some of us for the dicopper(II) complex of formula $[\text{Cu}_2(\text{dmphen})_2(\text{dca})_4]$ (dmphen = 2,9-dimethyl-1,10-phenanthroline and dca = dicyanamide) where a very weak magnetic coupling ($J = -3.3 \text{ cm}^{-1}$) between the two copper(II) ions through the two μ -15-dca bridges occurs.^[94]

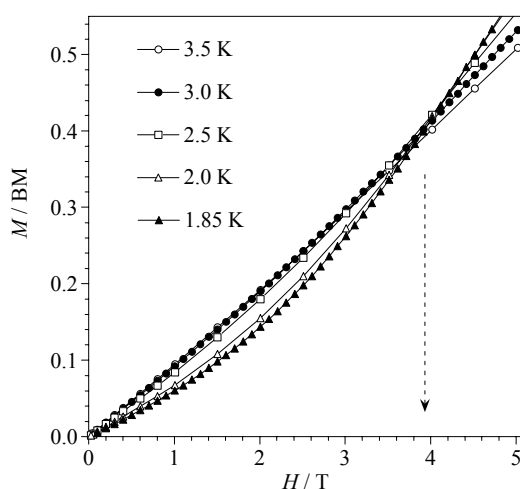


Figure 3-8. Magnetization versus H plot for **6** at $T = 1.85, 2.0, 2.5, 3.0$ and 3.5 K .

The magnetic properties of **8** under the form of $\chi_M T$ versus T plot [χ_M is the magnetic susceptibility per two copper(II) ions] are shown in Figure 3-9. This plot is similar to that of the previous compound but in the present case, no maximum of the magnetic susceptibility was observed in the temperature range explored, the value of $\chi_M T$ at 1.9 K being significantly above that of **6** ($0.56 \text{ cm}^3 \text{ mol}^{-1} \text{ K}$ in **8** versus $0.10 \text{ cm}^3 \text{ mol}^{-1} \text{ K}$ in **6**). These features are consistent with the occurrence of a very small antiferromagnetic interaction in **8** (weaker than that found in **6**). In agreement with the dinuclear structure of **8**, we analyze its magnetic data through a simple Bleaney-Bowers expression [eqn. (2)]^[95]

$$\chi_M = (2N\beta^2 g^2 / kT) [3 + \exp(-J/kT)]^{-1} \quad (2)$$

which is derived through the Hamiltonian $H = -J \mathbf{S}_1 \cdot \mathbf{S}_2 + \beta H (g_1 \mathbf{S}_1 + g_2 \mathbf{S}_2)$ where J is the exchange coupling parameter, $S_1 = S_2 = 1/2$ (interacting local spins), $g = g_1 = g_2 = g$ (average Landé factor) and N , β and k have their usual meanings. Least-squares fit through eqn. (2) led to the following set of parameters: $J = -0.40(1) \text{ cm}^{-1}$ and $g = 2.08(1)$ with $R = 8.7 \times 10^{-6}$ (R is the agreement factor defined as $\sum_i [(\chi_M T)_{\text{obs}}(i) - (\chi_M T)_{\text{calc}}(i)]^2 / \sum_i [(\chi_M T)_{\text{obs}}(i)]^2$).

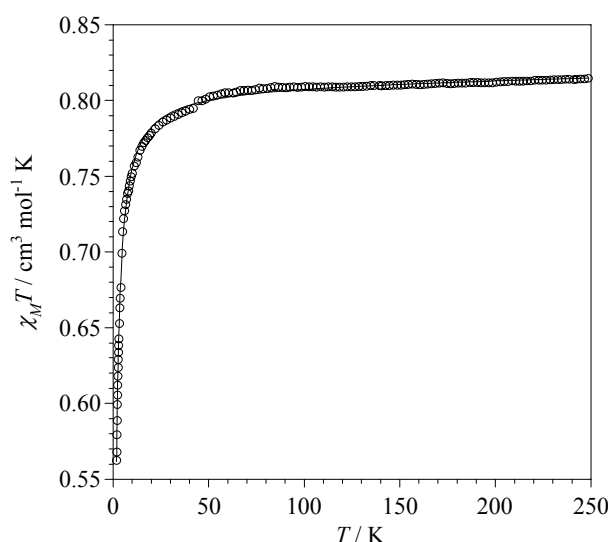


Figure 3-9. Thermal variation of $\chi_M T$ for **8** under an applied magnetic field of 0.1 T: (o) experimental data; (—) best-fit curve through eqn. (2) (see text).

The shape of the magnetization versus H plot at 1.9 K is in agreement with the occurrence of a very weak antiferromagnetic interaction, the value of the

magnetisation at 5 T (the maximum available magnetic field in our SQUID) is ca. 1.8 BM, a value somewhat below that expected for two uncoupled spin doublets.

The magnetic behaviour of **8** is practically identical to that previously reported for the parent compound of formula $[\text{Cu}_2(\text{N}_3)_4(1,3\text{-tpbd})]$.^[39]

The magnetic properties of **10** under the form of $\chi_M T$ versus T plot [χ_M is the magnetic susceptibility per two copper(II) ions] are shown in Figure 3-10. At room temperature, $\chi_M T$ is equal to $0.85 \text{ cm}^3 \text{ mol}^{-1} \text{ K}$, a value which is as expected for two magnetically non-interacting spin doublets. Upon cooling, the value of $\chi_M T$ increases, attaining a maximum at 4.0 K and then decreasing slightly. This behavior is typical of a ferromagnetically coupled dinuclear copper(II) complex, the small decrease of $\chi_M T$ in the low temperature region being due to zero-field splitting effects (D) and/or intermolecular interactions. The susceptibility data of **10** were analysed by the corresponding expression^[30] for a dicopper(II) unit which is derived through the Hamiltonian for two magnetically interacting local spin doublets derived from the Hamiltonian $H = -J \mathbf{S}_1 \cdot \mathbf{S}_2 + \mathbf{S}_1 \cdot \mathbf{D} \cdot \mathbf{S}_2 + \beta H (g_1 \mathbf{S}_1 + g_2 \mathbf{S}_2)$ where D is zero-field splitting of the triplet state. Best-fit results are: $J = +8.5(1) \text{ cm}^{-1}$, $g = 2.08(1)$ and $|D| = 0.9(2) \text{ cm}^{-1}$ with $R = 1.6 \times 10^{-5}$ ($\sum_i [(\chi_M T)_{\text{obs}}(i) - (\chi_M T)_{\text{calc}}(i)]^2 / \sum_i [(\chi_M T)_{\text{obs}}(i)]^2$). The theoretical curve matches very well the experimental in the whole temperature range as is indicated by the low value of the agreement factor R . It should be noted that the value of D is the maximum one because of the contribution of the intermolecular magnetic interactions that would also occur and we did not take into consideration. Anyway, the quality of the fit and the values of J and g remain practically unchanged when performing the fit with the inclusion of a θ parameter to account for the intermolecular interactions. The fact that the nature and magnitude of the magnetic interaction in **10** is very close to that observed for compound **a**, where the perchlorate bridge is present instead of the dithionate, reveals that the exchange pathway is the same in the two dicopper(II) complexes.

The magnetic properties of the tetracopper(II) complex **9** under the form of $\chi_M T$ against T [χ_M is the magnetic susceptibility per four copper(II) ions] are shown in Figure 3-11. At room temperature, $\chi_M T$ is equal to $1.68 \text{ cm}^3 \text{ mol}^{-1} \text{ K}$, a value which is as expected for four magnetically isolated spin doublets [ca. $1.65 \text{ cm}^3 \text{ mol}^{-1} \text{ K}$ with g

$= 2.10]$. $\chi_M T$ smoothly increases when cooling to reach a maximum value of $1.74 \text{ cm}^3 \text{ mol}^{-1} \text{ K}$ at 4.0 K and further decreases sharply to reach $1.43 \text{ cm}^3 \text{ mol}^{-1} \text{ K}$ at 1.9 K .

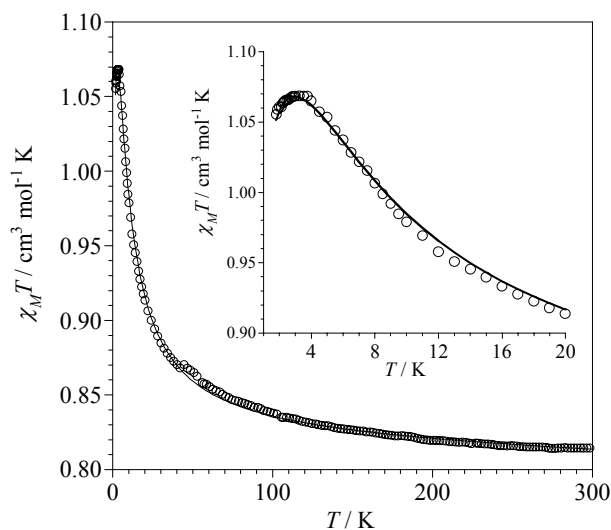


Figure 3-10. Thermal variation of $\chi_M T$ for **10** under applied magnetic fields of 0.1 T ($T \geq 50 \text{ K}$) and 500 G ($T < 50 \text{ K}$): (o) experimental data; (—) best-fit curve (see text). The inset shows the maximum of $\chi_M T$ in the low temperature region.

These features are consistent with the occurrence of weak ferro- and antiferromagnetic interactions.

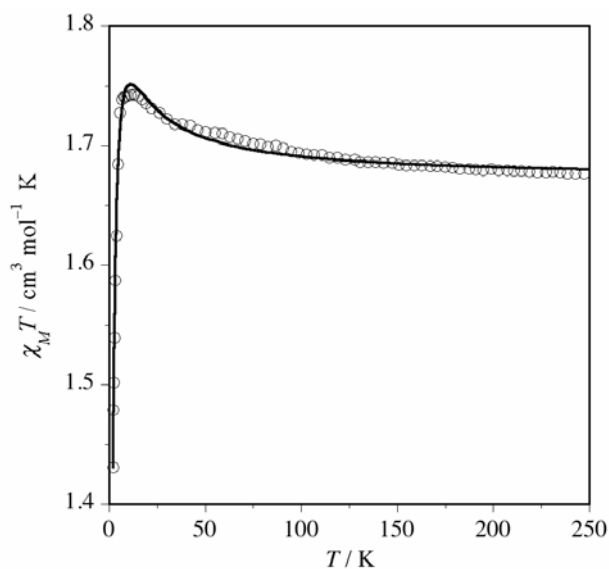


Figure 3-11. Thermal dependence of $\chi_M T$ for **9**: (o) experimental data; (—) best-fit curve (see text).

Having in mind the tetranuclear structure of **9**, its magnetic data were analyzed through the Hamiltonian $H = -J_{13} \mathbf{S}_1 \cdot \mathbf{S}_3 - J_{12} \mathbf{S}_1 \cdot \mathbf{S}_2 - J_{24} \mathbf{S}_2 \cdot \mathbf{S}_4 + \beta H (g_1 \mathbf{S}_1 + g_2 \mathbf{S}_2 + g_3 \mathbf{S}_3 + g_4 \mathbf{S}_4)$ where J_{ij} are the magnetic coupling parameters associated to the interaction between the i and j local spins.

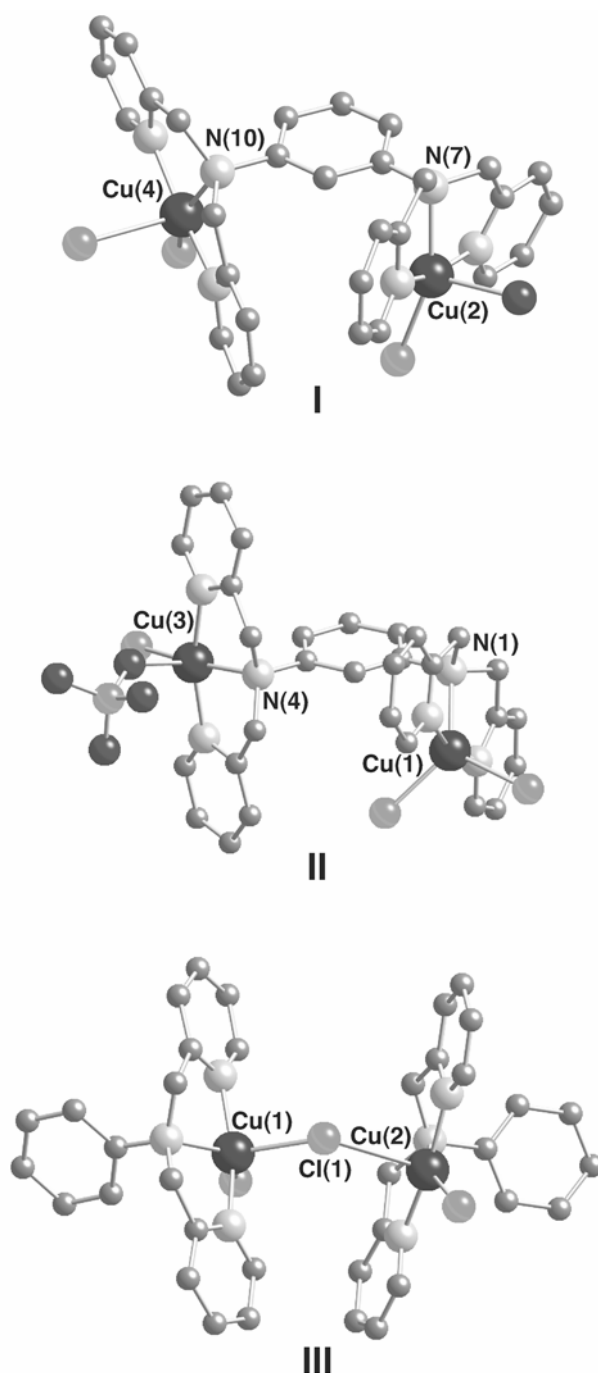


Figure 3-12. Model systems (I-III) of the dinuclear copper(II) fragments of **9** which were used to perform the DFT type calculations (see text).

In order to avoid overparametrisation in the fitting procedure, we assumed that $g_1 = g_2 = g_3 = g_4 = g$. Regardless, the fit of the magnetic data remains complicated because of the smooth variation of the experimental data and the possible correlation among the four variable parameters. So, in order to avoid physically meaningless sets of J_{ij} values in the fitting procedure, theoretical calculations of the DFT type (see paragraph of Computational Methodology in the Exp. Sect.) were performed on the dicopper(II) models shown in Figure 3-12 to visualize and evaluate the efficiency of the intramolecular exchange pathways involved. These models reproduce the three intramolecular exchange pathways in **9** (**I** and **II** for the outer interactions and **III** for the inner one) and their bond distances and angles are those of the real structure.

The unpaired electron on each copper(II) ion (that is the SOMO) in **I** lies in the basal plane of the metal atom [comprising of atoms N(7), N(8), N(9) and Cl(3) for Cu(2) and N(10), N(11), N(12) and Cl(4) for Cu(4)]. These two SOMOs are nearly perpendicular to the phenylenediamine plane and lie below this plane. This situation corresponds to the structures of compounds **10** and **a** where significant and nearly identical ferromagnetic interactions occur [$+8.5$ (**10**) and $+9.3 \text{ cm}^{-1}$ (**a**)]. The theoretical analysis carried out previously for **a** accounted for this ferromagnetic interaction:^[34] the direct overlap between the $d_{x^2-y^2}$ type magnetic orbitals of the copper atoms and the π system of the pyridyl ligand allows the unpaired spin of the metal to induce a polarisation of spin on the bridging skeleton, the alternating spin rule prevailing and leading thus to a parallel alignment of the peripheral spins. The calculated value of the magnetic coupling for **I** (J_{24}) is $+30.0 \text{ cm}^{-1}$. Its nature is as predicted, but its value is *ca.* three times that observed in **10** and **a**.

In **II**, although the SOMO of the Cu(3) atom is also of the $d_{x^2-y^2}$ type [orbital located in the basal plane built by the N(4)N(5)N(6)Cl(5) set of atoms], its orientation is such that is bisected by the phenylene ring and the exchange pathway is the σ -type. At the other copper atom [Cu(1)], the magnetic orbital is of the d_z^2 type [the ternary axis roughly corresponding to the N(2)···N(3) vector]. A weak spin density is expected on the N(1) atom and the exchange pathway is of the π -type at this side. In such a situation, the overlap between the SOMOs of Cu(3) and Cu(1) through the multiatomic Cu(3)-N(4)-C(45)-C(44)-C(43)-N(7)-Cu(2) pathway is expected to be very poor and could be zero by accidental orthogonality. Consequently, the value of the magnetic coupling is expected to be very weak but ferro- or antiferromagnetic in

nature.^[96, 97] The small magnitude of the calculated value of the magnetic coupling for **II** ($J_{13} = +0.20 \text{ cm}^{-1}$ fully agrees with this prediction).

Finally, the interacting SOMOs in model **III** are of d_z^2 [at Cu(1)] and $d_{x^2-y^2}$ [at Cu(2)] types, as described above. However in the present case the exchange pathway is monoatomic and the bridging atom fills the apical position of the square pyramid at Cu(2) and one equatorial position of the trigonal bipyramid at Cu(1). The orthogonality between the two SOMOs is predicted for such a situation for values of the angle at the bridging chloro (θ) close to 180° . As the value of the Cu(1)-Cl(2)-Cl(2) angle is 141.6° , a very weak antiferromagnetic coupling could be expected due to the poor overlap between the magnetic orbitals [equatorial (at Cu(1))-axial (at Cu(2)) exchange pathway]. This conclusion is not supported by the DFT calculations which afford a calculated value of the magnetic coupling for **III** of $J_{12} = +11.1 \text{ cm}^{-1}$.

The fact that the calculated ferromagnetic coupling for **I** is three times that predicted (that is the coupling observed for the complexes **a** and **10**) and the non-negligible value for the magnetic coupling of **III** deserve a brief comment. Highly charged molecules or molecules formed by fragments with well localized charges, *i.e.* systems that can be considered not covalent, cause problems in the evaluation of the energy and consequently, on the values of J by methods of computational chemistry. In the present case, it is clear that an overestimation of the ferromagnetic contributions has been derived. Anyway, once the ability of the different dinuclear model fragments to mediate magnetic interactions is evaluated by DFT calculations, we proceed to attempt a fit of the experimental magnetic data based on these results, that is $|J_{24}| > |J_{13}|$, $|J_{12}| \approx 0$ and $J_{24} > 0$. The analysis of the magnetic data of **9** through numerical matrix diagonalisation techniques using a Fortran program^[98] with the spin Hamiltonian specified above and fixing $J_{12} = 0 \text{ cm}^{-1}$ led to the following set of best-fit parameters: $J_{24} = +8.0 \text{ cm}^{-1}$, $J_{13} = -3.0 \text{ cm}^{-1}$ and $g = 2.114$ ($R = 1.7 \times 10^{-5}$). These results show that the ferromagnetic coupling between Cu(2) and Cu(4) is ensured whereas an antiferromagnetic interaction is involved between Cu(1) and Cu(3). In order to check the influence of the possible intermolecular magnetic interactions on the values of the intramolecular magnetic couplings, a last fit was performed considering a new parameter accounting for them (θ) and fixing $J_{12} = 0 \text{ cm}^{-1}$. A better agreement between the experimental and calculated magnetic data is achieved, the best-fit parameters being $J_{24} = +10.4 \text{ cm}^{-1}$, $J_{13} = -0.4 \text{ cm}^{-1}$, $\theta = -0.4$

cm^{-1} and $R = 9.0 \times 10^{-6}$. Now the values of J_{24} and J_{13} fully agree with those observed in the parent complexes **a** and **10** ($J = +9.3$ and $+8.4 \text{ cm}^{-1}$, respectively) and **8** ($J = -0.40 \text{ cm}^{-1}$). This is very satisfying because the relative arrangement of the bridging aromatic ring and the magnetic orbitals in **8** and **II** is very close and the same occurs when comparing **I** with **a** and **10**. In consequence, we have taken the results of these last fits as the more realistic ones.

3.3 Conclusion

A series of copper(II) complexes of the isomeric hexadentate ligands based on phenylenediamine, 1,*n*-tpbd ($n = 2-4$) has been prepared and the exchange polarization mechanism successfully tested once more. However, the main aim concerning a thorough comparison of the magnetic properties of stoichiometrically identical, structurally isomeric dicopper(II) complexes of 1,*n*-tpbd without auxiliary bridging ligands still eludes us because of the lack of X-ray quality crystals of the dinuclear $[\text{Cu}(1,n\text{-tpbd})\text{Cu}]^{4+}$ core as chloride, dithionate, perchlorate or hexafluorophosphate salts.^[26, 86] Thus the effect of *meta* against *para* versus *ortho* substitution on the magnetic properties still cannot be assessed satisfactorily in order to test the spin polarisation mechanism. Even though a mononuclear complex of 1,2-tpbd was obtained, formation of dinuclear complexes can be envisaged given the possibility of different ligand conformations (e.g. a twist around one of the phenylenediamine C-N bonds) and appropriate *capping* ligands. An optimization of the synthesis of 1,2-tpbd is required before our work can continue with this ligand.

3.4 Experimental Section

3.4.1 Materials and Methods.

Reagents and solvents used were of commercially available reagent grade quality. The phenylenediamine ligands were recrystallized prior to use. UV-vis spectra were measured on a Hewlett Packard 8452A or a Shimadzu UV-3100 spectrophotometer. ^1H NMR spectra were recorded on a Bruker AM-300 300-MHz spectrometer. IR spectra were determined on a Mattson Polaris FT-IR spectrometer (Nujol mulls) or as KBr disks using a Hitachi 270-30 IR spectrometer. EI mass spectra were recorded on a Varian MAT311A spectrometer and FAB mass spectra on a Kratos MS-50 spectrometer. Elemental analyses were performed at the Chemistry Department II at

the Copenhagen University, Atlantic Microlab, Inc., Norcross, Georgia 30091, U. S. A., or at the University of Erlangen. 1,4-Bis[bis(2-pyridylmethyl)amino]benzene (1,4-tpbd), its copper(II) complexes **b** and $[\text{Cu}_2(1,4\text{-tpbd})\text{Cl}_4]_n$ (**11**),^[86] as well as *N,N*-Bis(2-pyridylmethyl)aniline (phbpa)^[87] were prepared through the previously reported procedures.

Caution! Perchlorate salts are potentially explosive and they should be handled with care. Our preparations were carried out on mmol scale and heating was avoided.

3.4.2 Preparation of the Ligands and Complexes.

1,3-Bis[bis(2-pyridylmethyl)amino]benzene (1,3-tpbd). The synthesis of 1,3-tpbd was performed as described earlier^[26] but could be improved by using an excess of 2-chloromethylpyridine hydrochloride (molar ratio of 2-(chloromethyl)pyridine to 1,3-phenylenediamine 1:5). In contrast to the previously published synthesis, one recrystallization from acetone with a small amount of active charcoal was sufficient to purify the crude product and no trace of the trisubstituted phenylenediamine, *N,N,N'*-tris(2-pyridylmethyl)benzene-1,3-diamine was detected. The analytical data are the same as reported earlier but the yield was increased to 70% (to be compared to 25% obtained previously).

[CuCl₂(phbpa)] (6). CuCl₂ × 2 H₂O (31 mg, 0.1818 mmol) in 2 mL of methanol was added to a methanolic solution (5 ml) of phbpa (50 mg, 0.1818 mmol). The product precipitates as light green needles after 2 days. Yield 50.1 mg, 67.3%. Anal. Calcd. for C₁₈H₁₇Cl₂CuN₃: C, 52.76; H, 4.18; N, 10.25. Found: C, 52.57; H, 4.24; N, 10.14). FAB-MS *m/z* 373 ([CuCl(phbpa)]⁺, 100%), 338 ([Cu(phbpa)]²⁺, 55%). UV-Vis (MeOH) λ, nm (ε, dm³ mol⁻¹cm⁻¹): 258 (13161), 306 (2238), 378 (shoulder, 404), 702 (187).

[Cu(1,2-tpbd)](PF₆)₂ × 2H₂O (7). *o*-Phenylenediamine (0.5 g, 4.63 mmol) and 2(chloromethyl-)pyridine hydrochloride (3.8 g, 23.11 mmol) were dissolved in water (10 mL) under an argon atmosphere. NaOH (0.925 g, 23.11 mmol) in a minimum amount of water was added over a period of 2h. The pH was kept at 9.0 during the next 7-10 days by the occasional addition of NaOH (in all, 0.740 g, 18.45 mmol) in 7 mL of water. The solution was extracted with 5 × 30 mL of CH₂Cl₂ and the combined organic phases were dried over Na₂SO₄. Evaporation of the solvent yielded a yellow

oil, which contained the desired ligand, 1,2-Bis[bis(2-pyridylmethyl)amino]benzene (1,2-tpbd) and the major by-product, tri-*N,N,N'*-(2-pyridylmethyl)-1,2-benzenediamine. Complex formation was achieved by reacting this mixture (ca. 0.1 mmol in 1,2-tpbd based on NMR integrations) with $\text{Cu}(\text{NO}_3)_2 \times 5 \text{H}_2\text{O}$ (0.1 mmol) and further addition of NH_4PF_6 (0.5 mmol) in MeOH (5 mL). $[\text{Cu}(1,2\text{-tpbd})](\text{PF}_6)_2 \times 2\text{H}_2\text{O}$ was deposited as blue crystals overnight in variable yields. (Found : C, 41.67; H 3.27; N, 9.82. $\text{C}_{30}\text{H}_{32}\text{CuF}_{12}\text{N}_6\text{O}_2\text{P}_2$ requires : C, 41.79; H, 3.74; N, 9.75.)

$[\text{Cu}_2\text{Cl}_4(1,3\text{-tpbd})] \times \text{H}_2\text{O} \times \text{CH}_3\text{OH}$ (8). $\text{CuCl}_2 \times 2 \text{H}_2\text{O}$ (0.36 g, 2.1 mmol) dissolved in 10 mL water was added to a suspension of 1,3-tpbd (0.5 g, 1 mmol) in 10 mL of methanol. After stirring for 10 minutes, the solution was filtered and left standing overnight. The green crystals deposited were filtered and dried in air. Yield 0.4 g, 50.5%. Anal. Calcd. for $\text{C}_{31}\text{H}_{34}\text{N}_6\text{Cu}_2\text{O}_2\text{Cl}_4 \times \text{H}_2\text{O} \times \text{CH}_3\text{OH}$ (8): C, 47.04; H, 4.33; N, 10.62. Found: C, 47.05; H, 4.13; N, 10.82. UV-Vis (MeOH) λ , nm (ϵ , $\text{dm}^3\text{mol}^{-1}\text{cm}^{-1}$): 375 (shoulder, 702), 726 (268).

$[\{\text{Cu}_2\text{Cl}_2(\text{ClO}_4)(1,3\text{-tpbd})\}\text{Cl}\{\text{Cu}_2\text{Cl}_2(\text{OH}_2)(1,3\text{-tpbd})\}](\text{ClO}_4)_2$ (9). $\text{CuCl}_2 \times 2 \text{H}_2\text{O}$ (0.11 g, 0.63 mmol) and $\text{Cu}(\text{ClO}_4)_2 \times 6 \text{H}_2\text{O}$ (0.23 g, 0.63 mmol) dissolved in 15 mL of water were added to a suspension of 1,3-tpbd (0.3 g, 0.63 mmol) in 15 mL of methanol. After stirring for 10 minutes the solution was filtered and left standing for a few days. The green crystals deposited were filtered and dried in air. Yield 0.4 g, 50.5%. (Found C, 42.70; H, 3.34; N, 9.86. $\text{C}_{60}\text{H}_{56}\text{N}_{12}\text{Cu}_4\text{O}_{13}\text{Cl}_8$ requires C, 42.62; H, 3.34; N, 9.94). UV-Vis (MeOH) λ , nm (ϵ , $\text{dm}^3\text{mol}^{-1}\text{cm}^{-1}$): 375 (shoulder, 702), 726 (268).

$[\text{Cu}_2(\text{OH}_2)_2(\text{S}_2\text{O}_6)(1,3\text{-tpbd})]\text{S}_2\text{O}_6 \times 2 \text{H}_2\text{O} \times \text{CH}_3\text{OH}$ (10). $\text{Cu}(\text{BF}_4)_2 \times 6 \text{H}_2\text{O}$ (0.44 g, 1.26 mmol) dissolved in 15 mL water was added to a suspension of 1,3-tpbd (0.3 g, 0.63 mmol) in 15 mL of methanol. $\text{Na}_2\text{S}_2\text{O}_6$ (1 g, 4.13 mmol) in 50 mL of water was added and the solution was filtered after boiling for a few minutes. The green crystals which deposited overnight were filtered off and dried in air. Yield 0.4 g, 62.2%. Anal. Calcd. for $\text{C}_{31}\text{H}_{42}\text{Cu}_2\text{N}_6\text{O}_{17}\text{S}_4$ (10): C, 35.73; H, 4.06; N, 8.06. Found C, 35.16; H, 3.83; N, 8.23%.

3.4.3 Magnetic measurements.

Magnetic susceptibility data of polycrystalline samples of **6** and **8-10** were collected over the temperature range 1.9-300 K with a Quantum Design SQUID susceptometer and using applied magnetic fields of 0.1 T (**6** and **8-10**) and 500 G (**9** and **10**). Magnetization isotherms ($1.85 \leq T \leq 3.5$) varying the applied magnetic field in the range 0-5 T were performed for **6**. Diamagnetic corrections for the constituent atoms and corrections for the sample holder were performed. The correction for the temperature independent paramagnetism [$60 \times 10^{-6} \text{ cm}^3 \text{ mol}^{-1}$ per copper(II) ion] was also applied.

3.4.4 Computational Methodology.

The computational strategy used in this work has been described elsewhere and it is briefly outlined here.^[99] For the evaluation of the coupling constant for each dicopper(II) model fragment of **9** (I-III, Figure 13), two separate calculations were carried out using DFT, one for the triplet state and another one for the low-spin, broken symmetry state. The hybrid B3LYP method^[100] was used in the calculations as implemented in GAUSSIAN 98,^[100] with all-electron double- ζ basis proposed by Ahlrichs and co-workers except for copper where we have used a triple- ζ basis.^[101] The real dinuclear fragments of **9** were used in the calculations to estimate the values of the intramolecular magnetic couplings.

3.4.5 X-Ray Crystallography.

Single crystals were obtained directly from reaction mixtures. Due to solvent loss, crystals of **7**, **8** and **10** used for structural analysis show a slightly different lattice solvent composition than found in the elemental analysis. Data were collected on a Huber four-circle (for **6**) and on a Siemens SMART diffractometer^[102] for the other structures. Crystal data and experimental parameters are presented in Table 1. The data were corrected for Lorentz-polarization effects, absorption corrections were made by integration for **6** and **9** and by SADABS,^[70] a multi-scan technique for **7**, **8** and **10**. The structures were solved by direct methods, SHELX^[71] for **10** x 2 H₂O x CH₃OH and SIR97^[103] for **6**, **7** and **8** x 0.84 CH₃OH and refined by least-squares techniques using programs from SHELX^[71] or from KRYSTAL.^[104] Atomic scattering factors were taken from^[105] for **10** and from^[106] for the other structures. All non-

hydrogen atoms for **6** were refined anisotropically (on F) whereas the hydrogen atoms were refined isotropically. All non-hydrogen atoms for **8** x 0.84 CH₃OH were also anisotropically refined (on F), while the hydrogen atoms of the ligand were placed in fixed calculated positions (C-H = 0.95 Å). The molecules of methanol are disordered over two sites with occupancy factors of 0.53(1) and 0.31(1), and their hydrogen atoms were not included in the calculations. All non-hydrogen atoms for **10** x 2H₂O x CH₃OH were refined anisotropically (on F^2). The hydrogen atoms of the water molecule in this compound were refined isotropically whilst C-H distances were kept fixed (C-H = 0.97 and 0.93 Å for aliphatic and aromatic carbon atoms, respectively). The hydrogen atoms of the disordered methanol molecules were not included in the calculations. The absolute structure parameter^[107] was 0.005(5) indicating that the correct polarity has been chosen. All non-hydrogen atoms for **7** were refined anisotropically (on F) and the hydrogen atoms of the ligands were kept fixed in calculated positions (C-H = 0.95 Å).

Table 3-1. Summary of crystallographic data and experimental details for **6**, **7**, **8** x 0.84 CH₃OH, **9** and **10** x CH₃OH x 2 H₂O.

Compound	6	7	8 x 0.84CH ₃ OH	9	10 x CH ₃ OH x 2H ₂ O
Formula	C ₁₈ H ₁₇ N ₃ Cl ₂ Cu	C ₃₀ H ₂₈ N ₆ F ₁₂ P ₂ Cu	C _{30.84} H _{31.36} N ₆ O _{0.84} Cl ₄ Cu ₂	C ₆₀ H ₅₆ Cl ₈ Cu ₄ N ₁₂ O ₁₃	C ₃₁ H ₄₀ N ₆ O ₁₇ S ₄ Cu ₂
<i>a</i> [Å]	8.4065(8)	20.367(2)	8.6320(4)	8.2760(2)	8.5862(10)
<i>b</i> [Å]	14.133(1)	15.907(2)	27.471(1)	23.6354(4)	13.1174(2)
<i>c</i> [Å]	15.387(1)	22.082(2)	13.7959(7)	34.4974(5)	17.4616(3)
β [°]	110.7730(6)	115.489(1)	93.007(1)	90	87.873(1)
<i>V</i> [Å ³]	1709.3(2)	6458(1)	3266.7(3)	6747.9(3)	1965.3(1)
<i>Z</i>	4	8	4	4	2
Fw	409.80	826.07	768.41	1690.93	1024.05
space group	<i>P</i> 2 ₁ / <i>c</i> (no. 14)	<i>P</i> 2 ₁ / <i>c</i> (no. 14)	<i>P</i> 2 ₁ / <i>n</i> (no. 14)	<i>P</i> 2 ₁ 2 ₁ 2 ₁ (no. 19)	<i>P</i> 2 ₁ (no. 4)
<i>T</i> , K	294	120	295	200	200
λ, Å	0.71073	0.71073	0.71073	0.71073	0.71073
ρ _{calc} [g cm ⁻³]	1.592	1.699	1.562	1.664	1.730
μ [cm ⁻¹]	1.594	0.879	1.664	1.632	1.378
reflns collected	5877	82374	22243	71148	20197
reflns unique/ <i>R</i> _{int}	4945/0.032	18603/0.075	7912/0.048	16345/0.0987	9305/0.016
data/restraints/param	3648 ^a /0/286	10429 ^a /0/920	4095 ^a /11/408	16345 ^b /0/921	8980 ^b /1/591
<i>R</i> 1, <i>wR</i> 2	0.035/0.048 ^c	0.039/0.044 ^c	0.036/0.045 ^c	0.0586/0.0916 ^{d?}	0.022/0.054 ^d
^a $I > 3\sigma(I)$, ^b $I > 2\sigma(I)$ ^c $w = 1/[\sigma(F_o^2) + 1.03F_o^{2/2} - F_o]^2$ ^d $w = 1/[\sigma^2(F_o^2) + (0.0295P)^2 + 0.0474P]$ where $P = (F_o^2 + 2F_c^2)/3$.					

Table 3-2. Selected bond distances [Å] and angles [°] for **6**, **7**, **8** x 0.84 CH₃OH, **9** and **10** x CH₃OH x 2 H₂O.

Atoms	6	Atoms	7	Atoms	8 x 0.84 CH ₃ OH	Atoms	9	Atoms	10 x CH ₃ OH x 2 H ₂ O
Cu-Cl(1)	2.276(1)	Cu(1)-N(1)	2.091(2)	Cu(1)-Cu(2)	7.434(1)	Cu(1)-N(2)	1.985(4)	Cu(1)-Cu(2)	5.763(2)
Cu-Cl(2)	2.368(1)	Cu(1)-N(2)	2.013(2)	Cu(1)-Cl(1)	2.370(1)	Cu(1)-N(3)	1.993(4)	Cu(1)-N(3)	1.971(2)
Cu-N(1)	2.214(2)	Cu(1)-N(11)	2.054(3)	Cu(1)-Cl(2)	2.295(1)	Cu(1)-N(1)	2.143(4)	Cu(1)-N(1)	1.974(2)
Cu-N(11)	1.988(2)	Cu(1)-N(21)	2.102(3)	Cu(1)-N(1)	2.138(3)	Cu(1)-Cl(2)	2.310(2)	Cu(1)-O(13)	1.992(2)
Cu-N(21)	1.997(2)	Cu(1)-N(31)	1.970(3)	Cu(1)-N(11)	1.993(4)	Cu(1)-Cl(1)	2.412(2)	Cu(1)-N(2)	2.091(2)
		Cu(1A)-N(1A)	2.088(2)	Cu(1)-N(21)	2.003(4)	Cu(2)-N(8)	1.988(4)	Cu(1)-O(2)	2.275(2)
		Cu(1A)-N(2A)	2.022(2)	Cu(2)-Cl(3)	2.276(1)	Cu(2)-N(9)	1.994(4)	Cu(1)-O(8)	2.444(6)
		Cu(1A)-N(11A)	2.039(3)	Cu(2)-Cl(4)	2.375(1)	Cu(2)-N(7)	2.083(4)	Cu(2)-N(4)	1.970(2)
		Cu(1A)-N(21A)	2.098(2)	Cu(2)-N(2)	2.224(3)	Cu(2)-Cl(3)	2.230(2)	Cu(2)-N(6)	1.972(2)
		Cu(1A)-N(31A)	1.979(3)	Cu(2)-N(31)	1.997(4)	Cu(2)-Cl(1)	2.741(2)	Cu(2)-O(14)	1.994(2)
				Cu(2)-N(41)	1.992(3)	Cu(3)-N(6)	1.986(5)	Cu(2)-N(5)	2.110(2)
						Cu(3)-N(5)	1.993(4)	Cu(2)-O(1)	2.342(2)
						Cu(3)-N(4)	2.070(4)	Cu(2)-O(9A)	2.967(4)
						Cu(3)-Cl(5)	2.221(2)		
						Cu(3)-O(61)	2.371(4)		
						Cu(4)-N(12)	1.991(4)		
						Cu(4)-N(11)	1.996(4)		
						Cu(4)-N(10)	2.087(4)		
						Cu(4)-Cl(4)	2.245(2)		
						Cu(4)-O(4)	2.322(4)		
Cl(1)-Cu-Cl(2)	123.91(3)	N(1)-Cu(1)-N(2)	84.8(1)	Cl(1)-Cu(1)-Cl(2)	115.1(1)	N(2)-Cu(1)-N(3)	161.7(2)	N(3)-Cu(1)-N(1)	164.95(7)
Cl(1)-Cu-N(1)	127.55(6)	N(1)-Cu(1)-N(11)	127.7(1)	Cl(1)-Cu(1)-N(1)	103.8(1)	N(2)-Cu(1)-N(1)	80.6(2)	N(3)-Cu(1)-O(13)	94.10(7)
Cl(1)-Cu-N(11)	96.43(6)	N(1)-Cu(1)-N(21)	106.7(1)	Cl(1)-Cu(1)-N(11)	92.4(1)	N(3)-Cu(1)-N(1)	81.3(2)	N(1)-Cu(1)-O(13)	98.63(7)
Cl(1)-Cu-N(21)	95.28(6)	N(1)-Cu(1)-N(31)	83.9(1)	Cl(1)-Cu(1)-N(21)	95.7(1)	N(2)-Cu(1)-Cl(2)	96.5(2)	N(3)-Cu(1)-N(2)	83.46(6)
Cl(2)-Cu-N(1)	108.52(6)	N(2)-Cu(1)-N(11)	82.5(1)	Cl(2)-Cu(1)-N(1)	141.1(1)	N(3)-Cu(1)-Cl(2)	97.1(2)	N(1)-Cu(1)-N(2)	82.97(6)
Cl(2)-Cu-N(11)	91.32(6)	N(2)-Cu(1)-N(21)	81.4(1)	Cl(2)-Cu(1)-N(11)	96.8(1)	N(1)-Cu(1)-Cl(2)	130.5(2)	O(13)-Cu(1)-N(2)	173.03(7)
Cl(2)-Cu-N(21)	94.35(6)	N(2)-Cu(1)-N(31)	164.7(1)	Cl(2)-Cu(1)-N(21)	95.1(1)	N(2)-Cu(1)-Cl(1)	94.0(2)	N(3)-Cu(1)-O(2)	101.47(7)
N(1)-Cu-N(11)	79.97(8)	N(11)-Cu(1)-N(21)	121.0(1)	N(1)-Cu(1)-N(11)	81.2(1)	N(3)-Cu(1)-Cl(1)	92.9(2)	N(1)-Cu(1)-O(2)	86.93(6)
N(1)-Cu-N(21)	81.17(8)	N(11)-Cu(1)-N(31)	112.6(1)	N(1)-Cu(1)-N(21)	80.5(1)	N(1)-Cu(1)-Cl(1)	120.4(2)	O(13)-Cu(1)-O(2)	88.55(6)
N(11)-Cu-N(21)	161.14(9)	N(21)-Cu(1)-N(31)	91.9(1)	N(11)-Cu(1)-N(21)	161.2(1)	Cl(2)-Cu(1)-Cl(1)	109.1(1)	N(2)-Cu(1)-O(2)	98.33(6)
		N(1A)-Cu(1A)-N(2A)	84.5(1)	Cl(3)-Cu(2)-Cl(4)	129.6(1)	N(8)-Cu(2)-N(9)	164.5(2)	O(2)-Cu(1)-O(8)	166.95(5)
		N(1A)-Cu(1A)-N(11A)	127.4(1)	Cl(3)-Cu(2)-N(2)	124.5(1)	N(8)-Cu(2)-N(7)	82.5(2)	N(1)-Cu(1)-O(8)	83.25(5)
		N(1A)-Cu(1A)-N(21A)	110.1(1)	Cl(3)-Cu(2)-N(31)	95.2(1)	N(9)-Cu(2)-N(7)	83.2(2)	N(2)-Cu(1)-O(8)	89.01(5)
		N(1A)-Cu(1A)-N(31A)	83.3(1)	Cl(3)-Cu(2)-N(41)	95.7(1)	N(8)-Cu(2)-Cl(3)	98.0(2)	N(3)-Cu(1)-O(8)	90.04(5)
		N(2A)-Cu(1A)-N(11A)	82.7(1)	Cl(4)-Cu(2)-N(2)	105.9(1)	N(9)-Cu(2)-Cl(3)	97.5(2)	O(13)-Cu(1)-O(8)	84.46(5)
		N(2A)-Cu(1A)-N(21A)	81.7(1)	Cl(4)-Cu(2)-N(31)	92.6(1)	N(7)-Cu(2)-Cl(3)	157.3(2)	N(4)-Cu(2)-N(6)	162.20(7)
		N(2A)-Cu(1A)-N(31A)	164.4(1)	Cl(4)-Cu(2)-N(41)	91.7(1)	N(8)-Cu(2)-Cl(1)	85.5(2)	N(4)-Cu(2)-O(14)	96.21(7)
		N(11A)-Cu(1A)-N(21A)	118.0(1)	N(2)-Cu(2)-N(31)	80.3(1)	N(9)-Cu(2)-Cl(1)	90.1(2)	N(6)-Cu(2)-O(14)	93.09(7)
		N(11A)-Cu(1A)-N(31A)	112.5(1)	N(2)-Cu(2)-N(41)	81.4(1)	N(7)-Cu(2)-Cl(1)	95.3(2)	N(4)-Cu(2)-N(5)	83.29(6)
		N(21A)-Cu(1A)-N(31A)	93.4(1)	N(31)-Cu(2)-N(41)	161.7(1)	Cl(3)-Cu(2)-Cl(1)	107.4(1)	N(6)-Cu(2)-N(5)	83.91(7)
						N(6)-Cu(3)-N(5)	162.8(2)	O(14)-Cu(2)-N(5)	165.43(7)
						N(6)-Cu(3)-N(4)	81.6(2)	N(4)-Cu(2)-O(1)	97.68(6)
						N(5)-Cu(3)-N(4)	81.3(2)	N(6)-Cu(2)-O(1)	98.26(6)

Chapter 3

N(6)-Cu(3)-Cl(5)	97.3(2)	O(14)-Cu(2)-O(1)	84.72(7)
N(5)-Cu(3)-Cl(5)	98.7(2)	N(5)-Cu(2)-O(1)	109.80(6)
N(4)-Cu(3)-Cl(5)	166.6(2)	O(1)-Cu(2)-O(9A)	161.98(5)
N(6)-Cu(3)-O(61)	103.5(2)	N(4)-Cu(2)-O(9A)	76.29(5)
N(5)-Cu(3)-O(61)	80.9(2)	N(5)-Cu(2)-O(9A)	86.60(5)
N(4)-Cu(3)-O(61)	96.1(2)	N(6)-Cu(2)-O(9A)	90.65(5)
Cl(5)-Cu(3)-O(61)	97.2(2)	O(14)-Cu(2)-O(9A)	79.17(5)
N(12)-Cu(4)-N(11)	163.2(2)		
N(12)-Cu(4)-N(10)	83.8(2)		
N(11)-Cu(4)-N(10)	81.5(2)		
N(12)-Cu(4)-Cl(4)	98.4(2)		
N(11)-Cu(4)-Cl(4)	98.3(2)		
N(10)-Cu(4)-Cl(4)	156.5(2)		
N(12)-Cu(4)-O(4)	85.3(2)		
N(11)-Cu(4)-O(4)	88.6(2)		
N(10)-Cu(4)-O(4)	97.3(2)		
Cl(4)-Cu(4)-O(4)	106.2(2)		

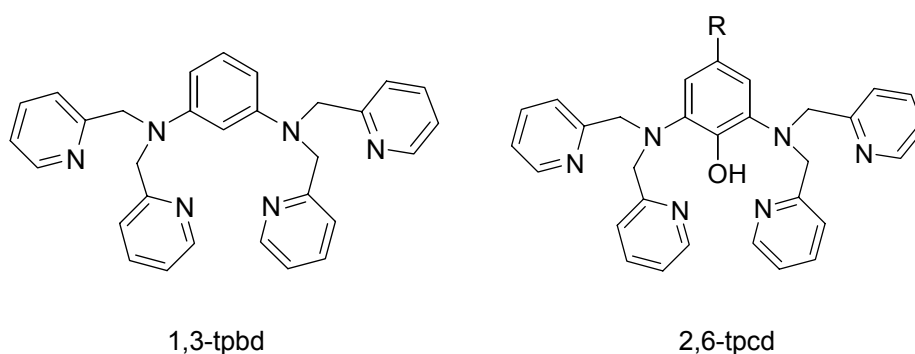
Chapter 4 - Syntheses, Characterization and Reactivity of Iron(II), Nickel(II), Copper(II) and Zinc(II) Complexes of the Ligand 1,3-Bis[bis(2-pyridylmethyl)amino]benzene (1,3-tpbd) and its phenol derivative 2,6-Bis[bis(2-pyridylmethyl)amino]-p-cresol (2,6-tpcd).

This work has been published previously in the *European Journal of Inorganic Chemistry*.

Foxon, S.; Xu, J.-Y.; Turba, S.; Leibold, M.; Hampel, F.; Heinemann, F. W.; Walter, O.; Würtele, C.; Holthausen, M. C.; Schindler, S., *Eur. J. Inorg. Chem.* 2007, 429-443.

4.1 Introduction

Previously we have demonstrated that the ligand 1,3-Bis[bis(2-pyridylmethyl)amino]benzene (1,3-tpbd) shown in Scheme 4-1 can coordinate two copper ions in close proximity.^[26, 34, 39] In this regard copper complexes of 1,3-tpbd or its phenol derivative 2,6-Bis[bis(2-pyridylmethyl)amino]-p-cresol (2,6-tpcd) (Scheme 4-1) represent good structural models of the histidine rich environments found in many dinuclear copper proteins (such as *hemocyanin* and *tyrosinase*).^[4, 5, 10, 26, 108]



Scheme 4-1. The ligands 1,3-Bis[bis(2-pyridylmethyl)amino]benzene (1,3-tpbd) and 2,6-Bis[bis(2-pyridylmethyl)amino]-p-cresol (2,6-tpcd; R = CH₃).

Furthermore, the intramolecular magnetic coupling observed in a series of copper(II) complexes with 1,3-tpbd could be tuned from ferromagnetic to antiferromagnetic.^[34, 39] Similar ferromagnetic coupling has been observed for copper complexes with a related *m*-phenylenediamine based ligand system.^[33, 40] Recently, a 1,3-tpbd

platinum complex has been used in mechanistic studies.^[109] However to date, only a small number of transition metal complexes of related derivatives of the 1,3-tpbd ligand system have been investigated.^[25, 27, 86, 87, 110-116]

To gain further understanding of the ligating ability of 1,3-tpbd, we herein describe the synthesis and characterization of a series of iron(II), zinc(II) and copper(II) complexes with 1,3-tpbd as well as a copper(II) complex of the phenol analogue of 1,3-tpbd. A similar complex with the phenol derivative ligand shown in Scheme 4-1 (R = *t*-butyl) and its interesting properties (e.g. interactions with DNA) was recently reported by Karlin and co-workers.^[112, 113]

4.2 Results and Discussion

4.2.1 Ligand Syntheses

1,3-Bis[bis(2-pyridylmethyl)amino]benzene (1,3-tpbd). 1,3-tpbd was prepared in modest yields from commercially available *m*-phenylenediamine and picolylchloride hydrochloride as previously reported.^[26] Single Crystals of 1,3-tpbd, suitable for structural characterization, were obtained by slow evaporation of a methanol solution of 1,3-tpbd in a glove box. Attempts to recrystallize the ligand outside of the glove box often caused the formation of nearly colourless crystals in a slightly brown mother liquid. The solution turned to an intensive red colour during a couple of days affecting the crystals as well (most likely the ligand is partially oxidized) and as a consequence numerous attempts to solve the crystal structure failed due to poor refinement. A summary of crystal structure data and refinement parameters is presented in Table 4-1, selected bond lengths and angles in Table 4-3. The molecular structure of 1,3-tpbd is shown in Figure 4-1. The two pyridyl units bonded at each amine nitrogen atom are separated from each other by a large distance similar to the previously reported molecular structure of 1,4-tpbd.^[86] 1,3-tpbd crystallizes with one additional methanol solvent molecule per unit, oxygen bound hydrogen atoms of the methanol solvent molecule were located in a difference fourier map and isotropically refined.

Protonation of 1,3-tpbd or coordination of 1,3-tpbd to metal ions has the consequence that the pyridyl units move much closer together.

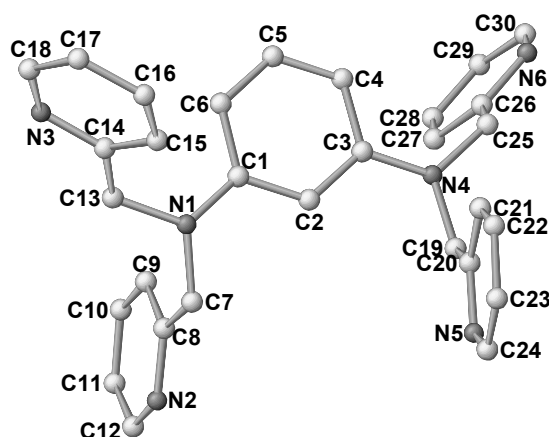


Figure 4-1. Molecular structure of 1,3-tpbd. Hydrogen atoms are omitted for clarity.

In Figure 4-2 the molecular structure of the cation of $[1,3\text{-tpbdH}_2](\text{ClO}_4)_2$ is shown (crystal structure data and refinement parameters, bond lengths and angles are presented in Tables 4-1 and 4-3).

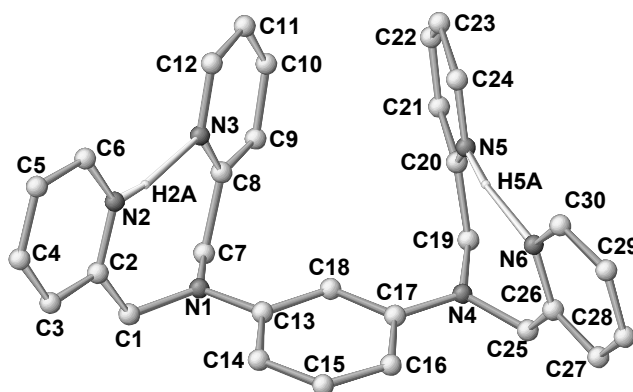


Figure 4-2. Molecular structure of the cation of $[1,3\text{-tpbdH}_2](\text{ClO}_4)_2$. Only hydrogen atoms involved in hydrogen bonding are shown.

$[1,3\text{-tpbdH}_2](\text{ClO}_4)_2$ crystallizes with two molecules per crystallographically independent unit of the unit cell together with three molecules of acetonitrile. Two of the ClO_4^- anions are disordered. The H atoms of the protonated N atoms were localized in a difference fourier map and refined isotropically. The crystal structures of 1,3-tpbd and $[1,3\text{-tpbdH}_2]^{2+}$ display similar metrical parameters. The immediate geometry around the aliphatic amine nitrogen atoms is nearly planar with C(1)-N(1) 1.388(2) Å in 1,3-tpbd and C(13)-N(1) 1.396(4) Å in $[1,3\text{-tpbdH}_2](\text{ClO}_4)_2$ indicating delocalization of the nitrogen lone pair of electrons with the aromatic π -systems. All the inter-bond angles around the aliphatic amine nitrogen atoms are close to 120° . However, as discussed above, the positions of the pyridine rings in 1,3-tpbd and its

protonated derivative are quite different. In $[1,3\text{-tpbdH}_2]^{2+}$ adjacent pyridine nitrogen atoms on each ligand “arm” [N(2) and N(3), N(5) and N(6)] are strongly hydrogen-bonded to one another. The average distance between the hydrogen-bonded pyridine nitrogen atoms is 2.741 Å. Additionally we obtained the protonated triflate salt of 1,3-tpbd (see Table 4-1 and 4-2.) of which the cation is identical to $[1,3\text{-tpbdH}_2](\text{ClO}_4)_2$. However, the two crystal structures differ from each other due to the crystal packing arrangement of the anions and furthermore the inclusion of additional solvent molecules. In principle these protonated ligand salts are comparable to the metal complexes (see below) and the protons in $[1,3\text{-tpbdH}_2]^{2+}$ can be regarded as small metal cations. The previously reported crystal structure of $[1,4\text{-tpbdH}_2]^{2+}$ displays similar bond distances and angles to the $[1,3\text{-tpbdH}_2]^{2+}$ structure described above.^[86]

Syntheses of the complexes.

4.2.2 Iron complexes.

Ligands capable of coordinating two iron ions in close proximity have been employed as structural models for dinuclear iron metalloproteins (e. g. the oxygen carrier protein hemerythrin).^[3, 117, 118] Prior to the investigations of the oxygen sensitive iron(II) model compounds, we tried to synthesize and structurally characterize an iron(III) complex of 1,3-tpbd. However, all our efforts to date in obtaining an iron(III) 1,3-tpbd complex were unsuccessful. Numerous attempts (employing different reaction conditions) to synthesize $[\text{Fe}_2(1,3\text{-tpbd})]^{6+}$ derivatives, such as $[\text{Fe}_2(1,3\text{-tpbd})(\text{DMF})_6]^{6+}$ or $[\text{Fe}_2(1,3\text{-tpbd})(\text{RCOO})_n]^{(6-n)+}$, by the reaction of 1,3-tpbd with $\text{Fe}(\text{ClO}_4)_3$ in different solvents (coordinating or non-coordinating), with and without addition of anions such as AsO_4^{3-} , $\text{C}_6\text{H}_5\text{COO}^-$, CH_3COO^- or Cl^- only afforded the protonated free ligand and unreacted iron salts. Over a period of weeks single crystals, suitable for X-ray structural analysis, of $[1,3\text{-tpbdH}_2](\text{SO}_3\text{CF}_3)_2$ (see Experimental Section) and $[1,3\text{-tpbdH}_2](\text{ClO}_4)_2$ described above (Figure 4-3) were obtained. Furthermore, efforts in obtaining an iron(III) 1,3-tpbd complex by oxidizing the corresponding iron(II) precursor complex (described below) failed. These results clearly indicate that the 1,3-tpbd ligand has a low affinity for iron(III). In the presence of water, protonation of the ligand occurs, however in the absence of protons no complexation of the iron(III) ions was observed either. Other pyridyl containing

ligands are known to stabilize iron(II) relative to iron(III), however in these cases it was still possible to synthesize, isolate and characterize the according iron(III) complexes.^[119]

An iron(II) complex of 1,3-tpbd was prepared and single crystals of $[\text{Fe}_2(1,3\text{-tpbd})(\text{CH}_3\text{CN})_6](\text{ClO}_4)_4 \times 2 \text{ CH}_3\text{CN} \times 0.5 \text{ H}_2\text{O}$ (**12**) were grown. The molecular structure of the cation $[\text{Fe}_2(1,3\text{-tpbd})(\text{CH}_3\text{CN})_6]^{4+}$ of **12** is shown in Figure 4-3 (crystal structure data and refinement parameters, bond lengths and angles are presented in Tables 4-1 and 4-3). The unit cell of **12** consists of two sets of crystallographically independent dinuclear cations, $[\text{Fe}_2(1,3\text{-tpbd})(\text{CH}_3\text{CN})_6]^{4+}$, and uncoordinated perchlorate anions, four acetonitrile solvent molecules and one water molecule. There are only minor structural differences between the two dinuclear cations. In each cation, the intramolecular Fe...Fe separation is 7.488(1) and 7.697(2) Å, respectively. The 1,3-tpbd ligand coordinates each iron(II) center via two pyridine nitrogen atoms and one aliphatic amine nitrogen atom, displaying $\text{N}_{\text{amine}}\text{-Fe-N}_{\text{pyridine}}$ angles averaging $\sim 81^\circ$ to accommodate the five-membered chelate rings.

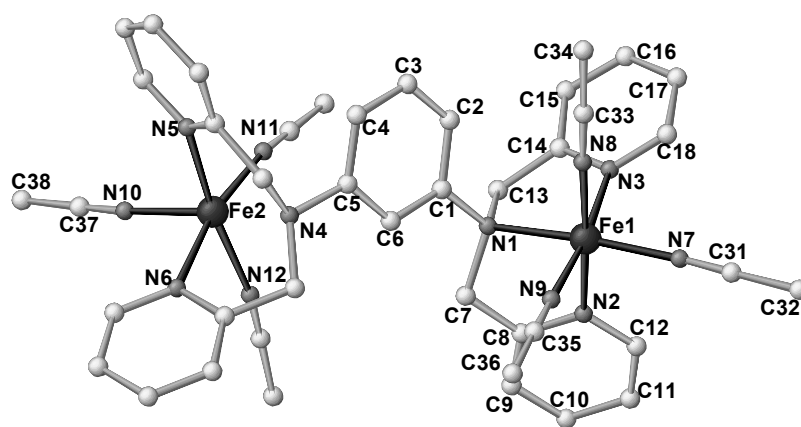


Figure 4-3. Molecular structure of the cation of $[\text{Fe}_2(1,3\text{-tpbd})(\text{CH}_3\text{CN})_6](\text{ClO}_4)_4 \times 2 \text{ CH}_3\text{CN} \times 0.5 \text{ H}_2\text{O}$ (**12**). Hydrogen atoms and solvent molecules are omitted for clarity.

As has been observed previously for Fe^{II} TPA complexes, the $\text{Fe-N}_{\text{amine}}$ distances ranging from 2.095(2) to 2.280(3) Å are characteristically longer than the $\text{Fe-N}_{\text{pyridine}}$ bond lengths of 1.966(3) to 2.188(3) Å.^[120-122] Three *fac*-coordinated acetonitrile molecules occupy the remaining coordination sites to complete the slightly distorted octahedral coordination geometry around each iron(II) center, with Fe-N-C angles ranging from 166.7(3) to 177.1(3)° and the Fe-N distances ranging from 1.953(3) to 2.183(3) Å. These shorter Fe-N distances indicate that the nitrile groups of the

acetonitrile solvent molecules are strongly coordinated to the iron(II) center. Intermolecular $\pi\cdots\pi$ interactions (ca. 3.675 Å) exist between C(26)-C(27)-C(28)-C(29)-C(30)-N(6) and C(56)-C(57)-C(58)-C(59)-C(60)-N(15) of adjacent pyridine rings from two independent dinuclear cations.

Furthermore, a second iron(II) complex, $[\text{Fe}_2(1,3\text{-tpbd})(\text{DMF})_6](\text{ClO}_4)_4$ (**13**), was prepared. The molecular structure of the cation of complex **13** is shown in Figure 4-4 (crystal structure data and refinement parameters, bond lengths and angles are presented in Tables 4-1 and 4-3). **13** crystallizes with half a molecule per crystallographic independent unit of the unit cell, the other half is generated by the crystallographic two-fold axis of the space group. Each iron(II) center lies in a distorted N_3O_3 octahedral coordination environment. The equatorial plane around Fe(1) comprises two pyridyl nitrogen atoms [N(2) and N(3)] from the *fac*-coordinated 1,3-tpbd ligand and two oxygen atoms [O(1) and O(2)] from coordinated DMF solvent molecules. Apical positions are occupied by the tertiary amine nitrogen N(1) of 1,3-tpbd and oxygen atom O(3) from a third DMF solvent molecule. The Fe- $\text{N}_{\text{pyridine}}$ bond lengths [2.152(2)-2.174(2) Å] are characteristically shorter than those of Fe- N_{amine} [2.312(2) Å] and the *cis* $\text{N}_{\text{pyridine}}\text{-Fe-}\text{N}_{\text{pyridine}}$ angles [92.03°] are entirely consistent with those found in **12**. The Fe- O_{DMF} distances [2.075(2) to 2.112(2) Å] and the average *cis*-coordinated angles [O-Fe-O 92.58°] indicate that the DMF molecules are strongly coordinated to the iron(II) center. The Fe \cdots Fe separation of 6.962 Å is shorter than in **12**, probably a consequence of the stronger $\pi\cdots\pi$ interaction (ca. 3.596 Å) between the two pyridine rings (C(2)-C(3)-C(4)-C(5)-C(6)-N(2) and C(2A)-C(3A)-C(4A)-C(5A)-C(6A)-N(2A)) each from a different tridentate end of the 1,3-tpbd molecule.

Both iron(II) complexes were found to only react slowly with dioxygen, however much faster with hydrogen peroxide. Preliminary kinetic studies of both oxidation reactions indicated complex reaction mechanisms that could not be elucidated. Most likely this is a consequence that 1,3-tpbd is not an innocent ligand and is also involved in the oxidation reactions (see below). Furthermore, efforts to isolate reaction products from these oxidations, such as the according iron(III) complexes described above, were unsuccessful. In contrast with 1,4-tpbd as a ligand only polymeric iron(II) complexes were obtained.^[115] With *N,N*-Bis(2-pyridylmethyl)aniline (phbpa), the half ligand system to 1,3-tpbd, a 2:1 ligand : metal ion ratio was observed, however, no crystal structures were reported.^[87]

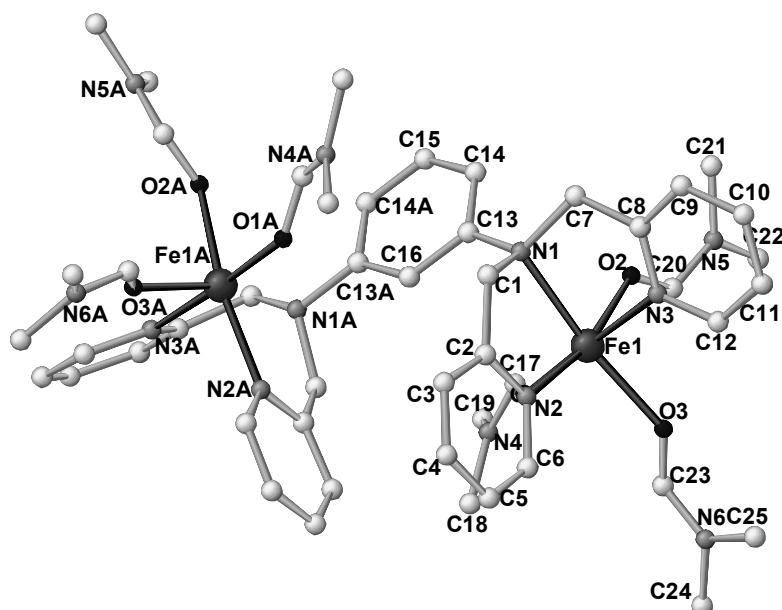


Figure 4-4. Molecular structure of the cation of $[\text{Fe}_2(1,3\text{-tpbd})(\text{DMF})_6](\text{ClO}_4)_4$ (**13**). Hydrogen atoms are omitted for clarity.

4.2.3 Nickel complex.

Reacting $[\text{Ni}(\text{DMF})_6](\text{ClO}_4)_2$ with 1,3-tpbd under anaerobic conditions in a glove box led to the nickel(II) analogue of **13**, $[\text{Ni}_2(1,3\text{-tpbd})(\text{DMF})_6](\text{ClO}_4)_4$ (**14**). Crystals suitable for X-ray crystallography were grown and isolated. **14** crystallizes with nearly identical cell parameters as **13** (Table 4-1) but the structure of **14** is much better described in the monoclinic space group C2 (**14**) than C2/c (**13**). Accordingly the systematic absences for the glide mirror plane in C2/c for **14** are not observed where for **13** these systematic absence conditions are fulfilled absolutely so that the structure of **13** is described correctly C2/c. However, a description of the structure of **14** in C2/c is possible but leads to a significant increase of the R_1 -value from 10 to 16 percent. Therefore even if it can be assumed from the cell parameters that **13** and **14** are isostructural the crystal structure of **14** here is presented in the lower symmetric space group C2. A figure of the molecular structure of the cation of **14** is shown in Figure 4-5. The crystal structure data and selected bond lengths and angles are presented in Table 4-1 and 4-3.

The asymmetric unit of complex **14** comprises two crystallographically independent “half” cation units and four ClO_4^- anions, of which three are disordered. The full

content of the unit cell is generated by applying symmetry operations to the asymmetric unit cell.

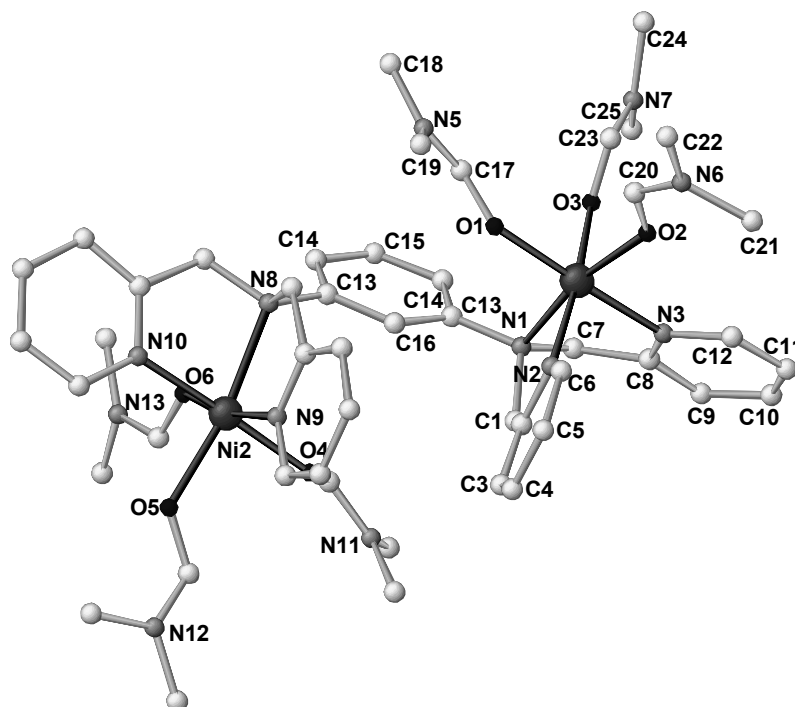


Figure 4-5. Molecular structure of the cation of $[\text{Ni}_2(1,3\text{-tpbd})(\text{DMF})_6](\text{ClO}_4)_4$ (**14**). Hydrogen atoms are omitted for clarity.

As the structure of **14** is very similar to that of **13** and the calculations might be performed as well in the centrosymmetric space group $C2/c$ the final absolute structure parameter is relatively high. The two crystallographically independent $[\text{Ni}_2(1,3\text{-tpbd})(\text{DMF})_6]^{2+}$ cations of **14** differ only marginally with regard to their bond lengths and angles.

4.2.4 Zinc complexes.

In investigating redox active metal complexes of iron and copper it is useful to study in comparison complexes with non-redox active centers such as zinc. Copper(II) ions can be substituted by zinc(II) ions and additionally show quite similar coordination behavior. Such zinc(II) complexes themselves can show interesting reaction properties, for example they can be used to hydrolyze diribonucleoside monophosphate diesters.^[123] However, in contrast to our expectations the synthesis of a zinc(II) complex of 1,3-tpbd turned out to be more difficult than the synthesis of the according copper(II) complexes. Mixing zinc(II) perchlorate and 1,3-tpbd in an

alcoholic solution, immediately led to white gelatinous like precipitates that could not be (re)crystallized. Only after a large number of experiments (applying different conditions), we obtained crystals of the zinc(II) complex $[\text{Zn}_2(1,3\text{-tpbd})(\text{CH}_3\text{CN})_2(\text{SO}_3\text{CF}_3)_2(\text{H}_2\text{O})](\text{SO}_3\text{CF}_3)_2$ (**15**) with triflate as a counter anion. The molecular structure of the cation of **15** in Figure 4-6 shows an unsymmetrical di-zinc unit, both ions linked by the *m*-phenylenediamine group and a triflate ion giving an intramolecular Zn...Zn distance of 6.007(1) Å, which is much shorter than in those complexes that are only bridged by 1,3-tpbd. However, it is close to the Cu...Cu distance [5.873(1) Å] in the analogous complex $[\text{Cu}_2(1,3\text{-tpbd})(\text{H}_2\text{O})_2(\text{ClO}_4)_3](\text{ClO}_4)$ with an additional perchlorate- instead of the triflate-bridge (crystal structure data and refinement parameters, selected bond lengths and angles are presented in Tables 4-2 and 4-3).^[26]

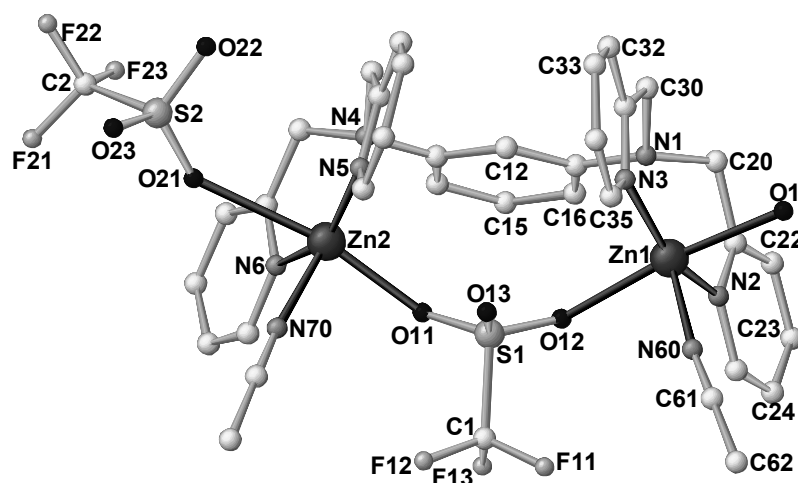
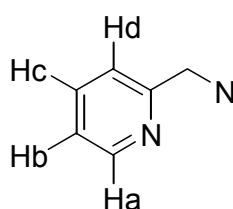


Figure 4-6. Molecular structure of the cation of $[\text{Zn}_2(1,3\text{tpbd})(\text{CH}_3\text{CN})_2(\text{SO}_3\text{CF}_3)_2(\text{H}_2\text{O})](\text{SO}_3\text{CF}_3)_2$ (**15**). Hydrogen atoms are omitted for clarity.

The coordination geometry around Zn(1) is best described as distorted octahedral. The equatorial plane around the zinc(II) center is occupied by three N-donor atoms of the meridional capping ligand 1,3-tpbd (N(1), N(2) and N(3)). Apical positions are occupied by O(12) of the bridging triflate anion and O(1) of a water molecule. The nature of the ligands around Zn(2) differs from Zn(1) in that a terminal triflate, instead of a water molecule, occupies one of the apical coordination sites. The $\text{N}_{\text{pyridine}}\text{-Zn-}\text{N}_{\text{pyridine}}$ bond angles of $156.1(2)^\circ$ and $152.3(2)^\circ$ in **15** are smaller than $\text{N}_{\text{pyridine}}\text{-Cu-}\text{N}_{\text{pyridine}}$ in $[\text{Cu}_2(1,3\text{-tpbd})(\text{H}_2\text{O})_2](\text{ClO}_4)_4 \times 4 \text{ H}_2\text{O}$ [$164.5(2)^\circ$] apparently owing to the

bigger steric hindrance of the triflate ion. Accordingly, both distances of Zn-N_{pyridine} in the range of 2.021(5)-2.046(5) Å and Zn-N_{amine} at 2.350(5) and 2.346(4) Å are longer than those in [Cu₂(1,3-tpbd)(H₂O)₂](ClO₄)₄ × 4 H₂O (av. Cu-N_{pyridine} 1.969(5) Å; Cu-N_{amine} 2.089(5) Å). This also applies for the distance of the acetonitrile substituent [Zn-N_{C≡N} av. 2.091(5) Å] instead of water [Cu-O_w 1.985(5) Å] at the fourth equatorial site. A triflate anion bridges the two zinc(II) centers *via* O(11) and O(12) [Zn(1)-O(12) = 2.242(4) Å and Zn(2)-O(11) = 2.122(4) Å]. The structure is “capped” at the apical positions by a water molecule [Zn(1)-O(1) 2.243(5) Å] for Zn(1) and by a terminal triflate anion [Zn(2)-O(21) 2.578(4) Å]. To the best of our knowledge there is only one further example of a crystal structure containing a bridging triflate anion linking two zinc(II) ions found in the Cambridge Crystallographic Database.^[124] Efforts to obtain crystals of the copper(II)-1,3-tpbd triflate analogue failed so far. Furthermore, using 1,4-tpbd as a ligand only a mononuclear zinc complex, [ZnCl₂(1,4-tpbd)], was obtained and its crystal structure has been reported.^[115]

In contrast to the according copper(II) complexes **15** is diamagnetic and can be studied in solution by ¹H NMR spectroscopy. Four types of pyridine proton resonances are found in the range 7.4- 8.6 ppm (see Experimental Section). These four proton resonances represent four symmetry equivalent sets of the pyridine protons found in the complex. Two triplets and two doublets are formed by the splitting of each pyridine proton by its adjacent proton(s). The splitting scheme is depicted in Scheme 4-2. H_a is split into a doublet by H_b (*J* = 5 Hz), and H_d is split into a doublet by H_c (*J* = 8 Hz). Proton H_a is assigned to the downfield doublet, and H_d as the upfield doublet. H_b is split by both H_a (*J* = 6 Hz) and H_c (*J* = 7 Hz) to form a triplet, and H_c is split by both H_b (*J* = 7 Hz) and H_d (*J* = 8 Hz) to form a triplet. H_c is assigned to the downfield triplet, and H_b is assigned to the upfield triplet. The assignments of H_c and H_b are based on greater stabilisation of electron withdrawal in the *para* position, compared to the *meta* position, and previous assignments of pyridine protons in related compounds.^[125]



Scheme 4-2. NMR-assignment in complexes **12**, **13** and **15**.

4.2.5 Heterodinuclear zinc(II) and copper(II) complexes.

After achieving the synthesis of a zinc(II) complex as well as the previously reported copper(I) and copper(II) complexes with the ligand 1,3-tpbd, it was obvious that we should try to prepare a heterodinuclear zinc(II) copper(II) complex as a model complex for the enzyme superoxide dismutase (CuZnSOD).^[126-132] However, mixing stoichiometric amounts of 1,3-tpbd together with zinc(II) and copper(II) chloride did not lead to the isolation of pure $[\text{CuZn}(1,3\text{-tpbd})\text{Cl}_4]$, but instead to a mixture of the three dinuclear complexes: $[\text{Zn}_2(1,3\text{-tpbd})\text{Cl}_4]$ (**16**), $[\text{Cu}_2(1,3\text{-tpbd})\text{Cl}_4]$ (**8**) and $[\text{CuZn}(1,3\text{-tpbd})\text{Cl}_4]$ (**17**). Structural characterization of all three complexes was achieved by picking individual crystals (that were different in color) from the reaction mixture. The molecular structure of **16** is shown in Figure 4-7 and that of **17** in Figure 4-8 (crystal structure data and refinement parameters, bond lengths and angles are presented in Tables 4-2 and 4-3).

The crystal structure of $[\text{Cu}_2(1,3\text{-tpbd})\text{Cl}_4]$ (**8**) has been obtained previously in a different study and crystallographic details will be published elsewhere.^[111] Due to the fact that here X-ray crystallography measurements do not allow the differentiation between zinc and copper ions, the presence of the different metal ions was further confirmed by photon-induced X-ray emission spectroscopy of the crystals of **16**, **8** and **17**.

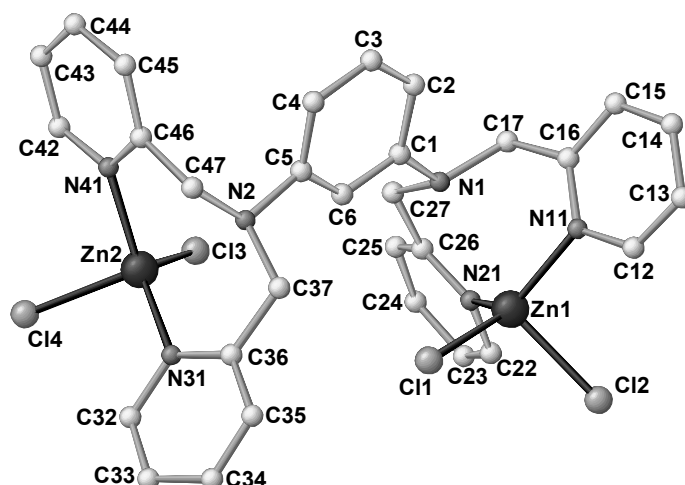


Figure 4-7. Molecular structure of $[\text{Zn}_2(1,3\text{-tpbd})\text{Cl}_4]$ (**16**). Hydrogen atoms are omitted for clarity.

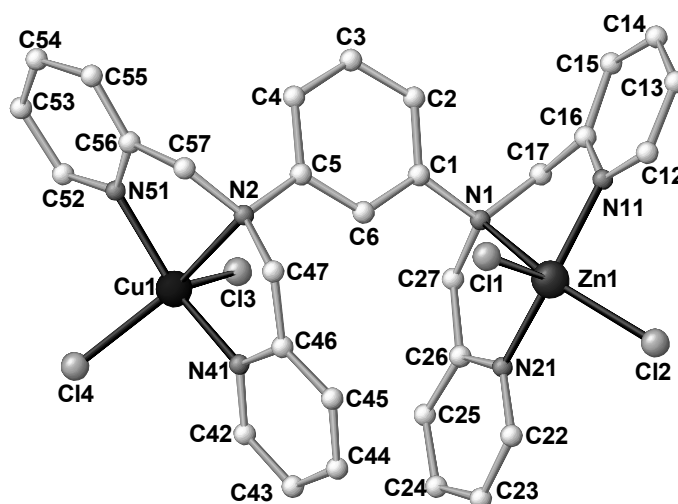


Figure 4-8. Molecular Structure of $[\text{CuZn}(1,3\text{-tpbd})\text{Cl}_4]$ (**17**). Hydrogen atoms are omitted for clarity.

The metal ions are linked *via* the 1,3-phenylenediamine group leading to an intramolecular $\text{Zn}\cdots\text{Zn}$ distance of 6.925 Å for **16** and $\text{Cu}\cdots\text{Zn}$ separation of 6.849 Å for **17**, both of them shorter than the $\text{Cu}\cdots\text{Cu}$ distance of 7.434 Å for **8**. In **16**, the zinc(II) ions are penta-coordinated by three nitrogen atoms of the 1,3-tpbd ligand and two chloride ions, with the following distances: $\text{Zn}(1)\text{-Cl}(1) = 2.248(2)$, $\text{Zn}(1)\text{-Cl}(2) = 2.305(2)$, average $\text{Zn}(1)\text{-N}_{\text{pyridine}} = 2.050(6)$ and $\text{Zn}(1)\text{-N}_{\text{amine}} = 2.646(2)$ Å. Considering such weak N_{amine} -ligation to zinc(II) ions, the coordination geometry around $\text{Zn}(1)$ and $\text{Zn}(2)$ can be described as distorted trigonal bipyramidal. The axial positions of the coordination sphere around $\text{Zn}(1)$ are occupied by $\text{N}(1)$ and $\text{Cl}(2)$ and the equatorial plane of the ZnN_3Cl_2 unit comprises $\text{N}(11)$, $\text{N}(22)$ and $\text{Cl}(1)$ with $\text{Zn}(1)$ lying out of the basal plane by 0.2956 Å. Compared to the mononuclear zinc(II) 1,4-tpbd complex with $\text{Zn-N}_{\text{pyridine}}$ average distance 2.14(1) Å and $\text{Zn-N}_{\text{amine}} = 2.26(1)$ Å, where the $\text{Zn-N}_{\text{pyridine}}$ distance is significantly longer and the $\text{Zn-N}_{\text{amine}}$ distance is significantly shorter than in **16**.^[115] In **17**, both coordination geometries around the copper(II) and zinc(II) centers are close to trigonal bipyramidal with $\text{N}(41)$ and $\text{N}(51)$ occupying the axial positions around $\text{Cu}(1)$ and $\text{N}(11)$ and $\text{N}(21)$ occupying the axial positions of $\text{Zn}(1)$. Similar to complex **16**, the three nitrogen atoms of one tridentate end of the 1,3-tpbd ligand and the metal center to which they are coordinated are almost coplanar, with $\text{Cu-N}_{\text{pyridine}}$ average distance 2.054(2) and $\text{Cu-N}_{\text{amine}} = 2.499(2)$ Å, $\text{Zn-N}_{\text{pyridine}}$ average distance 2.034(2) and $\text{Zn-N}_{\text{amine}} = 2.370(2)$ Å. The Cu-Cl distances are very close to each other [2.279(3) and 2.284(3) Å], likewise for the Zn-Cl bonds [2.307(4) and 2.333(3) Å]. The $\text{Zn-N}_{\text{pyridine}}$ and $\text{Cu-N}_{\text{pyridine}}$ distances are in

accordance to those determined for related mononuclear analogues, in contrast the Zn-N_{amine} and Cu-N_{amine} distances in the mononuclear complexes of 2.142(2) Å and 2.207(6) Å are significantly shorter.^[133, 134] However, these complexes are complexes with a different ligand to metal cation ratio (one metal ion and two coordinated bispicolylamine ligands) at the amine nitrogen atom and the hydrogen atom is not substituted by an organic group.

4.2.6 "Zinc ion assisted" formation of a dinuclear copper complex.

During our efforts to prepare model complexes for CuZnSOD described above, we observed a very surprising reaction behavior when stoichiometric mixtures of copper(II) and zinc(II) perchlorate salts were mixed with 1,3-tpbd. Instead of obtaining the heterodinuclear complex, we isolated a new dinuclear copper(II) complex, [Cu₂(1,3-tpbd)₂(H₂O)₂](ClO₄)₄ (**18**), in which two copper(II) ions had reacted with two 1,3-tpbd ligand units. The molecular structure of the cation of complex **18** is shown in Figure 4-9 (crystal structure data and refinement parameters, bond lengths and angles are presented in Tables 4-2 and 4-3).

Complex **18** is a so called "dimetallocyclophane" and it is interesting to compare its structure with the dinuclear complex, [Cu₂L'₂(H₂O)₂](ClO₄)₄ x 2 H₂O, obtained previously from an impurity that was formed during the synthesis of 1,3-tpbd.^[26] The "impurity" L' is a derivative of the 1,3-tpbd ligand, missing one pyridyl "arm" (derived from incomplete formation of 1,3-tpbd during synthesis). A schematic presentation of the complex with the "impurity" as ligand in comparison with **17** is shown in Scheme 4-3.

Complex **18** likewise crystallizes with an inversion center located in the middle of the "dimetallocyclophane" core. However, the metal coordination sphere is quite different to that of [Cu₂L'₂(H₂O)₂](ClO₄)₄ x 2 H₂O. The copper(II) ions in **18** exhibit a "4+1" square-based pyramidal geometry with three nitrogens (N(1), N(2) and N(3)) from one tridentate end of 1,3-tpbd in the meridional form, and the pyridine (N(5A)) from the symmetry-related ligand completing the basal plane, while a water molecule (O(1)) occupies the apical site. In **18** the tertiary amine (N(4A)) from the symmetry-related ligand is not bound to the copper(II) center with a long distance of 4.472 Å, while the corresponding nitrogen (N(2)) as a secondary amine is coordinated to the

copper(II) center with a bond length of 2.071(2) Å in the corresponding $[\text{Cu}_2\text{L}'_2(\text{H}_2\text{O})_2](\text{ClO}_4)_4 \times 2 \text{H}_2\text{O}$ complex.

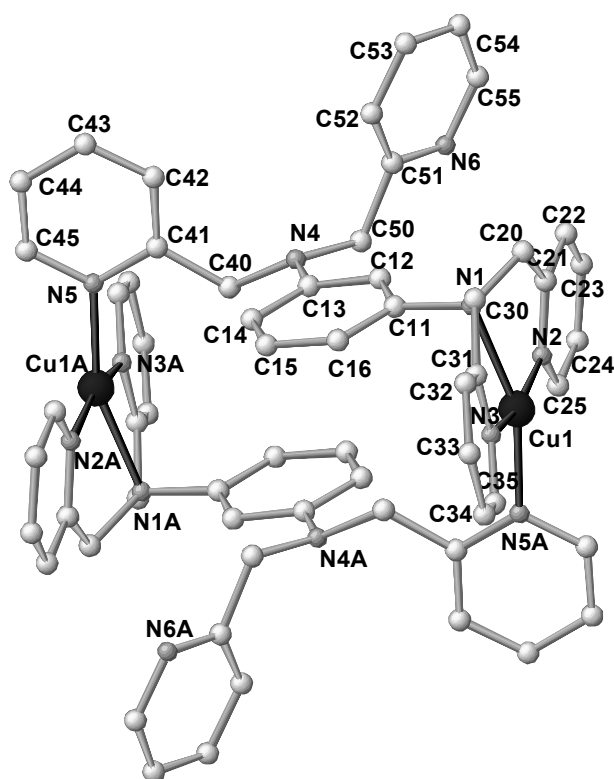
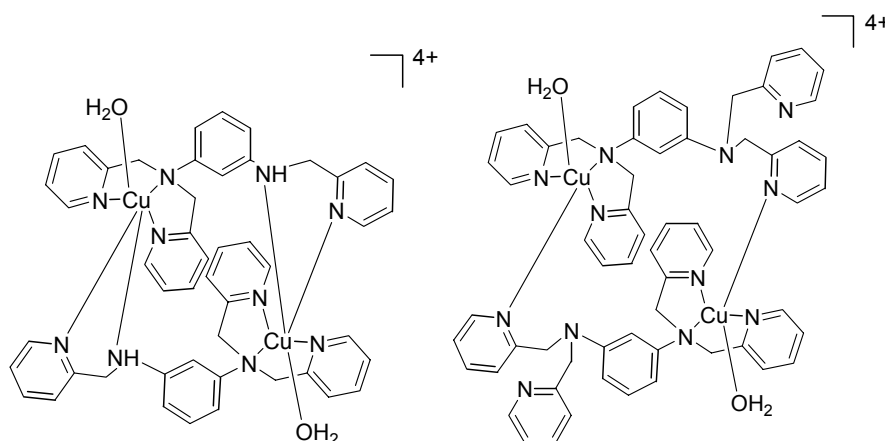


Figure 4-9. Molecular structure of the cation of $[\text{Cu}_2(1,3\text{-tpbd})_2(\text{H}_2\text{O})_2](\text{ClO}_4)_4$ (**18**). Water molecules and Hydrogen atoms are omitted for clarity.

The two pyridyl “arms” from the same tertiary amine are *trans* to one another [N(2)-Cu(1)-N(3) 164.8(2)°], [Cu(1)-N(2) = 1.986(3), Cu(1)-N(3) = 1.976(3) Å]. However, the corresponding two pyridyl nitrogens in $[\text{Cu}_2\text{L}'_2(\text{H}_2\text{O})_2](\text{ClO}_4)_4 \times 2 \text{H}_2\text{O}$ are *cis*-coordinated to copper(II) with a N(11)-Cu(1)-N(12) angle of 86.2(5)°. In complex **18**, all the Cu-N_{pyridine} lengths are in general slightly shorter than the *trans* Cu-N(1)_{amine} [2.074(3) Å]. The steric influence of the non-coordinated pyridine ring results in the different coordination geometry and an intramolecular distance of Cu⋯Cu (8.820(1) Å) which is 1.3 Å longer than that of $\text{Cu}_2\text{L}'_2(\text{H}_2\text{O})_2(\text{ClO}_4)_4 \times 2\text{H}_2\text{O}$.

The finding that **18** forms despite the presence of zinc(II) ions is extremely surprising due to the results described above that zinc(II) can substitute copper(II) ions perfectly well in complexes of the ligand 1,3-tpbd. Furthermore, **18** can also be prepared if only a small amount (e.g. 5%) of zinc(II) ions are present.

This result clearly suggests that zinc(II) ions should not be necessarily present and that it should be possible to synthesize **18** by mixing copper(II) perchlorate and 1,3-tpbd in a one to one stoichiometric ratio (Scheme 4-4) since the reaction in a stoichiometric ratio of one (1,3-tpbd) to two $\text{Cu}(\text{ClO}_4)_2$ affords the dinuclear copper(II) complex $[\text{Cu}_2(1,3\text{-tpbd})(\text{H}_2\text{O})_2(\text{ClO}_4)_3](\text{ClO}_4)$ that has been structurally characterized previously.^[26]

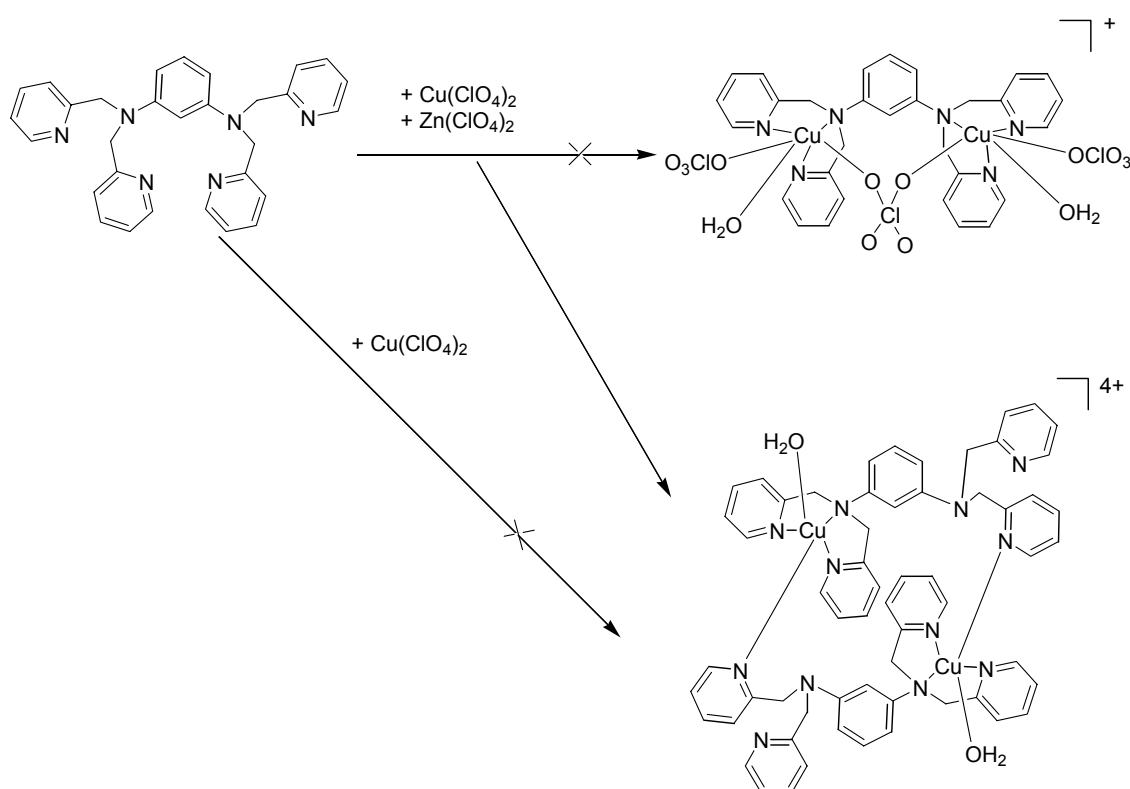


Scheme 4-3. Schematic representation of the complex with the "impurity" L' as ligand (left) in comparison to **18** (right).

However, in contrast a series of experiments showed that **18** cannot be prepared under aerobic conditions without the presence of zinc(II) ions. For example a mixture of 1,3-tpbd and one equivalent of copper(II) perchlorate in methanol/ H_2O , acetonitrile or DMF exposed to air caused the effect that the green solutions rapidly started to turn to a deep-red colour within a day.

Such a phenomenon has precedence with other related *m*-phenyldiamine derivatives where radical reactions were observed during oxidation reactions.^[135-137] A possible mechanism (shown in Scheme 4-5) can be postulated according to these previous findings (most likely an oxygen atom reacts with the benzene ring of the 1,3-tpbd ligand.^[136] Unfortunately, all our efforts to identify this "red" material in order to ascertain whether 1,3-tpbd has been modified have been unsuccessful (only oily dark red reaction mixture products could be obtained so far).

However, this part of the postulated mechanism of ligand oxidation could readily explain the zinc(II) assisted crystallization of **18**.

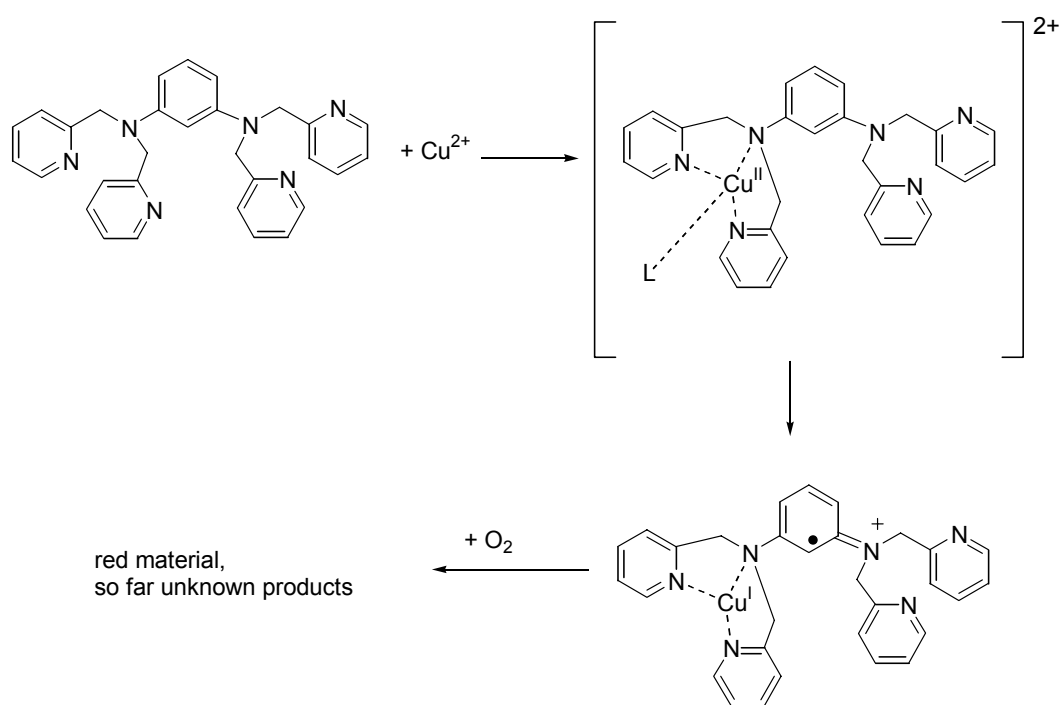


Scheme 4-4. Scheme of reactions observed during the "zinc assisted" formation of **18**.

If enough copper(II) ions are present the formation of the radical intermediate shown in Scheme 4-5 will be suppressed because both coordination sites are blocked with the copper(II) ions and dinuclear copper(II) complexes such as $[\text{Cu}_2(1,3\text{-tpbd})(\text{H}_2\text{O})_2(\text{ClO}_4)_3]\text{ClO}_4$ can be easily prepared.

If non-redox active zinc(II) ions are present they will (as outlined above) coordinate to 1,3-tpbd as well. Most likely - and not for an obvious reason - they seem to prefer coordination only to one of the ligand sites as observed previously with the 1,4-tpbd derivative as ligand (see above), where even the crystal structure of this 1:1 complex was reported.^[115]

Then, the other coordination site will be filled with a copper(II) ion and in a consecutive reaction the zinc(II) ion will now be substituted by a copper(II) ion already coordinated to another 1,3-tpbd ligand molecule. Thus the zinc(II) ion will be liberated and can again interact with a different 1,3-tpbd ligand molecule (which would also explain why stoichiometric amounts of zinc(II) ions are not necessary). Once complex **18** is formed, radical oxidations are again suppressed and therefore allow the facile synthesis and isolation of complex **18**.



Scheme 4-5. Possible reaction scheme for the formation of an oxidation product of 1,3-tpbd.

In our efforts to get a better understanding of the assumed ligand oxidation processes we also reinvestigated the oxidation of the dinuclear copper(I) 1,3-tpbd complex with dioxygen described previously.^[26] In the past this reaction has been studied in methanol, a solvent less suitable for stabilizing reactive intermediates such as copper "dioxygen adduct" complexes.^[26] In our current experiments using more suitable solvents such as acetone we observed spectral changes that indicate the formation of a copper peroxo complex (even at ambient temperature), however, so far all efforts to isolate or to characterize this species in a pure form were unsuccessful.

As a complimentary means to obtain insights into the structure and energetics of possible dioxygen adduct complexes we performed quantum chemical calculations at the B3LYP/TZVP level of density functional theory. We optimized the structures of three isomers, i.e. the $(\eta^2:\eta^2)$ -peroxo, the bis- μ -oxo, and the trans- $(\eta^1:\eta^1)$ -peroxo species. These calculations corroborate the interpretation of a side-on bound $(\eta^2:\eta^2)$ -peroxo species as the most stable complex formed. According to the quantum chemical results, the bis- μ -oxo species is 3.2 kcal/mol less stable, followed by the

trans-peroxo species, which is 12.1 kcal/mol less stable than the side-on bound peroxo isomer. Key parameters of the optimized structures are shown in Figure 4-10.

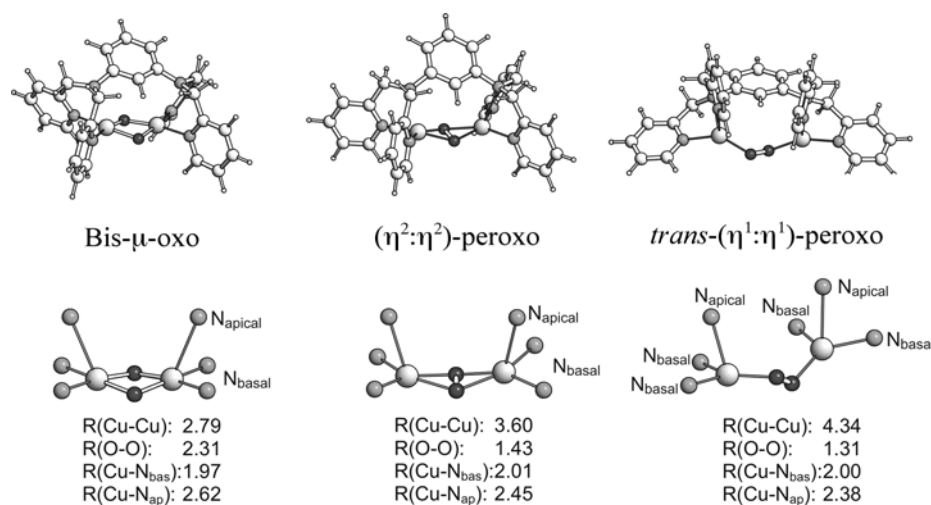


Figure 4-10. Calculated structures of the copper dioxygen adduct complex of 1,3-tpbd.

4.2.7 [Cu₂(2,6-tpcd)(H₂O)(Cl)](ClO₄)₂ x 2 H₂O (**19**).

So far our efforts to isolate and characterize the final oxidation product(s) have been unsuccessful. A possible product that could arise from an intramolecular ligand hydroxylation similar to oxidation reactions observed previously for related systems^[27] would lead to a phenol ligand shown in Figure 1 (R = H). Therefore we synthesized a derivative of this ligand (R = CH₃) from 2,6-Diamino-*p*-cresol dihydrochloride^[138] and 2-Chloromethylpyridine hydrochloride. The copper(II) complex was obtained easily when copper(II) perchlorate was mixed with the ligand and crystals suitable for crystallographic characterization could be isolated. The crystal structure of [Cu₂(2,6-tpcd)(H₂O)(Cl)](ClO₄)₂ x 2 H₂O (**19**) is shown in Figure 4-11 (crystal structure data and refinement parameters, bond lengths and angles are presented in Tables 4-2 and 4-3). The coordinated chloride ion is a consequence of the usage of the protonated ligand (isolation as the hydrochloride salt). The H atoms of water solvent molecules were derived from a difference fourier map and isotropically refined. **19** crystallizes with one coordinated and two additional water solvent molecules per unit.

In **19** both copper(II) ions are “4+1” coordinated forming a distorted square pyramidal geometry. The basal plane consists of two pyridine nitrogen atoms (N(2) and N(3)),

the amine nitrogen N(1) and the chloride anion Cl(1) while the apical plane consists of the phenol oxygen O(1).

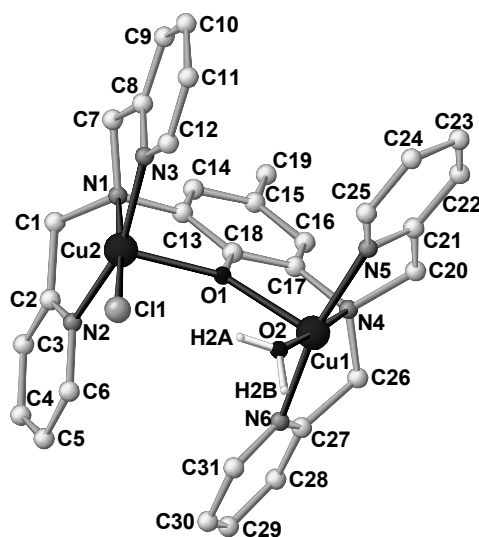


Figure 4-11. Molecular structure of the cation of $[\text{Cu}_2(2,6\text{-tpcd})(\text{H}_2\text{O})(\text{Cl})](\text{ClO}_4)_2$ (**19**). Only water bound hydrogen atoms are shown.

The distance between both copper(II) ions is 4.027 Å. Interestingly the distance Cu(1)-O(1) with 2.153(1) Å is slightly longer than the corresponding distance Cu(2)-O(1) (2.106(2) Å).

Parallel to our work, Karlin and co-workers investigated the reactivity of a dinuclear copper(I) complex with a nearly identical ligand (PD'OH) (Figure 1, R = t-butyl). Besides selective DNA interactions of this complex^[112] they furthermore reported in that regard a very interesting hydroxylation reaction of nitriles to aldehyde and cyanide during oxidation. A hydroperoxo complex has been postulated as reactive species in these reactions.^[113]

4.2.8 Conclusion

1,3-tpbd is a versatile ligand that can be used successfully to coordinate two metal ions in close proximity. While the nickel complex shows normal coordination behavior, redox active metal centers such as iron or copper ions demonstrate that 1,3-tpbd is a non-innocent ligand. Interestingly 1,3-tpbd does not coordinate iron(III) ions, instead protonation of the ligand is preferred. Oxidations of iron(II) complexes or copper(I) complexes of 1,3-tpbd led to reaction product mixtures that could not be

characterized so far. Theoretical calculations support the formation of a dinuclear side-on copper peroxo complex during the reaction of the copper(I) complex with dioxygen. Intramolecular ligand hydroxylation might occur during the oxidation reaction, however, could not be proved experimentally. The possible reaction product, a phenolate bridged derivative of the 1,3-tpbd complex could be synthesized in an independent way. Most interestingly is the reaction if only one equivalent of copper(II) salt is reacted with one equivalent of 1,3-tpbd. Under aerobic conditions a red product was formed after a short while, suggesting ligand oxidation. However, this reaction could be suppressed completely in the presence of zinc ions. Here $[\text{Cu}_2(1,3\text{-tpbd})_2(\text{H}_2\text{O})_2](\text{ClO}_4)_4$ a so called “dimetallocyclophane” formed.

4.3 Experimental Section

4.3.1 General Remarks.

All chemicals were purchased from commercial sources and used as received.

CAUTION! *The perchlorate salts used in this study are potentially explosive and should be handled with care.*

4.3.2 Physical Measurements.

Elemental analyses were carried out on a Carlo Erba 1106 using a Mettler Toledo UMX-2. NMR spectra were recorded on a 400 MHz Bruker-Aspect 2000/3000. IR spectra were recorded on a Bruker Optics IFS25.

4.3.3 Ligand Syntheses.

The ligand 1,3-Bis[bis(2-pyridylmethyl)amino]benzene (1,3-tpbd) was synthesized according to literature procedures.^[26] Slow evaporation of a methanol solution of 1,3-tpbd in a glove box afforded single crystals suitable for X-ray diffraction studies.

2,6-Bis[bis(2-pyridylmethyl)amino]-p-cresol (2,6-tpcd). A solution of sodium hydroxide (4.18 g, 0.1050 mol) in water (30 mL) was added dropwise with stirring to a mixture of 2,6-diamino-*p*-cresole \times 2 HCl^[138] (2 g, 0.0095 mol) and 2-chloromethylpyridine hydrochloride (7.82 g, 0.0475 mol) in 5 mL H₂O under inert conditions. The crude product was recrystallized several times from acetone and 0.5

g (0.001 mol) 10.5% 2,6-tpcd was obtained. ^1H NMR (CDCl_3/TMS , 400 MHz): δ (ppm) 8.48 (m, 4H, pyr-**Ha**), 7.48 (m, 4H, pyr-**Hc**), 7.45 (m, 8H, pyr-**Hb/Hd**), 7.39 (s, 2H, Ar-H), 4.75 (s, 8H, $-\text{CH}_2-$), 2.15 (s, 3H, $-\text{CH}_3$).

$[\text{H}_4(1,3\text{-tpbd})_2](\text{ClO}_4)_4 \times (\text{CH}_3\text{CN})_3$. A solution of iron(III) perchlorate hydrate (141.7 mg, 0.4 mmol) in water (3 mL) was added to a solution of 1,3-tpbd (95.2 mg, 0.2 mmol) in CH_3OH (7 mL). The reaction mixture (a brown suspension) was stirred for 1 h at room temperature and filtered. The precipitate was dissolved in CH_3CN (5 mL) and allowed to stand at room temperature for 2 days affording yellow block-shaped crystals suitable for X-ray diffraction analysis. $\text{C}_{66}\text{H}_{69}\text{Cl}_4\text{N}_{15}\text{O}_{16}$ (1470.16); Calculated: C, 53.92; H, 4.73; N, 14.29; Found: C, 53.78; H, 4.94; N, 14.51%.

$[\text{H}_4(1,3\text{-tpbd})_2](\text{SO}_3\text{CF}_3)_4$. The complex was obtained in a similar way as for the perchlorate salt described above, however, for this compound no analytical data were collected. The crystal structure and data are reported in Tables X and Y.

4.3.4 Syntheses of Complexes.

$[\text{Fe}_2(1,3\text{-tpbd})(\text{CH}_3\text{CN})_6](\text{ClO}_4)_4 \times (\text{CH}_3\text{CN})_2 \times (\text{H}_2\text{O})_{0.5}$ (12) and $[\text{Fe}_2(1,3\text{-tpbd})(\text{DMF})_6](\text{ClO}_4)_4$ (13). Complexes **12** and **13** were synthesized by the same procedure in a glove box differing only by the different solvents used. $\text{Fe}(\text{ClO}_4)_2 \times \text{H}_2\text{O}$ (101.9 mg; 0.4 mmol) and 1,3-tpbd (95.2 mg, 0.2 mmol) were dissolved in 10 mL of CH_3CN or DMF. The resulting clear light brown solution was stirred for 30 min at room temperature followed by vapor diffusion with diethyl ether (20 mL) at -11°C . Nearly colorless square crystals of **12** and light yellow plate crystals of **13** suitable for X-ray diffraction analysis were grown after three weeks. Yield: 161 mg (0.12 mmol, 61%) for **12** and 159 mg (0.11 mmol, 56%) for **13**. $\text{C}_{46}\text{H}_{53}\text{Cl}_4\text{Fe}_2\text{N}_{14}\text{O}_{16.50}$ (1319.52) (**12**): calc. C, 41.87; H, 4.05; N 14.86; found: C, 41.74; H, 3.99; N, 14.69; $\text{C}_{24}\text{H}_{35}\text{Cl}_2\text{FeN}_6\text{O}_{11}$ (710.33) (**13**): calcd. C, 40.58; H, 4.97; N 11.83; found: C, 40.65; H, 4.84; N, 11.87. ^1H NMR (CD_3CN , 400 MHz) for **12**: δ (ppm) 9.78 (d, 4H, $J_{\text{HH}} = 1.9$ Hz, pyr-**Ha**), 8.97 (t, 4H, $^3J_{\text{HH}} = 7.7$ Hz, pyr-**Hc**), 8.55 (t, 4H, $^3J_{\text{HH}} = 5.5$ Hz, pyr-**Hb**), 8.49 (d, 4H, $J_{\text{HH}} = 7.4$ Hz, pyr-**Hd**), 8.07 (t, 1H, $^3J_{\text{HH}} = 14.6$ Hz, Ar-H), 7.32 (s, 1H, Ar-H), 7.26 (dd, 2H, $J_{\text{HH}} = 6.99$ Hz, Ar-H), 6.00 (s, 8H, $-\text{CH}_2-$); (CD_3CN , 400 MHz) for **13**: δ (ppm) 8.40 (d, 4H, pyr-**Ha**), 8.00 (s, 1H, DMF-H), 7.59 (t, 4H, pyr-**Hc**), 7.05-7.16 (t/d, 8H, pyr-**Hb/-Hd**), 6.70 (t, 1H, Ar-H), 5.85-5.97 (s/d, 3H, Ar-H), 4.61 (s, 8H, $-\text{CH}_2-$), 2.71-2.87 (s, 36H, DMF- CH_3).

[Ni₂(1,3-tpbd)(DMF)₆](ClO₄)₄ (14). Similar to the above procedure for **12** and **13**, this complex was synthesized by adding a solution of [Ni(DMF)₆](ClO₄)₂^[139] in DMF to a solution of 1,3-tpbd in DMF under the inert conditions of a glove box. Crystals suitable for X-ray diffraction analysis were obtained by slow diffusion of diethyl ether into the solution. C₄₈H₇₀Cl₄Ni₂N₁₂O₂₂ (1426.38): calcd. C, 40.42; H, 4.95; N 11.78; found: C, 39.77; H, 4.48; N, 11.60. UV-vis (DMF), λ_{max}, nm: 612, 774, 937.

[Zn₂(1,3-tpbd)(CH₃CN)₂(SO₃CF₃)₂(H₂O)](SO₃CF₃)₂ (15). Zinc triflate (154 mg, 0.42 mmol) was added to a solution of 1,3-tpbd (100 mg, 0.21 mmol) in acetonitrile under an inert atmosphere. The solution was allowed to stir at room temperature for a further 2 h. The solvent was removed *in vacuo* and dichloromethane (5 mL) was added to the residual oil. Diethyl ether (20 mL) was added until the solution was slightly turbid. The vessel was placed in the freezer compartment of a fridge and within 3 days, large transparent blocks of **15** formed. IR (Nujol mull) / cm⁻¹: 3631 (w), 3629 (w), 3627 (w), 3549 (w), 3434 (w), 3245 (m), 3120 (m), 2972 (s), **2948 (s)**, 2885 (s), **2845 (s)**, 2726 (m), 2676 (m), 2416 (w), 2394 (w), 2317 (m), 2288 (m), 2211 (w), 2038 (w), 1923 (w), 1610 (m), 1582 (m), **1456 (s)**, **1376 (s)**, 1287 (s), 1246 (s), 1167 (s), 1105 (m), 1031 (s), 957 (m), 901 (m), 850 (m), 817 (m), 774 (m), 726 (m), 696 (m), 634 (m), 574 (m), 544 (m), 517 (m), 472 (w). ¹H NMR (CD₃CN, 300 MHz): δ (ppm) 8.60 (d, 4H, ³J_{HH} = 4.9 Hz, pyr-**Ha**), 8.10 (t, 4H, ³J_{HH} = 7.5 Hz, pyr-**Hc**), 7.63 (t, 4H, J_{HH} = 6.0 Hz, pyr-**Hb**), 7.44 (d, 4H, ³J_{HH} = 7.9 Hz, pyr-**Hd**), 6.90 (t, 1H, ³J_{HH} = 8.3 Hz, Ar-H), 6.33 (dd, 1H, ³J_{HH} = 1.9 Hz, 8.7 Hz, Ar-H), 5.96 (s, 1H, Ar-H), 4.60 (s, 8H, -CH₂-).

[Zn₂(1,3-tpbd)Cl₄]·H₂O (16), [Cu₂(1,3-tpbd)Cl₄] (8), [CuZn(1,3-tpbd)Cl₄] (17). Slow evaporation of an aqueous methanolic solution of a stoichiometric mixture of ZnCl₂, CuCl₂ and 1,3-tpbd led to a mixture of yellow and two different green colored crystals suitable for X-ray diffraction analysis.

[Cu₂(1,3-tpbd)₂(H₂O)₂] x (ClO₄)₄ x 2H₂O (18). A methanolic suspension of 1,3-tpbd (95.2 mg, 0.2 mmol) was added to an aqueous methanol solution of Cu(ClO₄)₂ x 6H₂O (64.1 mg, 0.2 mmol) and Zn(ClO₄)₂ x 6H₂O (74.4 mg, 0.2 mmol). The mixture was stirred for 2 h, filtered and allowed to slowly evaporate at room temperature. Large green blocks formed within 48 h. A single-crystal X-ray diffraction analysis was performed and the structure of the green crystals was determined to be [Cu₂(1,3-

tpbd)(OH₂)₂](ClO₄)₄. That no zinc ions were present at all was further confirmed by photon-induced X-ray emission.

[Cu₂(2,6-tpcd)(H₂O)(Cl)](ClO₄)₂ x 2 H₂O (19). A suspension of 2,6-tpcd (100 mg, 0.2 mmol) in 5 mL methanol was added to a solution of Cu(ClO₄)₂ x 6 H₂O (148.2 mg, 0.4 mmol) in 5 mL H₂O. The mixture was stirred for 30 min at room temperature and allowed to slowly evaporate at room temperature. Within two days small green needles of **19** suitable for X-ray diffraction analysis were formed.

4.3.5 Computational Methods.

Density functional calculations have been performed employing the B3LYP functional^[100, 140-142] as implemented in the Turbomole program.^[143-145] The TZVP basis set has been employed for all atoms.^[146] Solvent effects have partially been included in these calculations employing the COSMO continuum solvent model (dielectric constant $\epsilon=36.64$ at room temperature).^[147]

4.3.6 X-ray Crystallographic Studies.

X-ray crystallographic data for **1,3-tpbd** were collected on a STOE IPDS-diffractometer at 193 K equipped with a low temperature system (Karlsruher Glastechnisches Werk). Cell parameters were refined by using up to 5000 reflections. A sphere of data (210 frames) was collected with the ϕ -oscillation mode (0.9° frame width; Irradiation times/frame: 7 min.) No absorption corrections were applied. The structures were solved by Direct Methods in SHELXS97, and refined by using full-matrix least-squares in SHELXL97.^[71] The hydrogen atoms were positioned geometrically and all non-hydrogen atoms were refined anisotropically, if not mentioned otherwise.

All following data were corrected for Lorentz and polarization effects.

Intensity data of **12** were collected on a Bruker-Nonius KappaCCD diffractometer, intensity data for **15** and **18** were collected on a Siemens P4 four circle diffractometer. Absorption effects were corrected either by semi-empirical methods based on multiple scans (**12**)^[70] or on the basis of Psi-scans.^[148] The structures were solved by direct methods; full-matrix least-squares refinement was carried out on F^2 using SHELXTL NT 6.12.^[72] All non-hydrogen atoms were refined anisotropically.

Hydrogen atoms were geometrically positioned except for the hydrogen atoms of the water molecules or aqua ligands the positions of which were derived from a difference fourier synthesis; their isotropic displacement parameters were tied to those of their corresponding carrier atoms by a factor of 1.2 or 1.5. One of the perchlorate anions of **12** is disordered; two preferred orientations were refined resulting in occupancy factors of 50.1(6) and 49.9(6)%. In **18** both of the two independent perchlorate anions are subjected to disorder. Two preferred orientations refined led to occupancy factors of 72(2) and 28(2)% around Cl1 and 61(2) and 39(2)% around Cl2, respectively.

Intensity data of protonated tpbd, **13**, **14** and **19** were collected on a Siemens SMART CCD 1000 diffractometer by the ω -scan technique collecting a full sphere of data with irradiation times of 10 to 20 s per frame and $\Delta\omega$ ranges between 0.3° and 0.45° . The collected reflections were corrected for absorption effects.^[70] All structures were solved by direct methods and refined by least-squares techniques using the SHELX97 programme package.^[71] The hydrogen atoms were positioned geometrically and all non-hydrogen atoms were refined anisotropically, if not mentioned otherwise. Further data collection parameters are summarised in Table 1, 2 and supporting material.

Intensity data of **16** and **17** were collected on a Nonius MACH3 diffractometer. Cell parameters were obtained and refined from 25 reflections. Absorption corrections (psi-scans) were applied. The space groups were determined from systematic absences and subsequent least-squares refinement. The structures were solved by direct methods. The parameters were refined with all data by full-matrix-least-squares on F^2 using SHELXL-97.^[71] Non-hydrogen atoms were refined with anisotropic thermal parameters. The hydrogen atoms were fixed in idealized positions using a riding model. Scattering factors were taken from the literature.^[106]

CCDC 610594 (1,3-tpbd), CCDC 610424 ([1,3-tpbdH₂](ClO₄)₂), CCDC 615270 (**12**), CCDC 610425 (**13**), CCDC 610426 ([1,3-tpbdH₂](CF₃SO₃)₂), CCDC 610427 (**14**), CCDC 615271 (**15**), CCDC 611033 (**16**), CCDC 611034 (**17**), CCDC 615272 (**18**) and CCDC 610428 (**19**), contain the supplementary crystallographic data for this paper. These data can be obtained free of charge at www.ccdc.cam.ac.uk/conts/retrieving.html [or from the Cambridge Crystallographic

Data Center, 12, Union Road, Cambridge CB2 1EZ, UK; Fax: (internat.) +44-1223-336-033; E-mail: deposit@ccdc.cam.ac.uk

1 **Table 4-1.** Crystallographic data and experimental details for **1,3-tpbd** ligand and compounds **12-14**.

Compound	1,3-tpbd	[1,3-tpbdH ₂](ClO ₄) ₂	[1,3-tpbdH ₂](SO ₃ CF ₃) ₂	12	13	14
Empirical formula	C ₃₁ H ₃₂ N ₆ O	C ₆₆ H ₆₉ Cl ₄ N ₁₅ O ₁₆	C ₆₄ H ₆₀ F ₁₂ N ₁₂ O ₁₂ S ₄	C ₄₆ H ₅₃ Cl ₄ Fe ₂ N ₁₄ O _{16.5}	C ₂₄ H ₃₅ Cl ₂ FeN ₆ O ₁₁	C ₄₈ H ₇₀ Cl ₄ Ni ₂ N ₁₂ O ₂₂
<i>M_r</i>	504.63	1470.16	1545.48	1319.52	710.33	1426.38
Temperature [K]	193(2)	200(2)	200(2)	100(2)	200(2)	200(2)
Radiation (λ [Å])	0.71073	0.71073	0.71073	0.71073	0.71073	0.71073
Crystal size [mm]	0.48 × 0.32 × 1.48	0.8 × 0.6 × 0.6	0.5 × 0.15 × 0.15	0.25 × 0.21 × 0.07	0.8 × 0.8 × 0.4	0.4 × 0.4 × 0.2
Crystal system	Triclinic	monoclinic	triclinic	monoclinic	monoclinic	monoclinic
space group	<i>P</i> 1 (no. 2)	<i>P</i> 2 ₁ /c (no. 14)	<i>P</i> -no. 2)	<i>P</i> 2 ₁ (no. 4)	<i>C</i> 2/c (no. 15)	<i>C</i> 2 (no. 5)
<i>a</i> [Å]	8.0703(10)	21.818(2)	11.115(1)	14.532(2)	34.813(4)	34.675(8)
<i>b</i> [Å]	13.2071(17)	19.862(2)	16.712(2)	23.015(2)	11.056(2)	10.972(3)
<i>c</i> [Å]	14.379(2)	16.294(2)	19.038(2)	17.284(2)	19.807(2)	19.616(4)
α [°]	64.833(15)	90	86.573(2)	90	90	90
β [°]	81.997(16)	102.656(2)	77.580(2)	93.12(1)	121.515(2)	121.278(3)
γ [°]	88.423(15)	90	78.997(2)	90	90	90
<i>V</i> [Å ³]	1372.7(3)	6889.1(8)	3389.5(4)	5772(1)	6499(2)	6378(2)
<i>Z</i>	2	4	2	4	8	4
ρ _{calcd.} [g·cm ⁻³]	1.221	1.417	1.514	1.518	1.452	1.485
μ [mm ⁻¹]	0.077	0.251	0.245	0.767	0.692	0.840
<i>F</i> (000)	536	3064	1592	2716	2952	2968
Scan range θ [°]	2.78 to 28.05	1.64 to 28.30	1.64 to 28.33	3.32 to 27.10	1.97 to 28.31	1.37 to 28.36
Index ranges	-9 ≤ <i>h</i> ≤ 9	-29 ≤ <i>h</i> ≤ 28	-14 ≤ <i>h</i> ≤ 14	-18 ≤ <i>h</i> ≤ 18	-46 ≤ <i>h</i> ≤ 46	-46 ≤ <i>h</i> ≤ 46
	-17 ≤ <i>k</i> ≤ 16	-26 ≤ <i>k</i> ≤ 26	-21 ≤ <i>k</i> ≤ 21	-29 ≤ <i>k</i> ≤ 29	-14 ≤ <i>k</i> ≤ 14	-14 ≤ <i>k</i> ≤ 14
	-18 ≤ <i>l</i> ≤ 18	-21 ≤ <i>l</i> ≤ 21	-25 ≤ <i>l</i> ≤ 25	-22 ≤ <i>l</i> ≤ 22	-26 ≤ <i>l</i> ≤ 26	-26 ≤ <i>l</i> ≤ 25
Reflections collected	12413	81510	40908	140656	37816	31287
Unique reflections	6069	16875	16252	25407	7966	14865
<i>R</i> _{int}	0.0469	0.0513	0.0512	0.0542	0.0431	0.0896
Data/restraints/parameters	6069 / 0 / 356	16875 / 42 / 933	16252 / 0 / 965	25407 / 41 / 1536	7966 / 45 / 433	14865 / 1 / 880
Goodness-of-fit on <i>F</i> ²	1.042	1.032	0.932	1.026	1.056	1.065
<i>R</i> 1, ^[a] <i>wR</i> 2 [<i>I</i> > 4σ(<i>I</i>)] ^{[b][c]}	0.0511, 0.1290	0.0707, 0.1843	0.0518, 0.1114	0.0412, 0.0818	0.0460, 0.1192	0.1057, 0.2631
<i>R</i> 1, ^[a] <i>wR</i> 2 (all data) ^{[b][d]}	0.0847, 0.1464	0.1153, 0.2218	0.1260, 0.1351	0.0617, 0.0883	0.0709, 0.1308	0.1224, 0.2822
Flack parameter ^[107]	-	-	-	0.009(8)	-	-
Largest diff. peak/hole [e·Å ⁻³]	0.262, -0.205	1.107, -0.771	0.306/-0.551	0.689, -0.707	0.688, -0.846	1.292/-3.707

2 ^[a] $R1 = \sum \|F_o\| - \sum \|F_c\| / \sum \|F_o\|$. ^[b] $wR2 = [\sum [w(F_o^2 - F_c^2)] / \sum [w(F_o^2)]]^{1/2}$; $w = 1/[\sigma^2(F_o^2) + (aP)^2 + bP]$, $P = [\max(F_o^2 \text{ or } 0) + 2(F_c^2)]/3$. ^[c] Denotes the value of the residual considering only the reflections
3 with $I > 4\sigma(I)$. ^[d] Denotes the value of the residual considering all the reflections. ^[e] $S = [\sum w(F_o^2 - F_c^2)] / [(n - p)^{1/2}]$, n = number of data, p = parameters used.

Table 4-2. Crystallographic data and experimental details for compounds **15-19**.

Compound	15	16	17	18	19
Empirical formula	C ₄₀ H ₃₉ F ₁₂ N ₉ O ₁₃ S ₄ Zn ₂	C ₃₀ H ₃₀ Cl ₄ N ₆ OZn ₂	C ₃₀ H ₂₆ Cl ₄ CuN ₆ Zn	C ₆₀ H ₆₄ Cl ₄ Cu ₂ N ₁₂ O ₂₀	C ₃₁ H ₃₅ Cl ₃ Cu ₂ N ₆ O ₁₂
<i>M_r</i>	1340.78	763.14	743.29	1542.11	917.08
Temperature [K]	293(2)	173(2)	173(2)	293(2)	200(2)
Radiation (λ, [Å])	0.71073	0.71073	0.71073	0.71073	0.71073
Crystal size [mm]	0.62 × 0.50 × 0.42	0.20 × 0.10 × 0.10	0.30 × 0.20 × 0.20	0.65 × 0.50 × 0.32	0.25 × 0.35 × 0.2
Crystal system	Orthorhombic	monoclinic	monoclinic	monoclinic	triclinic
space group	<i>Pna</i> 2 ₁ (no. 33)	<i>P</i> 2 ₁ / <i>n</i> (no. 14)	<i>P</i> 2 ₁ (no. 4)	<i>P</i> 2 ₁ / <i>n</i> (no. 14)	<i>P</i> 1̄ (no. 2)
<i>a</i> [Å]	25.712(2)	9.177(2)	8.600(2)	10.859(1)	10.495(1)
<i>b</i> [Å]	9.569(1)	27.304(6)	13.002(3)	22.660(2)	12.184(2)
<i>c</i> [Å]	21.901(2)	12.287(3)	13.690(3)	13.072(1)	14.442(2)
α [°]	90	90	90	90	93.880(1)
β [°]	90	91.79(2)	103.24(3)	94.54(1)	95.284(1)
γ [°]	90	90	90	90	94.411(1)
<i>V</i> [Å ³]	5388.5(9)	3077.1(2)	1490.1(5)	3206.5(5)	1828.3(3)
<i>Z</i>	4	4	2	2	2
ρ _{calcd.} [g·cm ⁻³]	1.653	1.647	1.657	1.597	1.666
μ [mm ⁻¹]	1.154	1.943	1.910	0.916	1.453
<i>F</i> (000)	2712	1552	754	1588	936
Scan range θ [°]	2.27 to 27.00	2.68 to 26.33	2.56 to 33.67	2.27 to 27.00	1.68 to 28.31
Index ranges	-32 ≤ <i>h</i> ≤ 32 -12 ≤ <i>k</i> ≤ 12 -27 ≤ <i>l</i> ≤ 27	-11 ≤ <i>h</i> ≤ 11 -34 ≤ <i>k</i> ≤ 0 0 ≤ <i>l</i> ≤ 15	-10 ≤ <i>h</i> ≤ 0 -4 ≤ <i>k</i> ≤ 16 -17 ≤ <i>l</i> ≤ 16	-1 ≤ <i>h</i> ≤ 13 -28 ≤ <i>k</i> ≤ 1 -16 ≤ <i>l</i> ≤ 16	-13 ≤ <i>h</i> ≤ 13 -15 ≤ <i>k</i> ≤ 16 -18 ≤ <i>l</i> ≤ 19
Reflections collected	12077	6543	3407	8527	16512
Unique reflections	11763	6256	3196	7002	8570
<i>R</i> _{int}	0.0342	0.1193	0.0611	0.0214	0.0363
Data/restraints/parameters	11763 / 3 / 730	6256 / 0 / 388	3196 / 1 / 379	7002 / 5 / 507	8570 / 0 / 518
Goodness-of-fit on <i>F</i> ²	0.990	1.014	1.757	1.016	0.892
<i>R</i> 1, ^[a] _[c] <i>wR</i> 2 [<i>I</i> > 4σ (<i>I</i>)] ^[b] _[c]	0.0577, 0.0944	0.0610, 0.1181	0.0569, 0.2133	0.0500, 0.0993	0.0388, 0.0848
<i>R</i> 1, ^[a] _[d] <i>wR</i> 2 (all data) ^[b] _[d]	0.1128, 0.1130	0.1834, 0.1670	0.0704, 0.2198	0.0932, 0.1155	0.0693, 0.0923
Flack parameter ^[107]	-0.02(2)	-	-	-	-
Largest diff. peak/hole [e·Å ⁻³]	0.373, -0.375	0.829, -0.790	1.361, -1.294	0.459, -0.450	0.720, -0.651

^[a] $R1 = \sum \|F_o\| - \|F_c\| / \sum \|F_o\|$. ^[b] $wR2 = [\sum (w(F_o^2 - F_c^2)^2) / \sum (w(F_o^2)^2)]^{1/2}$; $w = 1/[\sigma^2(F_o^2) + (aP)^2 + bP]$, $P = [\max(F_o^2 \text{ or } 0) + 2(F_c^2)]/3$. ^[c] Denotes the value of the residual considering only the reflections with $I > 4\sigma(I)$. ^[d] Denotes the value of the residual considering all the reflections. ^[e] $S = [\sum w(F_o^2 - F_c^2)^2 / (n - p)]^{1/2}$, n = number of data, p = parameters used.

Table 4-3. Selected Bond Lengths [Å] and Angles [°] for 1,3-tpbd ligand and compounds **12-19**.

1,3-tpbd					
N(1)-C(1)	1.411(2)	N(5)-C(24)	1.326(4)	C(1)-N(1)-C(7)	120.7(2)
N(1)-C(7)	1.451(2)	N(5)-C(20)	1.336(2)	C(1)-N(1)-C(13)	118.5(2)
N(1)-C(13)	1.460(2)	N(6)-C(30)	1.333(3)	C(7)-N(1)-C(13)	115.1(2)
N(2)-C(8)	1.345(2)	N(6)-C(26)	1.339(2)	C(8)-N(2)-C(12)	117.2(2)
N(2)-C(12)	1.357(3)	C(7)-C(8)	1.514(3)	C(18)-N(3)-C(14)	117.2(2)
N(3)-C(18)	1.342(3)	C(8)-C(9)	1.382(3)	C(3)-N(4)-C(19)	121.4(2)
N(3)-C(14)	1.348(2)	C(9)-C(10)	1.381(3)	C(3)-N(4)-C(25)	120.4(2)
N(4)-C(3)	1.388(2)	C(10)-C(11)	1.370(3)	C(19)-N(4)-C(25)	117.9(2)
N(4)-C(19)	1.452(2)	C(11)-C(12)	1.371(4)	C(24)-N(5)-C(20)	117.1(2)
N(4)-C(25)	1.454(2)			C(30)-N(6)-C(26)	117.1(2)
[H₂1,3-tpbd](ClO₄)₂					
N(2)-H(2A)	0.84(4)	N(3)-C(8)	1.336(4)	C(13)-N(1)-C(1)	119.8(2)
N(5)-H(5A)	0.94(4)	N(3)-C(12)	1.343(4)	C(1)-N(1)-C(7)	118.6(2)
N(1)-C(13)	1.396(4)	C(7)-C(8)	1.517(4)	C(13)-N(1)-C(7)	119.7(2)
N(1)-C(1)	1.449(4)	C(8)-C(9)	1.386(5)	C(17)-N(4)-C(19)	121.3(2)
N(1)-C(7)	1.453(4)	C(9)-C(10)	1.388(6)	C(17)-N(4)-C(25)	119.6(2)
N(2)-C(6)	1.340(4)	N(4)-C(17)	1.397(4)	C(19)-N(4)-C(25)	118.8(2)
N(2)-C(2)	1.348(4)	N(4)-C(19)	1.447(4)	C(6)-N(2)-H(2A)	120(3)
C(1)-C(2)	1.514(4)	N(4)-C(25)	1.451(4)	C(2)-N(2)-H(2A)	118(3)
C(2)-C(3)	1.378(4)	N(5)-C(20)	1.334(4)	C(24)-N(5)-H(5A)	121(2)
C(3)-C(4)	1.388(5)	N(5)-C(24)	1.341(5)	C(20)-N(5)-H(5A)	116(2)
C(4)-C(5)	1.372(6)	N(6)-C(26)	1.337(5)		
C(5)-C(6)	1.372(5)	N(6)-C(30)	1.352(5)		
[H₂1,3-tpbd](SO₃CF₃)₂					
N(2)-H(1)	1.24(3)	N(3)-C(8)	1.344(3)	C(13)-N(1)-C(1)	119.5(2)
N(5)-H(2X)	0.92(7)	N(3)-C(12)	1.344(3)	C(1)-N(1)-C(7)	119.1(2)
N(1)-C(13)	1.394(3)	C(7)-C(8)	1.519(3)	C(13)-N(1)-C(7)	120.3(2)
N(1)-C(1)	1.453(3)	C(8)-C(9)	1.382(3)	C(17)-N(4)-C(19)	120.7(2)
N(1)-C(7)	1.455(3)	C(9)-C(10)	1.380(4)	C(17)-N(4)-C(25)	119.4(2)
N(2)-C(6)	1.345(3)	N(4)-C(17)	1.405(3)	C(19)-N(4)-C(25)	119.0(2)
N(2)-C(2)	1.346(3)	N(4)-C(19)	1.449(3)	C(6)-N(2)-H(1)	120(2)
C(1)-C(2)	1.509(3)	N(4)-C(25)	1.449(3)	C(2)-N(2)-H(1)	119(2)

C(2)-C(3)	1.369(3)	N(5)-C(20)	1.341(3)	C(24)-N(5)-H(2X)	119(4)
C(3)-C(4)	1.377(3)	N(5)-C(24)	1.342(3)	C(20)-N(5)-H(2X)	119(4)
C(4)-C(5)	1.371(4)	N(6)-C(26)	1.330(3)		
C(5)-C(6)	1.367(3)	N(6)-C(30)	1.349(3)		
[Fe₂(1,3-tpbd)(CH₃CN)₆](ClO₄)₄ x 2 CH₃CN x 0.5 (H₂O) (12)					
Fe(1)-N(3)	1.989(3)	N(3)-Fe(1)-N(9)	171.8(2)	N(11)-Fe(2)-N(6)	168.6(1)
Fe(1)-N(9)	1.997(3)	N(3)-Fe(1)-N(7)	95.0(2)	N(10)-Fe(2)-N(4)	165.6(2)
Fe(1)-N(7)	2.001(3)	N(9)-Fe(1)-N(7)	90.7(2)	N(5)-Fe(2)-N(4)	76.8(1)
Fe(1)-N(8)	2.007(3)	N(3)-Fe(1)-N(8)	84.5(2)	N(12)-Fe(2)-N(4)	98.0(1)
Fe(1)-N(2)	2.024(3)	N(9)-Fe(1)-N(8)	89.6(2)	N(11)-Fe(2)-N(4)	102.2(1)
Fe(1)-N(1)	2.131(2)	N(7)-Fe(1)-N(8)	90.4(2)	N(6)-Fe(2)-N(4)	74.7(1)
Fe(2)-N(10)	2.099(3)	N(3)-Fe(1)-N(2)	94.3(2)	N(19)-Fe(3)-N(20)	90.5(1)
Fe(2)-N(5)	2.146(3)	N(9)-Fe(1)-N(2)	91.3(2)	N(19)-Fe(3)-N(21)	89.5(1)
Fe(2)-N(12)	2.164(3)	N(7)-Fe(1)-N(2)	92.6(2)	N(20)-Fe(3)-N(21)	90.7(1)
Fe(2)-N(11)	2.183(3)	N(8)-Fe(1)-N(2)	176.8(2)	N(19)-Fe(3)-N(15)	93.5(1)
Fe(2)-N(6)	2.188(3)	N(3)-Fe(1)-N(1)	83.0(1)	N(20)-Fe(3)-N(15)	85.7(1)
Fe(2)-N(4)	2.263(3)	N(9)-Fe(1)-N(1)	92.3(1)	N(21)-Fe(3)-N(15)	175.4(1)
Fe(3)-N(19)	1.953(3)	N(7)-Fe(1)-N(1)	171.4(1)	N(19)-Fe(3)-N(14)	91.6(1)
Fe(3)-N(20)	1.955(3)	N(8)-Fe(1)-N(1)	97.7(1)	N(20)-Fe(3)-N(14)	177.7(1)
Fe(3)-N(21)	1.963(3)	N(2)-Fe(1)-N(1)	79.2(1)	N(15)-Fe(3)-N(14)	93.3(1)
Fe(3)-N(15)	1.966(3)	N(10)-Fe(2)-N(5)	95.6(2)	N(19)-Fe(3)-N(13)	171.7(1)
Fe(3)-N(14)	1.976(2)	N(10)-Fe(2)-N(12)	90.3(2)	N(22)-Fe(4)-N(24)	91.9(1)
Fe(3)-N(13)	2.095(2)	N(5)-Fe(2)-N(12)	173.6(2)	N(22)-Fe(4)-N(18)	93.0(1)
Fe(4)-N(22)	2.097(3)	N(10)-Fe(2)-N(11)	90.4(2)	N(24)-Fe(4)-N(18)	91.5(2)
Fe(4)-N(24)	2.100(3)	N(5)-Fe(2)-N(11)	93.6(1)	N(24)-Fe(4)-N(17)	172.4(2)
Fe(4)-N(18)	2.107(3)	N(12)-Fe(2)-N(11)	83.9(2)	N(18)-Fe(4)-N(17)	93.5(1)
Fe(4)-N(17)	2.124(3)	N(10)-Fe(2)-N(6)	94.3(2)	N(18)-Fe(4)-N(23)	172.6(2)
Fe(4)-N(23)	2.142(3)	N(5)-Fe(2)-N(6)	96.3(1)	N(17)-Fe(4)-N(23)	88.9(1)
Fe(4)-N(16)	2.280(3)	N(12)-Fe(2)-N(6)	85.6(1)		
[Fe₂(1,3-tpbd)(DMF)₆](ClO₄)₄ (13)					
Fe(1)-O(1)	2.075(2)	O(1)-Fe(1)-O(3)	89.45(8)	O(1)-Fe(1)-N(3)	177.19(8)
Fe(1)-O(2)	2.112(2)	O(1)-Fe(1)-O(2)	90.84(8)	O(3)-Fe(1)-N(3)	89.44(8)
Fe(1)-O(3)	2.110(2)	O(3)-Fe(1)-O(2)	97.45(8)	O(2)-Fe(1)-N(3)	86.74(8)
Fe(1)-N(1)	2.312(2)	O(1)-Fe(1)-N(2)	90.65(8)	N(2)-Fe(1)-N(3)	92.03(8)
Fe(1)-N(2)	2.152(2)	O(3)-Fe(1)-N(2)	95.89(8)	O(1)-Fe(1)-N(1)	105.90(7)

Fe(1)-N(3)	2.174(2)	O(2)-Fe(1)-N(2)	166.58(7)	O(3)-Fe(1)-N(1)	163.39(7)
N(3)-Fe(1)-N(1)	75.51(7)	O(2)-Fe(1)-N(1)	88.79(7)	N(2)-Fe(1)-N(1)	77.98(7)
[Ni₂(1,3-tpbd)(DMF)₆](ClO₄)₄ (14)					
Ni(1)-O(1)	2.039(4)	O(1)-Ni(1)-N(2)	87.2(2)	N(9)-Ni(2)-O(6)	90.8(6)
Ni(1)-N(2)	2.044(6)	O(1)-Ni(1)-O(2)	88.9(2)	N(9)-Ni(2)-N(10)	94.4(5)
Ni(1)-O(2)	2.048(5)	N(2)-Ni(1)-O(2)	96.2(2)	O(6)-Ni(2)-N(10)	95.7(4)
Ni(1)-O(3)	2.063(5)	O(1)-Ni(1)-O(3)	93.2(2)	N(9)-Ni(2)-O(4)	86.7(5)
Ni(1)-N(3)	2.073(4)	N(2)-Ni(1)-O(3)	169.9(2)	O(6)-Ni(2)-O(4)	94.1(4)
Ni(1)-N(1)	2.195(5)	O(2)-Ni(1)-O(3)	93.9(2)	N(10)-Ni(2)-O(4)	170.2(4)
Ni(2)-O(6)	2.06(2)	O(1)-Ni(1)-N(3)	178.2(2)	N(9)-Ni(2)-O(5)	176.7(5)
Ni(2)-N(10)	2.05(2)	N(2)-Ni(1)-N(3)	93.7(2)	O(6)-Ni(2)-O(5)	87.5(6)
Ni(2)-O(4)	2.07(2)	O(2)-Ni(1)-N(3)	89.4(2)	N(10)-Ni(2)-O(5)	88.6(5)
Ni(2)-O(5)	2.10(2)	O(3)-Ni(1)-N(3)	86.2(2)	O(4)-Ni(2)-O(5)	90.5(5)
Ni(2)-N(8)	2.20(2)	O(1)-Ni(1)-N(1)	102.8(2)	N(9)-Ni(2)-N(8)	79.7(4)
Ni(2)-N(9)	2.03(2)	O(2)-Ni(1)-N(1)	168.0(2)	N(10)-Ni(2)-N(8)	82.0(4)
		O(3)-Ni(1)-N(1)	88.3(2)	O(4)-Ni(2)-N(8)	88.6(3)
		N(3)-Ni(1)-N(1)	79.0(2)	O(5)-Ni(2)-N(8)	102.1(5)
		N(2)-Ni(1)-N(1)	81.8(2)	O(6)-Ni(2)-N(8)	170.0(5)
[Zn₂(1,3-tpbd)(CH₃CN)₂(SO₃CF₃)₂(H₂O)](SO₃CF₃)₂ (15)					
Zn(1)-N(1)	2.350(5)	N(1)-Zn(1)-N(2)	78.3(2)	N(4)-Zn(2)-N(5)	79.0(2)
Zn(1)-N(2)	2.032(5)	N(1)-Zn(1)-N(3)	78.9(2)	N(4)-Zn(2)-N(6)	79.1(2)
Zn(1)-N(3)	2.046(5)	N(2)-Zn(1)-N(3)	156.1(2)	N(5)-Zn(2)-N(6)	152.3(2)
Zn(1)-N(60)	2.078(5)	N(1)-Zn(1)-O(12)	93.1(2)	N(4)-Zn(2)-O(11)	97.6(2)
Zn(1)-O(1)	2.243(5)	N(2)-Zn(1)-O(12)	89.0(2)	N(5)-Zn(2)-O(11)	105.7(2)
Zn(1)-O(12)	2.242(4)	N(3)-Zn(1)-O(12)	99.4(2)	N(6)-Zn(2)-O(11)	93.9(2)
Zn(2)-N(4)	2.346(4)	O(1)-Zn(1)-O(12)	173.4(2)	O(11)-Zn(2)-O(21)	167.3(2)
Zn(2)-N(5)	2.024(4)	N(2)-Zn(1)-O(1)	89.2(2)	N(4)-Zn(2)-O(21)	88.3(2)
Zn(2)-N(6)	2.021(5)	O(1)-Zn(1)-N(1)	92.7(2)	N(5)-Zn(2)-O(21)	86.5(2)
Zn(2)-N(70)	2.104(5)	N(3)-Zn(1)-O(1)	84.8(2)	N(70)-Zn(2)-O(11)	90.1(2)
Zn(2)-O(11)	2.122(4)	N(60)-Zn(1)-O(1)	86.5(2)	N(5)-Zn(2)-N(70)	100.2(2)
Zn(2)-O(21)	2.578(4)	N(60)-Zn(1)-N(1)	178.9(2)	N(70)-Zn(2)-O(21)	84.0(2)
		N(2)-Zn(1)-N(60)	100.9(2)	N(6)-Zn(2)-O(21)	76.1(2)
		N(3)-Zn(1)-N(60)	101.7(2)	N(70)-Zn(2)-N(4)	172.3(2)
		N(60)-Zn(1)-O(12)	87.7(2)	N(6)-Zn(2)-N(70)	99.3(2)
[Zn₂(1,3-tpbd)Cl₄] (16)					

Zn(1)-N(11)	2.046(6)	N(11)-Zn(1)-N(21)	120.1(3)	N(41)-Zn(2)-N(31)	124.6(3)
Zn(1)-N(21)	2.055(6)	N(11)-Zn(1)-Cl(1)	116.6(2)	N(41)-Zn(2)-Cl(3)	105.6(2)
Zn(1)-Cl(1)	2.248(2)	N(21)-Zn(1)-Cl(1)	113.0(2)	N(31)-Zn(2)-Cl(3)	120.9(2)
Zn(1)-Cl(2)	2.305(2)	N(11)-Zn(1)-Cl(2)	98.3(2)	N(41)-Zn(2)-Cl(4)	99.1(2)
Zn(1)-N(1)	2.646(2)	N(1)-Zn(1)-N(11)	71.7(2)	N(2)-Zn(2)-N(31)	72.9(2)
Zn(2)-N(31)	2.066(7)	N(21)-Zn(1)-Cl(2)	100.8(2)	N(31)-Zn(2)-Cl(4)	98.6(2)
Zn(2)-N(41)	2.042(7)	Cl(1)-Zn(1)-Cl(2)	103.5(1)	Cl(3)-Zn(2)-Cl(4)	102.4(1)
Zn(2)-Cl(4)	2.314(3)	Zn(1)-Cl(1)-O(1)	89.9(2)	Zn(2)-Cl(3)-O(1)	110.2(2)
Zn(2)-Cl(3)	2.259(3)	C(16)-N(11)-Zn(1)	122.0(6)	C(32)-N(31)-Zn(2)	117.6(6)
Zn(2)-N(2)	2.594(3)	N(1)-Zn(1)-Cl(1)	94.8(2)	N(2)-Zn(2)-Cl(3)	97.4(2)
[CuZn(1,3-tpbd)Cl₄] (17)					
Zn(1)-N(11)	2.03(2)	N(11)-Zn(1)-N(21)	145.4(4)	N(41)-Cu(1)-N(51)	143.4(4)
Zn(1)-N(21)	2.04(2)	N(11)-Zn(1)-Cl(2)	95.1(3)	N(41)-Cu(1)-Cl(3)	102.2(3)
Zn(1)-Cl(2)	2.307(4)	N(21)-Zn(1)-Cl(2)	96.4(3)	N(51)-Cu(1)-Cl(3)	104.0(3)
Zn(1)-Cl(1)	2.333(3)	N(11)-Zn(1)-Cl(1)	99.2(3)	N(41)-Cu(1)-Cl(4)	96.7(3)
Zn(1)-N(1)	2.37(2)	N(21)-Zn(1)-Cl(1)	109.6(3)	N(51)-Cu(1)-Cl(4)	97.9(3)
Cu(1)-N(41)	2.04(2)	Cl(2)-Zn(1)-Cl(1)	103.3(2)	Cl(3)-Cu(1)-Cl(4)	110.0(2)
Cu(1)-N(51)	2.06(2)	N(11)-Zn(1)-N(1)	76.9(4)	N(41)-Cu(1)-N(2)	74.6(3)
Cu(1)-Cl(3)	2.279(3)	N(21)-Zn(1)-N(1)	77.2(4)	N(51)-Cu(1)-N(2)	74.1(3)
Cu(1)-Cl(4)	2.284(3)	Cl(2)-Zn(1)-N(1)	150.8(3)	Cl(3)-Cu(1)-N(2)	105.2(3)
Cu(1)-N(2)	2.499(2)	Cl(1)-Zn(1)-N(1)	105.6(3)	Cl(4)-Cu(1)-N(2)	144.8(3)
[Cu₂(1,3-tpbd)₂(H₂O)₂](ClO₄)₄ (18)					
Cu(1)-N(1)	2.074(3)	N(3)-Cu(1)-N(2)	164.8(2)	N(2)-Cu(1)-N(1)	82.4(2)
Cu(1)-N(2)	1.986(3)	N(3)-Cu(1)-N(5) ^[a]	98.4(2)	N(3)-Cu(1)-O(1)	89.4(2)
Cu(1)-N(3)	1.976(3)	N(2)-Cu(1)-N(5) ^[a]	96.8(2)	N(3)-Cu(1)-N(1)	83.5(2)
Cu(1)-N(5)	2.000(3)	N(5) ^[a] -Cu(1)-N(1)	157.4(2)	N(2)-Cu(1)-O(1)	87.0(2)
Cu(1)-O(1)	2.286(3)	N(5) ^[a] -Cu(1)-O(1)	104.1(2)	N(1)-Cu(1)-O(1)	98.5(1)
[Cu₂(2,6-tpcd)(H₂O)(Cl)](ClO₄)₂ x 2H₂O (19)					
Cu(1)-O(2)	1.993(2)	O(2)-Cu(1)-N(5)	94.3(1)	N(3)-Cu(2)-N(2)	159.1(1)
Cu(1)-N(5)	2.003(2)	O(2)-Cu(1)-N(6)	99.3(1)	N(3)-Cu(2)-N(1)	82.9(1)
Cu(1)-N(6)	2.013(2)	N(5)-Cu(1)-N(6)	163.8(1)	N(2)-Cu(2)-N(1)	81.9(1)
Cu(1)-N(4)	2.064(2)	O(2)-Cu(1)-N(4)	176.8(1)	N(3)-Cu(2)-O(1)	96.0(1)
Cu(1)-O(1)	2.153(2)	N(5)-Cu(1)-N(4)	82.9(1)	N(2)-Cu(2)-O(1)	96.5(1)
Cu(2)-N(3)	1.996(2)	N(6)-Cu(1)-N(4)	83.6(1)	N(1)-Cu(2)-O(1)	84.0(1)
Cu(2)-N(2)	2.007(2)	O(2)-Cu(1)-O(1)	94.9(1)	N(3)-Cu(2)-Cl(1)	97.8(1)

Chapter 4

Cu(2)-N(1)	2.076(2)	N(5)-Cu(1)-O(1)	94.9(1)	N(2)-Cu(2)-Cl(1)	96.6(1)
Cu(2)-O(1)	2.106(2)	N(6)-Cu(1)-O(1)	92.6(1)	N(1)-Cu(2)-Cl(1)	176.7(1)
Cu(2)-Cl(1)	2.280(1)	N(4)-Cu(1)-O(1)	83.7(1)	O(1)-Cu(2)-Cl(1)	99.1(1)

^[a] -x+1, -y+1, -z+1

Chapter 5 - Synthesis and characterization of 1,3,5-Triaminobenzene Trihydrochloride and the ligand 1,3,5-Tris[bis(2-pyridylmethyl)amino]benzene (1,3,5-hpbt).

This work in its final form is supposed to be submitted for publication in the *European Journal of Organic Chemistry*.

Sabrina Turba, Heike Hausmann, Peter R. Schreiner and Siegfried Schindler.

5.1 Introduction.

The Ligand 1,3-Bis[bis(2-pyridylmethyl)amino]benzene (1,3-tpbd, Scheme 4-1 in Chapter 4) and a series of its complexes with several transition metal ions were synthesized previously.^[26, 34, 39, 41]

Due to the interesting magnetic properties of the copper(II) complexes of 1,3-tpbd it was obvious to try to increase the complexity of this system by implementation of a further “coordinating arm” and therefore we attempted to synthesize the ligand 1,3,5-Tris[bis(2-pyridylmethyl)amino]benzene (1,3,5-hpbt, Figure 5-1).

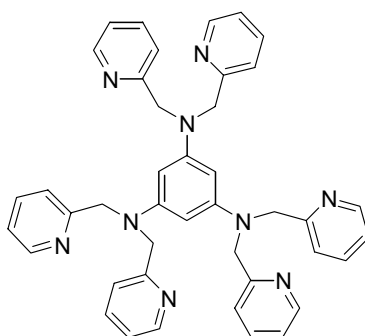


Figure 5-1. The ligand 1,3,5-Tris[bis(2-pyridylmethyl)amino]benzene (1,3,5-hpbt).

A copper(II) complex with the related ligand *N,N,N'*-1,3,5-benzenetris(oxamate) which is shown in Figure 5-1, (and also in Figure 1-8 in Chapter 1) was synthesized previously and its interesting magnetic properties were reported in detail.^[40]

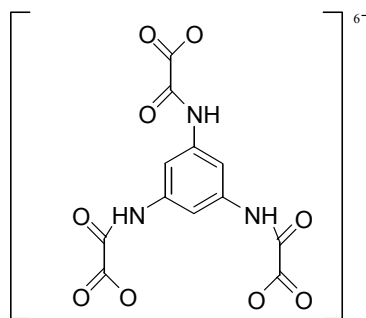


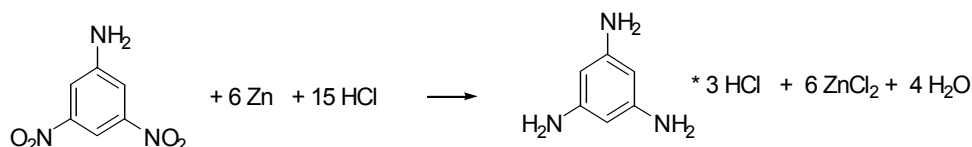
Figure 5-2. The ligand *N,N',N''*-1,3,5-benzenetris(oxamate).

5.2 Results and Discussion.

5.2.1 Synthesis of 1,3,5-triaminobenzene trihydrochloride.

To obtain the ligand 1,3,5-hpbt, the precursor compound 1,3,5-triaminobenzene needed to be synthesized (Scheme 5-1). The ligand *N,N',N''*-1,3,5-benzenetris(oxamate), shown in Figure 5. 1, is based on the same structural unit. It is well known from previous syntheses that 1,3,5-triaminobenzene is not very stable in its free form.^[40, 149] In contrast, the trihydrochloride of 1,3,5-triaminobenzene is much more stable compared with the unprotonated amine. It was prepared according to the method of Fromm and Ebert,^[138] similar to the synthesis of the precursor (2,6-diamino-*p*-cresole dihydrochloride) of the ligand 2,6-bis[bis(2-pyridylmethyl)amino]*p*-cresole (2,6-tpcd) described above (Chapter 4.3.3).^[41]

In the original synthesis tin was used as a reducing agent for 3,5-dinitroaniline, however, we could demonstrate in our experiments that zinc could be used in the same way according to Scheme 5-1. The formed zinc ions were removed from the solution as zinc sulfide that was obtained by bubbling H₂S through the solution.



Scheme 5-1. Synthesis of 1,3,5-triaminobenzene trihydrochloride.

The product was obtained in good yield in form of beige needles that could be characterized structurally. Figure 5-3 shows the crystal structure of 1,3,5-

triaminobenzene trihydrochloride and crystallographic data as well as selected bond lengths and angles are depicted in Table 5-1 and 5-2.

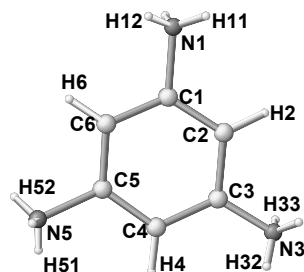


Figure 5-3. Molecular structure of 1,3,5-triaminobenzene trihydrochloride. Tetrachlorozincate and chloride ions as well as solvent molecules are omitted for clarity.

The angles between the benzene carbon atoms and the three amine-nitrogen atoms, with one exception, are in the range of 117.5(4) (for N(3)–C(3)–C(2)) to 119.(3) (for C(2)–C(1)–N(1)). The angle N(3)–C(3)–C(4) differs with a value of 122.9(4) remarkably. This distortion might be caused by the presence of another 1,3,5-triaminobenzene trihydrochloride molecule in the unit cell, that is responsible for an enlargement of this angle. All protons at the nitrogen atoms could be located. Interestingly, tetrachlorozincate was observed in the crystals, obviously the result of incomplete formation and separation of zinc sulfide. The tetrachlorozincate is located between two 1,3,5-triaminobenzene molecules.

Furthermore, 1,3,5-triaminobenzene trihydrochloride was characterized by NMR spectroscopy. The ^1H -NMR spectrum of 1,3,5-triaminobenzene trihydrochloride is shown in Figure 5-4. It is characterized by the signal of the benzene hydrogen atoms at 6.76 ppm (the solvent signal of d_6 -DMSO appears at 2.56 ppm).

The characterization of the substance 1,3,5 triaminobenzene trihydrochloride by NMR spectroscopy was of great interest because ten years ago, Barfield and Fagerness calculated it's chemical shifts by the use of DFT methods^[150] and therefore it was now possible to confirm their predicted results.

In 1,3,5 triaminobenzene trihydrochloride, the protonated amine groups are able to couple with the adjacent hydrogen atoms of the benzene ring and a triplet at 7.26

ppm is observed. Furthermore, a broad singlet at 9.20-10.00 ppm is observed in the NMR spectrum for the unprotonated form. The equilibrium for this protonation/deprotonation reaction is fast and could not be estimated.

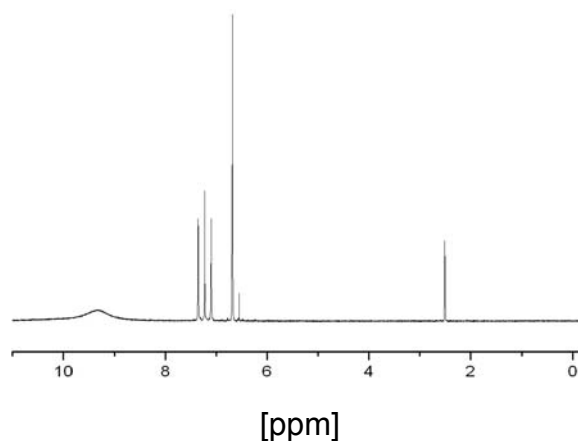
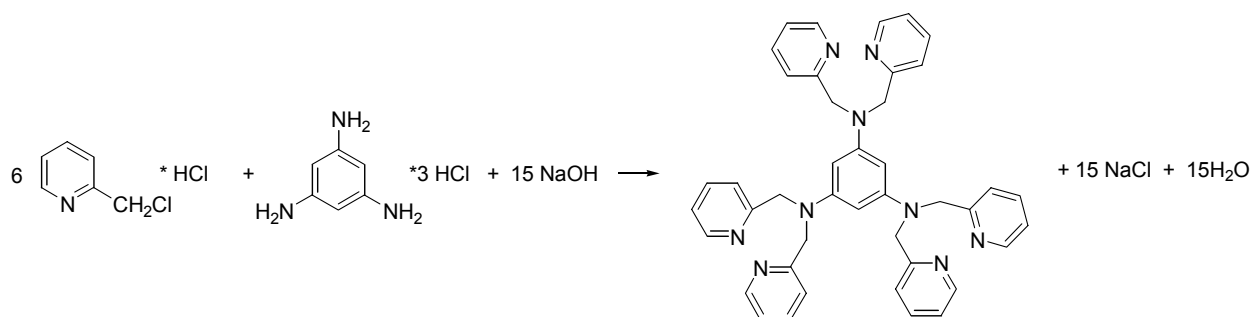


Figure 5-4. NMR-Spectra of 1,3,5-triaminobenzene trihydrochloride.

5.2.2 Synthesis of the ligand 1,3,5-hpbt.

In accordance with the synthesis of phbpa and 1,3-tpbd, 1,3,5-hpbt was obtained by a nucleophilic substitution reaction of 1,3,5-triaminobenzene trihydrochloride with 2-(chloromethyl)pyridine hydrochloride.^{[87] [26]} The reaction is shown in Scheme 5-2.^[26]



Scheme 5-2. Synthesis of 1,3,5-tris[bis(2-pyridylmethyl)amino]benzene (1,3,5-hpbt).

The crude product of 1,3,5-hpbt was obtained as a dark brown oil. Efforts to purify the product proved to be difficult, however using a soxhlet-apparatus, with petrol ether (40/60) as solvent allowed to obtain a quite pure product, identified by NMR spectroscopy, in extremely low yield.

Unfortunately, all efforts so far to obtain crystals of a copper complex of the ligand 1,3,5-hpbt, suitable for X-ray crystallography were unsuccessful.

5.3 Experimental Section

5.3.1 General Remarks.

All chemicals were purchased from commercial resources and used as received.

5.3.2 Physical Measurements.

NMR spectra were recorded with a Bruker Aspect 2000/3000.

5.3.3 Synthesis of 1,3,5-triaminobenzene trihydrochloride.^[138]

3,5-Dinitroaniline (2.02 g; 0.011 mol) and zinc (5.71 g; 0.048 mol) were mixed under an argon atmosphere. To this mixture, hydrochloric acid (37%, 24 mL) was added dropwise with stirring. The suspension was cooled in an ice bath and the resulting brown solution was stirred for 3 hours under these conditions. Subsequent removal of the excess of hydrochloric acid was accomplished by distillation and a brown-black solid was obtained. This material was dissolved in approximately 60 mL of water and the zinc ions were removed from the brown solution by bubbling H₂S through the solution. The precipitated zinc sulfide was filtered and the volume of the resulting light yellow solution was reduced by distillation with a rotary evaporator to about 25 mL. Storing the solution for one night in a refrigerator allowed the collection of brown yellow crystals (needles) of 1,3,5-triaminobenzene suitable for X-ray crystallography.

Yield: 2.12 g (0.009 mol; 82%)

¹H-NMR (DMSO-d₆, 400MHz): δ = 6.76 (s, 3 H, C2-, C4- and C6- Ar-H), 7.26 (t, protonated NH₂-substituents)

¹³C-{¹H}NMR (DMSO-d₆, 400MHz): δ = 107.1 (C2-, C4- or C6-Ar), 108.4 (C2-, C4- or C6-Ar), 135.0 (quaternary C1-, C3- or C5-Ar with NH₂- / NH₃⁺-substituent), 159.1 (quaternary C1-, C3- or C5-Ar with NH₂- / NH₃⁺-substituent)

5.3.4 Synthesis of the ligand 1,3,5-hpbt.^[26]

A solution of sodium hydroxide (4.34 g; 0.1075 mol) in water (20 mL) was added dropwise with stirring to a mixture of 1,3,5-triaminobenzene trihydrochloride (1.00 g; 0.0043 mol) and 2-(chloromethyl)pyridine hydrochloride (5.64 g; 0.0344 mol) in 20 mL water under inert conditions during the time of one week. The brown and oily crude product was separated and purified using a soxhlet-apparatus with petrol ether (40/60) as solvent. The product was obtained in form of a few brown-yellow needles.

¹H-NMR (CDCl₃, 400 MHz): δ = 4.69 (s, 8 H, -CH₂-), 6.05-6.15 (m, 3 H, C2-, C4- and C6- Ar-H), 6.95 (t, 1H, C5- Ar-H), 7.10-7.25 (m, 8 H, C4- and C5- Pyr-H), 7.50-7.60 (m, 4 H, C3- Pyr-H), 8.45-8.55 (m, 4 H, C6- Pyr-H)

¹³C-{¹H}NMR (CDCl₃, 400 MHz): δ = 57.3 (-CH₂-), 97.3 (C2-Ar), 102.5 (C4- and C6-Ar), 120.9 (C5-Pyr), 121.8 (C3-Pyr), 129.9 (C5-Ar), 136.6 (C4-Pyr), 149.4 (C6-Pyr), 149.6 (C1- and C3-Ar), 159.0 (C2-Pyr)

5.3.5 X-ray Crystallographic Studies.

Intensity data of 1,3,5-triaminobenzene trihydrochloride were collected on a Siemens SMART CCD 1000 diffractometer by the ω -scan technique collecting a full sphere of data with irradiation times of 10 to 20 s per frame and $\Delta\omega$ ranges between 0.3° and 0.45°. The collected reflections were corrected for absorption, Lorentz and polarization effects^[70] All structures were solved by direct methods and refined by least-squares techniques using the SHELX-97 programme package^[71]. The hydrogen atoms were positioned geometrically and all non-hydrogen atoms were refined anisotropically, if not mentioned otherwise. Further data collection parameters are summarised in Table 5-1.

Table 5-1. Crystallographic data and experimental details.

Compound	1,3,5-triaminobenzene trihydrochloride
Empirical formula	C ₆ H ₁₄ Cl ₅ N ₃ Ozn
<i>M_r</i>	386.82
Temperature [K]	200(2)
Radiation (λ [Å])	Mo-K _α , 0.71073
Crystal shape	beige block
Crystal size [mm]	0.25 × 0.25 × 0.25
Crystal system	Triclinic
Space group	P-1 (No. 2)
<i>a</i> [Å]	7.127(1)
<i>b</i> [Å]	9.665(2)
<i>c</i> [Å]	11.080(2)
α [°]	98.490(2)
β [°]	100.186(2)
γ [°]	109.087(2)
<i>V</i> [Å ³]	692.4(2)
<i>Z</i>	2
ρ _{calcd.} [g·cm ⁻³]	1.855
μ [mm ⁻¹]	2.721
<i>F</i> (000)	388
Scan range θ [°]	1.91 to 28.29
Index ranges	−9 ≤ <i>h</i> ≤ 9 −12 ≤ <i>k</i> ≤ 12 −14 ≤ <i>l</i> ≤ 14
Reflections collected	8522
Unique reflections	3351
<i>R</i> _{int}	0.0396
Data/restraints/parameters	3351/72/191
Goodness-of-fit on <i>F</i> ²	1.032
Final <i>R</i> indices [<i>I</i> > 2σ(<i>I</i>)]	<i>R</i> 1 = 0.0492 <i>wR</i> 2 = 0.1115
<i>R</i> indices (all data)	<i>R</i> 1 = 0.0725 <i>wR</i> 2 = 0.1214
Largest diff. peak/hole [e·Å ⁻³]	0.728/−0.489

Table 5-2. Selected bond lengths and angles.

Atoms	1,3,5-triaminobenzene trihydrochloride
N(1)–C(1)	1.469(5)
N(1)–H(11)	0.73(2)
N(1)–H(12)	0.73(2)
N(1)–H(13)	0.73(2)
N(3)–C(3)	1.348(5)
N(3)–H(31)	0.72(2)
N(3)–H(32)	0.72(2)
N(3)–H(33)	0.72(2)
N(5)–C(5)	1.464(5)
N(5)–H(51)	0.73(2)
N(5)–H(52)	0.73(2)
N(5)–H(53)	0.73(2)
C(1)–C(2)	1.377(6)
C(1)–C(6)	1.383(6)
C(2)–C(3)	1.397(6)
C(2)–H(2)	0.9300
C(3)–C(4)	1.392(6)
C(4)–C(5)	1.381(6)
C(4)–H(4)	0.9300
C(5)–C(6)	1.372(6)
C(6)–H(6)	0.9300
C(1)–N(1)–H(11)	113(4)
C(1)–N(1)–H(12)	108(4)
H(11)–N(1)–H(12)	111(2)
C(1)–N(1)–H(13)	103(5)
H(11)–N(1)–H(13)	110(2)
H(12)–N(1)–H(13)	110(3)
C(3)–N(3)–H(31)	111(8)
C(3)–N(3)–H(32)	110(4)
H(31)–N(3)–H(32)	114(3)
C(3)–N(3)–H(33)	90(4)
H(31)–N(3)–H(33)	116(3)
H(32)–N(3)–H(33)	114(3)
C(5)–N(5)–H(51)	110(5)
C(5)–N(5)–H(52)	108(7)
H(51)–N(5)–H(52)	113(3)
C(5)–N(5)–H(53)	103(7)
H(51)–N(5)–H(53)	111(3)
H(52)–N(5)–H(53)	112(3)
C(2)–C(1)–C(6)	122.9(4)
C(2)–C(1)–N(1)	119.3(4)
C(6)–C(1)–N(1)	117.7(4)
C(1)–C(2)–C(3)	118.9(4)
C(1)–C(2)–H(2)	120.5
C(3)–C(2)–H(2)	120.5
N(3)–C(3)–C(4)	122.9(4)
N(3)–C(3)–C(2)	117.5(4)
C(4)–C(3)–C(2)	119.6(4)
C(5)–C(4)–C(3)	118.7(4)
C(5)–C(4)–H(4)	120.6
C(3)–C(4)–H(4)	120.6
C(6)–C(5)–C(4)	123.3(4)
C(6)–C(5)–N(5)	118.1(4)
C(4)–C(5)–N(5)	118.7(4)
C(5)–C(6)–C(1)	116.6(4)
C(5)–C(6)–H(6)	121.7
C(1)–C(6)–H(6)	121.7

Summary

Syntheses and characterisations of metal complexes with the ligand 1,3-bis[bis(2-pyridylmethyl)amino]benzene(1,3-tpbd) and its derivatives *N*, *N*-bis(2-pyridylmethyl)aniline (phbpa), 2,6-bis[bis(2-pyridylmethyl)amino]-*p*-cresole (2,6-tpcd) und 1,3,5-tris[bis(2-pyridylmethyl)amino]benzene (1,3,5-hpbt) as well as its *ortho*- and *para*-substituted analogues 1,2-bis[bis(2-pyridylmethyl)amino]benzene (1,2-tpbd) and 1,4-bis[bis(2-pyridylmethyl)amino]benzene (1,4-tpbd) are reported herein. These investigations are based on the previous studies on the complex $[\text{Cu}_2(1,3\text{-tpbd})(\text{H}_2\text{O})_2(\text{ClO}_4)_3]\text{ClO}_4$, which showed quite interesting magnetic behaviour. As briefly described in chapter 2 and 3, the magnetic properties of the copper(II) complexes with the ligand 1,3-tpbd were strongly dependent on the presence of additional ligands/anions. These investigations have been successfully continued in this work and in cooperation with the researchers mentioned in the previous chapters, the following copper(II), iron(II), nickel(II) and zinc(II) complexes with the ligand 1,3-tpbd could be synthesized and characterized using X-ray diffraction methods.

- $[\text{Cu}_4(1,3\text{-tpbd})_2(\text{H}_2\text{O})_4(\text{NO}_3)_4](\text{NO}_3)_4 \times 13 \text{ H}_2\text{O}$ (**1**)
- $[\text{Cu}_4(1,3\text{-tpbd})_2(\text{AsO}_4)(\text{ClO}_4)_3(\text{H}_2\text{O})](\text{ClO}_4)_2 \times 2 \text{ H}_2\text{O} \times 0.5 \text{ CH}_3\text{OH}$ (**2**)
- $[\text{Cu}_4(1,3\text{-tpbd})_2(\text{PO}_4)(\text{ClO}_4)_3(\text{H}_2\text{O})](\text{ClO}_4)_2 \times 2 \text{ H}_2\text{O} \times 0.5 \text{ CH}_3\text{OH}$ (**3**)
- $[\text{Cu}_2(1,3\text{-tpbd})((\text{PhO})_2\text{P}(\text{O})\text{OH})_2(\text{H}_2\text{O})_2](\text{ClO}_4)_2$ (**4**)
- $[\text{Cu}_2(1,3\text{-tpbd})((\text{PhO})\text{PO}_3)_2(\text{H}_2\text{O})_{0.69}(\text{CH}_3\text{CN})_{0.31}]_2(\text{BPh}_4)_4 \times \text{Et}_2\text{O} \times \text{CH}_3\text{CN}$ (**5**)
- $[\text{Cu}_2\text{Cl}_4(1,3\text{-tpbd})] \times 0.84 \text{ CH}_3\text{OH}$ (**8**)
- $[\{\text{Cu}_2\text{Cl}_2(\text{ClO}_4)(1,3\text{-tpbd})\}\text{Cl}\{\text{Cu}_2\text{Cl}_2(\text{OH}_2)(1,3\text{-tpbd})\}](\text{ClO}_4)_2$ (**9**)
- $[\text{Cu}_2(\text{OH}_2)_2(\text{S}_2\text{O}_6)(1,3\text{-tpbd})]\text{S}_2\text{O}_6 \times 2 \text{ H}_2\text{O} \times \text{CH}_3\text{OH}$ (**10**)
- $[\text{Fe}_2(1,3\text{-tpbd})(\text{CH}_3\text{CN})_6](\text{ClO}_4)_4 \times 2 \text{ CH}_3\text{CN} \times 0.5 \text{ H}_2\text{O}$ (**12**)
- $[\text{Fe}_2(1,3\text{-tpbd})(\text{DMF})_6](\text{ClO}_4)_4$ (**13**)
- $[\text{Ni}_2(1,3\text{-tpbd})(\text{DMF})_6](\text{ClO}_4)_4$ (**14**)

- $[\text{Zn}_2(1,3\text{-tpbd})(\text{CH}_3\text{CN})_2(\text{SO}_3\text{CF}_3)_2(\text{H}_2\text{O})](\text{SO}_3\text{CF}_3)_2$ (**15**)
- $[\text{Zn}_2(1,3\text{-tpbd})\text{Cl}_4]$ (**16**)
- $[\text{CuZn}(1,3\text{-tpbd})\text{Cl}_4]$ (**17**)
- $[\text{Cu}_2(1,3\text{-tpbd})_2(\text{H}_2\text{O})_2](\text{ClO}_4)_4$ (**18**)

Furthermore, the following copper(II) complexes with the ligands phbpa, 1,2-tpbd and 1,4-tpbd could be synthesized and furthermore, with the exception of complex $[\text{Cu}_2\text{Cl}_4(1,4\text{-tpbd})]$, they could be structurally characterized.

- $[\text{CuCl}_2(\text{phbpa})]$ (**6**)
- $[\text{Cu}(1,2\text{-tpbd})](\text{PF}_6)_2$ (**7**)
- $[\text{Cu}_2\text{Cl}_4(1,4\text{-tpbd})]$ (**11**)

The complexes $[\text{Cu}_4(1,3\text{-tpbd})_2(\text{AsO}_4)(\text{ClO}_4)_3(\text{H}_2\text{O})](\text{ClO}_4)_2 \times 2 \text{ H}_2\text{O} \times 0.5 \text{ CH}_3\text{OH}$ and $[\text{Cu}_4(1,3\text{-tpbd})_2(\text{PO}_4)(\text{ClO}_4)_3(\text{H}_2\text{O})](\text{ClO}_4)_2 \times 2 \text{ H}_2\text{O} \times 0.5 \text{ CH}_3\text{OH}$ are tetranuclear compounds and in each the arsenate/phosphate ion acts as a bridge between four copper(II) ions. Hence, the Cu(1)···Cu(2)-distances in these compounds are with 4.358/4.226 Å significantly shorter than in the complexes that were synthesized previously. The investigation of the magnetic properties of the complex $[\text{Cu}_4(1,3\text{-tpbd})_2(\text{PO}_4)(\text{ClO}_4)_3(\text{H}_2\text{O})](\text{ClO}_4)_2 \times 2 \text{ H}_2\text{O} \times 0.5 \text{ CH}_3\text{OH}$ showed the expected paramagnetic behaviour.

Furthermore, detailed magnetic investigations on the complexes $[\text{CuCl}_2(\text{phbpa})]$ (**6**), $[\text{Cu}_2\text{Cl}_4(1,3\text{-tpbd})] \times 0.84 \text{ CH}_3\text{OH}$ (**8**), $[\{\text{Cu}_2\text{Cl}_2(\text{ClO}_4)(1,3\text{-tpbd})\}\text{Cl}\{\text{Cu}_2\text{Cl}_2(\text{OH}_2)(1,3\text{-tpbd})\}](\text{ClO}_4)_2$ (**9**) and $[\text{Cu}_2(\text{OH}_2)_2(\text{S}_2\text{O}_6)(1,3\text{-tpbd})]\text{S}_2\text{O}_6 \times 2 \text{ H}_2\text{O} \times \text{CH}_3\text{OH}$ (**10**) were performed. For the complex $[\{\text{Cu}_2\text{Cl}_2(\text{ClO}_4)(1,3\text{-tpbd})\}\text{Cl}\{\text{Cu}_2\text{Cl}_2(\text{OH}_2)(1,3\text{-tpbd})\}](\text{ClO}_4)_2$ (**9**) theoretical calculations of the DFT type were performed to visualize and evaluate the efficiency of the intramolecular exchange pathways involved.

However, the main aim concerning a thorough comparison of the magnetic properties of stoichiometrically identical, structurally isomeric dicopper(II) complexes of 1,*n*-tpbd without auxiliary bridging ligands is still missing because of the lack of X-ray quality crystals of the dinuclear $[\text{Cu}(1,n\text{-tpbd})\text{Cu}]^{4+}$ core as chloride, dithionate, perchlorate or hexafluorophosphate salts. Thus the effect of *meta* against *para* versus *ortho*

substitution on the magnetic properties still cannot be assessed satisfactorily in order to test the spin polarisation mechanism. Even though a mononuclear complex of 1,2-tpbd was obtained, formation of dinuclear complexes with this ligand are unlikely.

The ligand 1,3-tpbd in its unprotonated as well as in its protonated form could be characterized crystallographically. It is remarkable that the protons (in the protonated compounds $[H_2(1,3\text{-tpbd})](ClO_4)_2$ and $[H_2(1,3\text{-tpbd})](CF_3SO_3)_2$) are, similar to small metal cations, coordinated between the pyridine nitrogen atoms of the ligand.

While the nickel complex shows normal coordination behavior, redox active metal centers such as iron or copper ions demonstrate that 1,3-tpbd is a non-innocent ligand. Interestingly 1,3-tpbd does not coordinate iron(III) ions, instead protonation of the ligand is preferred. Oxidations of iron(II) complexes or copper(I) complexes of 1,3-tpbd led to reaction product mixtures that could not be characterized so far. Theoretical calculations support the formation of a dinuclear side-on copper peroxo complex during the reaction of the copper(I) complex with dioxygen. Intramolecular ligand hydroxylation was not observed during the oxidation reaction, however, preliminary experiments showed the formation of a violet coloured peroxo-intermediate. Unfortunately this reaction could not be reproduced for reasons that are not clear at all. The reaction product that would have formed if an intramolecular hydroxylation reaction would occur during oxidation, a phenolate bridged derivative of the 1,3-tpbd complex, using the ligand 2,6-tpcd, could be synthesized in an independent way. The thus obtained $[Cu_2(2,6\text{-tpcd})(H_2O)(Cl)](ClO_4)_2 \times 2 H_2O$ (**19**) could be structurally characterized.

Most interestingly is the reaction if only one equivalent of copper(II) salt is reacted with one equivalent of 1,3-tpbd. Under aerobic conditions a red product was formed after a short while, suggesting ligand oxidation. However, this reaction could be suppressed completely in the presence of zinc ions. Here $[Cu_2(1,3\text{-tpbd})_2(H_2O)_2](ClO_4)_4$ a so called "dimetallocyclophane" formed.

To increase the complexity of the 1,3-tpbd ligand a further "ligand arm" was introduced, forming the new ligand 1,3,5-Hpbt. Efforts to obtain the trinuclear copper complex of this ligand were unsuccessful. However, the precursor compound prepared for the synthesis of this ligand, the protonated 1,3,5-triaminobenzene (that

could be structurally characterized), proved to be very interesting for detailed NMR studies.

Zusammenfassung

In dieser Arbeit wird die Synthese und Charakterisierung von Metall-Komplexen mit dem Liganden 1,3-Bis[bis(2-pyridylmethyl)amino]benzol (1,3-tpbd) und seinen Derivaten *N, N*-Bis(2-pyridylmethyl)anilin (phbpa), 2,6-Bis[bis(2-pyridylmethyl)amino]-*p*-kresol (2,6-tpcd) und 1,3,5-Tris[bis(2-pyridylmethyl)amino]benzol (1,3,5-hpbt) sowie seinen *ortho*- und *para*-substituierten Analoga 1,2-Bis[bis(2-pyridylmethyl)amino]benzol (1,2-tpbd) und 1,4-Bis[bis(2-pyridylmethyl)amino]benzol (1,4-tpbd) beschrieben. Ausgangspunkt war der Komplex $[\text{Cu}_2(1,3\text{-tpbd})(\text{H}_2\text{O})_2(\text{ClO}_4)_3]\text{ClO}_4$, dessen ungewöhnliche magnetische Eigenschaften von großem Interesse waren. Wie in Kapitel 2 und 3 beschrieben, konnten die magnetischen Eigenschaften der bisher dargestellten Kupfer(II)-Komplexe mit dem Liganden 1,3-tpbd durch zusätzliche Liganden/Anionen variiert werden. Im Rahmen dieser Arbeit wurden diese Untersuchungen erfolgreich fortgesetzt und in Kooperation mit den in den jeweiligen Kapiteln aufgeführten Wissenschaftlern konnten die folgenden Kupfer(II)-, Eisen(II), Nickel(II) und Zink(II)-Komplexe dargestellt und kristallographisch charakterisiert werden.

- $[\text{Cu}_4(1,3\text{-tpbd})_2(\text{H}_2\text{O})_4(\text{NO}_3)_4](\text{NO}_3)_4 \times 13 \text{ H}_2\text{O}$ (**1**)
- $[\text{Cu}_4(1,3\text{-tpbd})_2(\text{AsO}_4)(\text{ClO}_4)_3(\text{H}_2\text{O})](\text{ClO}_4)_2 \times 2 \text{ H}_2\text{O} \times 0.5 \text{ CH}_3\text{OH}$ (**2**)
- $[\text{Cu}_4(1,3\text{-tpbd})_2(\text{PO}_4)(\text{ClO}_4)_3(\text{H}_2\text{O})](\text{ClO}_4)_2 \times 2 \text{ H}_2\text{O} \times 0.5 \text{ CH}_3\text{OH}$ (**3**)
- $[\text{Cu}_2(1,3\text{-tpbd})((\text{PhO})_2\text{P}(\text{O})\text{OH})_2(\text{H}_2\text{O})_2](\text{ClO}_4)_2$ (**4**)
- $[\text{Cu}_2(1,3\text{-tpbd})((\text{PhO})\text{PO}_3)_2(\text{H}_2\text{O})_{0.69}(\text{CH}_3\text{CN})_{0.31}]_2(\text{BPh}_4)_4 \times \text{Et}_2\text{O} \times \text{CH}_3\text{CN}$ (**5**)
- $[\text{Cu}_2\text{Cl}_4(1,3\text{-tpbd})] \times 0.84 \text{ CH}_3\text{OH}$ (**8**)
- $[\{\text{Cu}_2\text{Cl}_2(\text{ClO}_4)(1,3\text{-tpbd})\}\text{Cl}\{\text{Cu}_2\text{Cl}_2(\text{OH}_2)(1,3\text{-tpbd})\}](\text{ClO}_4)_2$ (**9**)
- $[\text{Cu}_2(\text{OH}_2)_2(\text{S}_2\text{O}_6)(1,3\text{-tpbd})]\text{S}_2\text{O}_6 \times 2 \text{ H}_2\text{O} \times \text{CH}_3\text{OH}$ (**10**)
- $[\text{Fe}_2(1,3\text{-tpbd})(\text{CH}_3\text{CN})_6](\text{ClO}_4)_4 \times 2 \text{ CH}_3\text{CN} \times 0.5 \text{ H}_2\text{O}$ (**12**)
- $[\text{Fe}_2(1,3\text{-tpbd})(\text{DMF})_6](\text{ClO}_4)_4$ (**13**)
- $[\text{Ni}_2(1,3\text{-tpbd})(\text{DMF})_6](\text{ClO}_4)_4$ (**14**)

- $[\text{Zn}_2(1,3\text{-tpbd})(\text{CH}_3\text{CN})_2(\text{SO}_3\text{CF}_3)_2(\text{H}_2\text{O})](\text{SO}_3\text{CF}_3)_2$ (**15**)
- $[\text{Zn}_2(1,3\text{-tpbd})\text{Cl}_4]$ (**16**)
- $[\text{CuZn}(1,3\text{-tpbd})\text{Cl}_4]$ (**17**)
- $[\text{Cu}_2(1,3\text{-tpbd})_2(\text{H}_2\text{O})_2](\text{ClO}_4)_4$ (**18**)

Zudem wurden folgende Kupfer(II) Komplexe mit den Liganden phbpa, 1,2-tpbd und 1,4-tpbd dargestellt. Diese konnten, mit Ausnahme des Komplexes $[\text{Cu}_2\text{Cl}_4(1,4\text{-tpbd})]$, erfolgreich kristallographisch charakterisiert werden.

- $[\text{CuCl}_2(\text{phbpa})]$ (**6**)
- $[\text{Cu}(1,2\text{-tpbd})](\text{PF}_6)_2$ (**7**)
- $[\text{Cu}_2\text{Cl}_4(1,4\text{-tpbd})]$ (**11**)

Bei den Komplexen $[\text{Cu}_4(1,3\text{-tpbd})_2(\text{AsO}_4)(\text{ClO}_4)_3(\text{H}_2\text{O})](\text{ClO}_4)_2 \times 2 \text{ H}_2\text{O} \times 0.5 \text{ CH}_3\text{OH}$ und $[\text{Cu}_4(1,3\text{-tpbd})_2(\text{PO}_4)(\text{ClO}_4)_3(\text{H}_2\text{O})](\text{ClO}_4)_2 \times 2 \text{ H}_2\text{O} \times 0.5 \text{ CH}_3\text{OH}$ gelang es erstmals Komplextetramere darzustellen, bei welchen das Arsenat- bzw. das Phosphat-Ion sowohl intra- als auch intermolekular verbrückend zwischen den Kupfer(II)-Atomen wirkt. Demzufolge sind die $\text{Cu}(1)\cdots\text{Cu}(2)$ -Abstände bei diesen beiden Verbindungen mit 4,358 bzw. 4,226 Å deutlich kleiner als bei den bisher synthetisierten Komplexen. Eine Untersuchung der magnetischen Eigenschaften des Komplexes $[\text{Cu}_4(1,3\text{-tpbd})_2(\text{PO}_4)(\text{ClO}_4)_3(\text{H}_2\text{O})](\text{ClO}_4)_2 \times 2 \text{ H}_2\text{O} \times 0.5 \text{ CH}_3\text{OH}$ ergab das erwartete paramagnetische Verhalten.

Zudem wurden detaillierte magnetische Untersuchungen an den Komplexen $[\text{CuCl}_2(\text{phbpa})]$ (**6**), $[\text{Cu}_2\text{Cl}_4(1,3\text{-tpbd})] \times 0.84 \text{ CH}_3\text{OH}$ (**8**), $[\{\text{Cu}_2\text{Cl}_2(\text{ClO}_4)(1,3\text{-tpbd})\}\text{Cl}\{\text{Cu}_2\text{Cl}_2(\text{OH}_2)(1,3\text{-tpbd})\}](\text{ClO}_4)_2$ (**9**) und $[\text{Cu}_2(\text{OH}_2)_2(\text{S}_2\text{O}_6)(1,3\text{-tpbd})]\text{S}_2\text{O}_6 \times 2 \text{ H}_2\text{O} \times \text{CH}_3\text{OH}$ (**10**) durchgeführt. Für den Komplex $[\{\text{Cu}_2\text{Cl}_2(\text{ClO}_4)(1,3\text{-tpbd})\}\text{Cl}\{\text{Cu}_2\text{Cl}_2(\text{OH}_2)(1,3\text{-tpbd})\}](\text{ClO}_4)_2$ wurde ausserdem eine DFT-Rechnung durchgeführt, um den Mechanismus des stattfindenden intramolekularen magnetischen Austauschs visualisieren zu können.

Jedoch konnte in diesem Zusammenhang eines der Hauptziele dieses Aufgabengebietes, welches darin bestand, die magnetischen Eigenschaften der isomeren, dinuklearen unverbrückten Kupfer(II)-Komplexe der 1,*n*-tpbd-Reihe

miteinander zu vergleichen, nicht erreicht werden. Unzureichende Qualität einzelner Röntgenstrukturanalysen machte einen aussagekräftigen Vergleich des Einflusses der *meta*- gegen *para*- und *ortho*-Substitution auf die magnetischen Eigenschaften unmöglich.^[26, 86]

Erstmals gelang es im Rahmen dieser Arbeit, die Struktur des Liganden 1,3-tpbd, sowohl in reiner als auch in deprotonierter Form kristallographisch zu charakterisieren. Erwähnenswert ist in diesem Zusammenhang, dass die Protonen in den Strukturen X und Y wie kleine Metallkationen zwischen den Pyridin-Stickstoffatomen des Liganden koordiniert sind.

Während der beschriebene Nickel (II) Komplex mit dem Liganden 1,3-tpbd normales Koordinationsverhalten zeigt, demonstrieren redox-aktive Metallzentren wie Eisen- oder Kupfer-Ionen, dass 1,3-tpbd durchaus in der Lage ist, an den jeweiligen Redox-Reaktionen teilzunehmen. Interessanterweise, koordiniert 1,3-tpbd beispielsweise keine Eisen(III) Kationen, stattdessen wird eine Protonierung des Liganden bevorzugt. Oxidationen von Eisen(II)- oder Kupfer(I)-Komplexen mit 1,3-tpbd resultieren in Reaktionsgemischen, die bisher noch nicht weiter charakterisiert werden konnten. Theoretische Rechnungen sagen die Bildung eines zweikernigen side-on Kupfer-Peroxo Komplexes bei der Reaktion des Kupfer(I)-Komplexes mit molekularem Sauerstoff voraus und erste Experimente zeigten die Bildung eines violetten Intermediates, was auf die Bildung eines solchen Peroxo-Komplexes hindeutet. Jedoch ließ sich diese Reaktion bislang nicht reproduzieren. Eine intramolekulare Hydroxylierung des Liganden wird hier nicht beobachtet. Das mögliche Oxidationsprodukt einer intramolekularen Hydroxylierungsreaktion, das phenolatverbrückte Derivat des Kupfer(II)-1,3-tpbd Komplexes, konnte auf eigenständige Weise unter Verwendung des Liganden 2,6-tpcd synthetisiert werden. Der so erhaltene Komplex $[\text{Cu}_2(2,6\text{-tpcd})(\text{H}_2\text{O})(\text{Cl})](\text{ClO}_4)_2 \times 2 \text{ H}_2\text{O}$ (**19**) wurde kristallographisch charakterisiert.

Ein weiteres, sehr interessantes Ergebnis wurde erhalten, als man ein Äquivalent eines Kupfer(II) Salzes mit ebenfalls einem Äquivalent 1,3-tpbd zur Reaktion brachte. Dabei wurde unter aeroben Bedingungen nach kurzer Zeit ein rotes Produkt erhalten, welches klar zeigt, dass eine Oxidation des Liganden stattgefunden haben muss. Jedoch konnte diese Reaktion durch die Präsenz von Zink(II) Kationen vollständig

unterdrückt werden. In diesem Fall wurde die Bildung von $[\text{Cu}_2(1,3\text{-tpbd})_2(\text{H}_2\text{O})_2](\text{ClO}_4)_4$, einem so genannten "Dimetallocyclophan" beobachtet.

Um die Komplexizität des 1,3-tpbd Ligandensystems zu erhöhen, wurde ein weiterer "koordinierender Arm" eingeführt. Daraus resultierte der neue Ligand 1,3,5-Hpbt. Bisher konnten leider noch keine dreikernigen Kupfer(II) Komplexe mit diesem Liganden dargestellt werden. Die Vorstufe für die Synthese dieses Liganden, 1,3,5-Triaminobenzol Trihydrochlorid, (welches zudem kristallographisch charakterisiert werden konnte) erwies sich als sehr interessantes Untersuchungsobjekt für ausführliche NMR-spektroskopische Analysen.

Publications

- S. Turba, S. P. Foxon, F. W. Heinemann, K. Petukhov, P. Müller, O. Walter, S. Schindler, *Eur. J. Inorg. Chem.* **submitted**.
- S. Turba, O. Walter, S. Schindler, L. Preuss Nielsen, A. Hazell, R. Hazell, C. J. McKenzie, F. Lloret, J. Cano, M. Julve, *Inorg. Chem.* **submitted**.
- S. P. Foxon, J.-Y. Xu, S. Turba, M. Leibold, F. Hampel, F. W. Heinemann, O. Walter, C. Würtele, M. C. Holthausen, S. Schindler, *Eur. J. Inorg. Chem.* **2007**, 429-443.
- S. Turba, H. Hausmann, P. R. Schreiner, S. Schindler, *Eur. J. Org. Chem.* supposed to be submitted.

Curriculum Vitae

Sabrina Turba

geboren am 10. September 1979

in Gießen

ledig

Ausbildung

Hausbergschule, Grundschule, Hoch-Weisel 09/1985-07/1990

Weidigschule, Gymnasium, Butzbach 09/1990-06/1999

Justus-Liebig-Universität, Gießen 10/1999-03/2004

Studium der Chemie

Justus-Liebig-Universität, Gießen,

Institut für anorganische und analytische Chemie 05/2004-11/2004

- Diplomarbeit im Arbeitskreis von Prof. Dr. S. Schindler. Thema: „Synthese, Charakterisierung und Eigenschaften von Kupferkomplexen mit dem Liganden 1,3-Bis[bis(2-pyridylmethylamino)]benzol und Derivaten“

Justus-Liebig-Universität, Gießen,

Institut für anorganische und analytische Chemie 12/2004-02/2008

- Promotion bei Prof. Dr. S. Schindler. Thema: „Syntheses, structures and properties of metal complexes of bis(2-pyridylmethyl) derivatives of o-, m-, and p-phenylenediamine and aniline.“

Berufstätigkeit

Steria Mummert Consulting AG, Hamburg 07/1997-09/1997

Aushilfs- und Werksstudententätigkeiten 07/1998-09/1998

05/2001-09/2001

Curriculum Vitae

Commerzbank AG, Frankfurt/ Main 07/1999-09/1999

Aushilfs- und Werksstudententätigkeiten 07/2000-09/2000

Justus-Liebig-Universität, Gießen,

Institut für anorganische und analytische Chemie 03/2002-03/2005

Studentische Hilfskraft in den chemischen Praktika
für Nebenfachstudenten

Justus-Liebig-Universität, Gießen,

Institut für anorganische und analytische Chemie 04/2005-02/2008

Wissenschaftliche Mitarbeiterin, Betreuung des
Anorganisch Chemischen Grundpraktikums für
Chemiker und Materialwissenschaftler
(AC1a bzw. BK02) sowie des Fortgeschrittenen
Praktikums für Chemiker.

Matthaes Medien, Stuttgart 01/2006-02/2008

Freie Mitarbeit als Redakteurin für die
Zeitschriften „Reiterjournal“ und „Züchterforum“

Bibliography

- [1] W. Kaim, B. Schwederski, *Bioanorganische Chemie*, Teubner Verlag, Stuttgart, **1991**, S. 204 ff.
- [2] S. J. Lippard, J. M. Berg, *Bioinorganic Chemistry*, University Science Books, Mill Valley, CA, **1994**.
- [3] M. Costas, M. P. Mehn, M. P. Jensen, L. Que, Jr., *Chem. Rev.* **2004**, *104*, 939-986.
- [4] L. M. Mirica, X. Ottenwaleder, T. D. P. Stack, *Chem. Rev.* **2004**, *104*, 1013-1045.
- [5] E. A. Lewis, W. B. Tolman, *Chem. Rev.* **2004**, *104*, 1047-1076.
- [6] *Bioinorganic Catalysis*, (Eds.: J. Reedijk, E. Bouwman), Marcel Dekker, New York, **1993**.
- [7] E. I. Solomon, P. Chen, M. Metz, S.-K. Lee, A. E. Palmer, *Angew. Chem. Int. Ed.* **2001**, *40*, 4570-4590.
- [8] J. P. Klinman, *Chem. Rev.* **1996**, *96*, 2541-2561.
- [9] E. I. Solomon, U. M. Sundaram, T. E. Machonkin, *Chem. Rev.* **1996**, *96*, 2563-2605.
- [10] S. Schindler, *Eur. J. Inorg. Chem.* **2000**, 2311-2326.
- [11] J. Markl, *Chemie in unserer Zeit* **1996**, *30*, 6-18.
- [12] *Bioinorganic Chemistry of Copper*, (Eds.: K. D. Karlin, Z. Tyeklár), Chapman & Hall, New York, **1993**.
- [13] H. Decker, R. Dillinger, F. Tuczec, *Angew. Chem. Int. Ed.* **2000**, *39*, 1591-1595.
- [14] M. Pascaly, I. Jolk, B. Krebs, *Chemie in unserer Zeit* **1999**, *33*, 334-341.
- [15] R. L. Jolley, L. H. Evans, N. Makino, H. S. Mason, *J. Biol. Chem.* **1974**, *249*, 335-345.
- [16] E. Kim, E. E. Chufa'n, K. Kamaraj, K. D. Karlin, *Chem. Rev.* **2004**, *104*, 1077-1133.
- [17] K. D. Karlin, Y. Gultneh, *Prog. Inorg. Chem.* **1987**, 219-327.
- [18] Z. Tyeklar, K. D. Karlin, *Acc. Chem. Res.* **1989**, *22*, 241-248.
- [19] Z. Tyeklar, R. R. Jacobson, N. Wei, N. N. Murthy, J. Zubieta, K. D. Karlin, *J. Am. Chem. Soc.* **1993**, *115*, 2677-2689.
- [20] R. R. Jacobson, Z. Tyeklar, A. Farooq, K. D. Karlin, S. Liu, J. Zubieta, *J. Am. Chem. Soc.* **1988**, *110*, 3690-3692.

-
- [21] C. Würtele, E. Gaoutchenova, K. Harms, M. C. Holthausen, J. Sundermeyer, S. Schindler, *Angew. Chem. Int. Ed.* **2006**, *45*, 3867-3869.
- [22] M. Schatz, V. Raab, S. P. Foxon, G. Brehm, S. Schneider, M. Reiher, M. C. Holthausen, J. Sundermeyer, S. Schindler, *Angew. Chem. Int. Ed.* **2004**, *43*, 4360-4363.
- [23] K. A. Magnus, B. Hazes, H. Ton-That, C. Bonaventura, J. Bonaventura, W. G. J. Hol, *Proteins: Struct. Funct. Genet.* **1994**, *19*, 302-309.
- [24] R. H. Holm, P. Kenepohl, E. I. Solomon, *Chem. Rev.* **1996**, *96*, 2239-2314.
- [25] T. N. Sorrell, M. L. Garrity, D. J. Ellis, *Inorg. Chim. Acta* **1989**, *166*, 71-77.
- [26] S. Schindler, D. J. Szalda, C. Creutz, *Inorg. Chem.* **1992**, *31*, 2255-2264.
- [27] N. N. Murthy, M. Mahroof-Tahir, K. D. Karlin, *J. Am. Chem. Soc.* **1993**, *115*, 10404-10405.
- [28] O. Kahn, *Comm. Inorg. Chem.* **1984**, *3*, 105-133.
- [29] O. Kahn, *Angew. Chem., Int. Ed.* **1985**, *24*, 834-850.
- [30] O. Kahn, *Molecular Magnetism*, VCH, Weinheim, **1993**.
- [31] K.-S. Bürger, P. Chaudhuri, K. Wieghardt, B. Nuber, *Chem. Eur. J.* **1995**, *1*, 583-593.
- [32] A. Caneschi, D. Gatteschi, R. Sessoli, *Acc. Chem. Res.* **1989**, *22*, 392-398.
- [33] I. Fernández, R. Ruiz, J. Faus, M. Julve, F. Lloret, J. Cano, X. Ottenwaelder, Y. Journaux, M. C. Muñoz, *Angew. Chem. Int. Ed.* **2001**, *40*, 3039-3042.
- [34] S. P. Foxon, G. R. Torres, O. Walter, J. Z. Pedersen, H. Toftlund, M. Hüber, K. Falk, W. Haase, J. Cano, F. Lloret, M. Julve, S. Schindler, *Eur. J. Inorg. Chem.* **2004**, 335-343.
- [35] A. M. W. Cargill Thompson, D. Gatteschi, J. A. McCleverty, J. A. Navas, E. Rentschler, M. D. Ward, *Inorg. Chem.* **1996**, *35*, 2701-2703.
- [36] V. A. Ung, A. M. W. Cargill Thompson, D. A. Bardwell, D. Gatteschi, J. C. Jeffery, J. A. McCleverty, F. Totti, M. D. Ward, *Inorg. Chem.* **1997**, *36*.
- [37] H. M. McConnell, *J. Chem. Phys.* **1963**, *39*, 1910.
- [38] N. Mataga, *Theor. Chim. Acta* **1968**, *10*, 372-376.
- [39] S. P. Foxon, O. Walter, R. Koch, H. Rupp, P. Müller, S. Schindler, *Eur. J. Inorg. Chem.* **2004**, 344-348.
- [40] X. Ottenwaelder, J. Cano, Y. Journaux, E. Rivière, C. Brennan, M. Nierlich, R. Ruiz-Garcia, *Angew. Chem.* **2004**, *116*, 868-870.

-
- [41] S. P. Foxon, J.-Y. Xu, S. Turba, M. Leibold, F. Hampel, F. W. Heinemann, O. Walter, C. Würtele, M. C. Holthausen, S. Schindler, *Eur. J. Inorg. Chem.* **2007**, 429-443.
- [42] P. de Hoog, P. Gamez, M. Lüken, O. Roubeau, B. Krebs, J. Reedijk, *Inorg. Chim. Acta* **2004**, 357, 213-218.
- [43] H. Grove, J. Sletten, M. Julve, F. Lloret, J. Cano, *Dalton Trans.* **2001**, 259-265.
- [44] P. Gómez-Saiz, J. García-Tojal, P. Díez-Gómez, R. Gil-García, J. L. Pizarro, M. I. Arriortua, T. Rojo, *Inorg. Chem. Commun.* **2005**, 8, 259-262.
- [45] A. W. Addison, T. N. Rao, J. Reedijk, J. van Rijn, G. C. Verschoor, *Dalton Trans.* **1984**, 1349-1356.
- [46] R. P. Doyle, P. E. Kruger, M. Julve, F. Lloret, M. Nieuwenhuyzen, *Cryst. Eng. Comm.* **2002**, 4, 13-16.
- [47] Y. Li, G. De, M. Yuan, E. Wang, R. Huang, C. Hu, N. Hu, H. Jia, *Dalton Trans.* **2003**, 331-334.
- [48] T. Soumahoro, E. Burkholder, W. Ouellette, J. Zubieta, *Inorg. Chim. Acta* **2005**, 358, 608-616.
- [49] Y. Hou, S. Wang, E. Shen, D. Xiao, E. Wang, Y. Li, L. Xu, C. Hu, *J. Mol. Struct.* **2004**, 689, 81-88.
- [50] B. Krebs, K. Schepers, B. Bremer, G. Henkel, E. Althaus, W. Müller-Warmuth, K. Griesar, W. Haase, *Inorg. Chem.* **1994**, 33, 1907-1914.
- [51] A. E. True, R. C. Scarrow, C. R. Randall, R. C. Holz, L. J. Que, *J. Am. Chem. Soc.* **1993**, 115, 4246-4255.
- [52] J.-S. Lim, M. A. S. Aquino, A. G. Sykes, *Inorg. Chem.* **1996**, 35, 614-618.
- [53] A. Neves, M. A. de Brito, I. Vencato, V. Drago, K. Griesar, W. Haase, *Inorg. Chem.* **1996**, 35, 2360-2368.
- [54] I. Kawafune, G. Matsubayashi, *Bull. Chem. Soc. Jpn.* **1994**, 67, 694-698.
- [55] M. Pohl, Y. Lin, T. J. R. Weakley, K. Nomiya, M. Kaneko, H. Weiner, R. G. Finke, *Inorg. Chem.* **1995**, 34, 767-777.
- [56] R. Neiher, C. Trojanowski, R. Mattes, *Dalton Trans.* **1995**, 2521-2528.
- [57] R. Finn, J. Zubieta, *Chem. Comm.* **2000**, 1321-1322.
- [58] Y. Zhang, A. Clearfield, R. C. Haushalter, *Chem. Mater.* **1995**, 7, 1221-1225.
- [59] X. Bu, P. Feng, G. D. Stucky, *Chem. Comm.* **1995**, 1337-1338.

-
- [60] V. Soghmanian, Q. Chen, Y. Zhang, R. C. Haushalter, C. J. O'Connor, C. Tao, J. Zubieta, *Inorg. Chem.* **1995**, *34*, 3509-3519.
- [61] A. M. W. Cargill Thompson, D. A. Bardwell, J. C. Jeffery, M. D. Ward, *Inorg. Chim. Acta* **1998**, *267*, 239-247.
- [62] M. Raidt, M. Neuburger, T. A. Kaden, *Dalton Trans.* **2003**, 1292-1298.
- [63] S. L. Tobey, B. D. Jones, E. V. Anslyn, *J. Am. Chem. Soc.* **2003**, *125*, 4026-4027.
- [64] S. L. Tobey, E. V. Anslyn, *J. Am. Chem. Soc.* **2003**, *125*, 14807-14815.
- [65] T. Z. Zhang, E. V. Anslyn, *Tetrahedron* **2004**, *60*, 11117-11124.
- [66] S. L. Tobey, E. V. Anslyn, *Org. Lett.* **2003**, *5*, 2029-2031.
- [67] M. Wall, R. C. Hynes, J. Chin, *Angew. Chem. Int. Ed.* **1993**, *32*, 1633-1635.
- [68] Y. Moreno, A. Vega, S. Ushak, R. Baggio, O. Pena, E. Le Fur, J.-Y. Pivan, S. Spodine, *J. Mater. Chem* **2003**, *13*, 2381-2387.
- [69] P. Phuengphai, S. Youngme, C. Pakavatchai, G. A. van Albada, M. Quesada, J. Reedijk, *Inorg. Chem. Commun.* **2006**, *9*, 147-151.
- [70] in *SADABS*, 2.26 ed., Bruker AXS, Inc., Madison, WI, USA, **2002**.
- [71] G. M. Sheldrick, *SHELX-97*, Universität Göttingen, **1997**.
- [72] in *SHELXTL NT 6.12*, Bruker AXS, Inc., Madison, WI, USA, **2002**.
- [73] H. M. McConnell, *J. Chem. Phys.* **1961**, *35*, 1520-1521.
- [74] C. Kollmar, O. Kahn, *Acc. Chem. Res.* **1993**, *26*, 259-265.
- [75] J. S. Miller, A. J. Epstein, *Angew. Chem. Int. Ed.* **1994**, *33*, 385-415.
- [76] O. Kahn, *Adv. Inorg. Chem.* **1995**, *43*, 179-257.
- [77] S. Mitsubori, T. Ishida, T. Nogami, H. Iwamura, *Chem. Lett.* **1994**, *23*, 285-288.
- [78] H. Oshio, H. Ichida, *J. Phys. Chem* **1995**, *99*, 3294-3302.
- [79] F. Lloret, G. De Munno, M. Julve, J. Cano, R. Ruiz, A. Caneschi, *Angew. Chem. Int. Ed.* **1998**, *37*, 135-138.
- [80] E. Pardo, J. Faus, M. Julve, F. Lloret, C. Muñoz, J. Cano, X. Ottenwaelde, Y. Journaux, R. Carrasco, G. Blay, I. Fernández, R. Ruiz-García, *J. Am. Chem. Soc.* **2003**, *125*, 10770-10771.
- [81] E. Pardo, K. Bernot, M. Julve, F. Lloret, J. Cano, R. Ruiz-García, F. S. Delgado, C. Ruiz-Pérez, X. Ottenwaelde, Y. Journaux, *Inorg. Chem.* **2004**, *43*, 2768-2770.

-
- [82] E. Pardo, I. Morales-Osorio, M. Julve, F. Lloret, J. Cano, R. Ruiz-García, J. Pasán, C. Ruiz-Pérez, X. Ottenwaelde, Y. Journaux, *Inorg. Chem.* **2004**, *43*, 7594-7596.
- [83] D. A. Dougherty, *Acc. Chem. Res.* **1991**, *24*, 88-94.
- [84] H. Iwamura, N. Koga, *Acc. Chem. Res.* **1993**, *26*, 346-351.
- [85] A. Rajca, *Chem. Rev.* **1994**, *94*, 871-893.
- [86] T. Buchen, A. Hazell, L. Jessen, C. J. McKenzie, L. Preuss Nielsen, J. Z. Pedersen, D. Schollmeyer, *Dalton Trans.* **1997**, 2697-2704.
- [87] A. Hazell, C. J. McKenzie, L. P. Pedersen, *Polyhedron* **2000**, *19*, 1333-1338.
- [88] A. Nielsen, A. D. Bond, C. J. McKenzie, *Acta Cryst. E* **2005**, *61*, 478-480.
- [89] A. Nielsen, S. Veltzé, A. D. Bond, C. J. McKenzie, *Polyhedron* **2007**, *26*, 1649-1657.
- [90] F. Ugozzoli, C. Massera, A. M. Manotti Lanfredi, N. Marsich, A. Camus, *Inorg. Chim. Acta* **2002**, *340*, 97-104.
- [91] M. Sato, Y. Mori, I. Takeaki, *Synthesis* **1992**, 539-540.
- [92] J. W. Hall, University of North Carolina (Chapel Hill, NC), **1977**.
- [93] J. C. Bonner, M. E. Fisher, *Phys. Rev. A* **1964**, *135*, 640-658.
- [94] J. Carranza, J. Sletten, F. Lloret, M. Julve, *Inorg. Chim. Acta* **2004**, *357*, 3304-3316.
- [95] B. Bleaney, K. Bowers, *Proc. Roy. Soc., Sect. A* **1952**, *214*, 451-465.
- [96] T. R. Felthouse, E. N. Duesler, D. N. Hendrickson, *J. Am. Chem. Soc.* **1978**, *100*, 618-619.
- [97] T. R. Felthouse, D. N. Hendrickson, *J. Am. Chem. Soc.* **1978**, *100*, 2636-2648.
- [98] J. Cano, University of Valencia, **2003**.
- [99] E. Ruiz, P. Alemany, S. Alvarez, J. Cano, *J. Am. Chem. Soc.* **1997**, *119*, 1297-1303.
- [100] A. D. Becke, *J. Chem. Phys.* **1993**, *98*, 5648-5652.
- [101] A. Schäfer, H. Horn, R. Ahlrichs, *J. Chem. Phys.* **1992**, *97*, 2571-2577.
- [102] Siemens, Siemens Analytical X-ray Instruments Inc., Madison, WI, **1995**.
- [103] A. Altomare, G. Cascarano, C. Giacovazzo, A. Guagliardi, A. G. G. Moliterni, M. C. Burla, G. Polidori, M. Camalli, R. Spagna, University of Bari, **1997**.
- [104] A. Hazell, Aarhus University, Denmark, **1995**.
- [105] *International Tables for X-RAY Crystallography*, The Kynoch Press, Birmingham, **1992**.

-
- [106] *International Tables for X-RAY Crystallography*, The Kynoch Press, Birmingham, **1974**.
- [107] H. D. Flack, *Acta Cryst.* **1983**, A39, 876-881.
- [108] L. Q. Hatcher, K. D. Karlin, *J. Biol. Inorg. Chem.* **2004**, 9, 669-683.
- [109] A. Hofmann, R. van Eldik, *Dalton Trans.* **2003**, 2979-2985.
- [110] N. N. Murthy, K. D. Karlin, I. Bertini, L. C., *J. Am. Chem. Soc.* **1997**, 119, 2156-2162.
- [111] S. Turba, O. Walter, S. Schindler, L. Preuss Nielsen, A. Hazell, C. J. McKenzie, F. Lloret, J. Cano, M. Julve, *Inorg. Chem.* **submitted**.
- [112] L. Li, K. D. Karlin, S. E. Rokita, *J. Am. Chem. Soc.* **2005**, 127, 520-521.
- [113] L. Li, A. A. Narducci Sarjeant, M. A. Vance, L. N. Zakharov, A. N. Rheingold, E. I. Solomon, K. D. Karlin, *J. Am. Chem. Soc.* **2005**, 127, 15360-15361.
- [114] T. N. Sorrell, C. O'Connor, O. P. Anderson, J. H. Reibenspies, *J. Am. Chem. Soc.* **1985**, 107, 4199-4206.
- [115] A. Hazell, C. J. McKenzie, L. Preuss Nielsen, *Dalton Trans.* **1998**, 1751-1756.
- [116] A. Mederos, P. Gili, S. Domínguez, A. Benítez, M. Soledad Palacios, M. Hernández-Padilla, P. Martín-Zarza, M. L. Rodríguez, C. Ruíz-Pérez, F. J. Lahoz, L. A. Oro, F. Brito, J. M. Arrieta, M. Vlassi, G. Germain, *Dalton Trans.* **1990**, 1477-1491.
- [117] E. Y. Tshuva, S. J. Lippard, *Chem. Rev.* **2004**, 104, 987-1012.
- [118] S. V. Kryatov, E. V. Rybak-Akimova, S. Schindler, *Chem. Rev.* **2005**.
- [119] I. Bernal, I. M. Jensen, K. B. Jensen, C. J. McKenzie, H. Toftlund, J. P. Tuchagues, *Dalton Trans.* **1995**, 3667-3675.
- [120] C. R. Randall, L. Shu, Y.-M. Chiou, K. S. Hagen, M. Ito, N. Kitajima, R. J. Lachicotte, Y. Zang, L. Que Jr., *Inorg. Chem.* **1995**, 34, 1036-1039.
- [121] A. Diebold, K. S. Hagen, *Inorg. Chem.* **1998**, 37, 215-223.
- [122] D. Mandon, A. Nopper, T. Litrol, S. Goetz, *Inorg. Chem.* **2001**, 40, 4803-4806.
- [123] M. Yashiro, H. Kaneiwa, K. Onaka, M. Komiyama, *Dalton Trans.* **2004**, 4, 605-610.
- [124] M. L. Hlavinka, M. J. Mc Nevin, R. Shoemaker, J. R. Hagadorn, *Inorg. Chem.* **2006**, 45, 1815-1822.
- [125] J. B. Mandel, C. Maricondi, B. E. Douglas, *Inorg. Chem.* **1988**, 27, 2990-2996.
- [126] I. Fridovich, *Annu. Rev. Biochem.* **1995**, 64, 97-112.
- [127] D. P. Riley, *Chem. Rev.* **1999**, 99, 2573-2587.

- [128] D. Ghosh, N. Kundu, G. Maity, A. Caneschi, A. Endo, M. Chaudhury, *Inorg. Chem.* **2004**, 43, 6015-6023.
- [129] V. Pelmeshnikov, P. E. M. Siegbahn, *Inorg. Chem.* **2005**, 44, 3311-3320.
- [130] H. Ohtsu, S. Itoh, S. Nagatomo, T. Kitagawa, S. Ogo, Y. Watanabe, S. Fukuzumi, *Chem. Comm.* **2000**, 1051-1052.
- [131] H. Ohtsu, Y. Shimazaki, A. Odani, O. Yamauchi, W. Mori, S. Itoh, S. Fukuzumi, *J. Am. Chem. Soc.* **2000**, 122, 5733-5741.
- [132] S. Fukuzumi, H. Ohtsu, K. Ohkubo, S. Itoh, H. Imahori, *Coord. Chem. Rev.* **2002**, 226, 71-80.
- [133] Y. Gultneh, A. Raza Khan, D. Blaise, S. Chaudry, B. Ahvazi, B. B. Marvey, R. J. Butcher, *J. Inorg. Biochem.* **1999**, 75, 7-18.
- [134] M. Palaniandavar, R. J. Butcher, A. W. Addison, *Inorg. Chem.* **1996**, 35, 467-471.
- [135] A. Calder, A. R. Forrester, P. G. James, G. R. Luckhurst, *J. Am. Chem. Soc.* **1969**, 91, 3724-3727.
- [136] F. Effenberger, W.-D. Stohrer, K.-E. Mack, F. Reisinger, W. Seufert, H. E. A. Kramer, R. Föll, E. Vogelmann, *J. Am. Chem. Soc.* **1990**, 112, 4849-4857.
- [137] M. M. Wienk, R. A. J. Janssen, *J. Am. Chem. Soc.* **1996**, 118, 10626-10628.
- [138] E. Fromm, R. Ebert, *J. Prakt. Chemie* **1924**, 108, 75-87.
- [139] W. Fee, D. Elholum, A. McPherson, D. Rundle, *Aust. J. Chem.* **1973**, 26, 1207-1225.
- [140] A. D. Becke, *Phys. Rev. A* **1988**, 38, 3098-3109.
- [141] C. Lee, W. Yang, R. G. Parr, *Phys. Rev. B* **1988**, 37, 785-789.
- [142] P. J. Stephens, F. J. Devlin, C. F. Chabalowski, M. J. Frisch, *J. Phys. Chem.* **1994**, 98, 11623-11627.
- [143] R. Ahlrichs, M. Bär, H. P. Baron, R. Bauernschmitt, S. Becker, M. Ehrig, K. Eichkorn, S. Elliott, F. Furche, F. Haase, M. Häser, C. Hättig, H. Horn, C. Huber, U. Huniar, M. Kattaneck, A. Köhn, C. Kölmel, M. Kollwitz, K. May, C. Ochsenfeld, H. Öhm, A. Schäfer, U. Schneider, O. Treutler, K. Tsereteli, B. Unterreiner, M. von Arnim, F. Weigend, P. Weis, H. Weiss, Universität Karlsruhe, **2002**.
- [144] R. Ahlrichs, in *Encyclopedia Computational Chemistry* (Ed.: P. v. R. Schleyer), Wiley, Chichester, **1998**, pp. 3123-3129.

- [145] R. Ahlrichs, M. Bär, M. Häser, H. Horn, C. Kölmel, *Chem. Phys. Lett.* **1989**, 162, 165-169.
- [146] A. Schäfer, C. Huber, R. Ahlrichs, *J. Chem. Phys.* **1994**, 100, 5829-5835.
- [147] A. Klamt, G. Schüürmann, *J. Chem. Soc., Perkin Trans. 2* **1993**, 799-805.
- [148] A. T. C. North, D. C. Phillips, F. S. Matthews, *Acta Cryst.* **1968**, A24, 351-359.
- [149] J. E. Gill, R. Mcac Gillivray, J. Munro, *J. Chem. Soc.* **1949**, 1753-1754.
- [150] M. Barfield, P. Fagerness, *J. Am. Chem. Soc.* **1997**, 119, 8699-8711.